

Carnegie Mellon University

CARNEGIE INSTITUTE OF TECHNOLOGY

THESIS

SUBMITTED IN PARTIAL FULFILLMENT OF THE REQUIREMENTS

FOR THE DEGREE OF Doctor of Philosophy

TITLE Optimization Models for Water Management in
Chemical Processes and Shale Gas Production

PRESENTED BY Linlin Yang

ACCEPTED BY THE DEPARTMENT OF

Chemical Engineering

IGNACIO GROSSMANN 10/13/14
IGNACIO GROSSMANN, ADVISOR DATE

LORENZ BIEGLER 10/13/14
LORENZ BIEGLER, DEPARTMENT HEAD DATE

APPROVED BY THE COLLEGE COUNCIL

VIJAYAKUMAR BHAGAVATULA 10/13/14
DEAN DATE

OPTIMIZATION MODELS FOR WATER MANAGEMENT IN
CHEMICAL PROCESSES AND SHALE GAS PRODUCTION

by

LINLIN YANG

SUBMITTED IN PARTIAL FULFILLMENT OF THE
REQUIREMENTS FOR THE DEGREE OF
DOCTOR OF PHILOSOPHY

at

CARNEGIE MELLON UNIVERSITY
DEPARTMENT OF CHEMICAL ENGINEERING
PITTSBURGH, PENNSYLVANIA

OCTOBER, 2014

Acknowledgments

I would like to express my sincerest gratitude to Professor Ignacio E. Grossmann for being such a wonderful advisor and mentor during the past five years. In addition to being knowledgeable and encouraging, his attentiveness to detail and strong work ethic have made deep impact not only during my studies but also in my life.

I am grateful to Professors Larry Biegler, Nick Sahinidis, Jeff Sirola and David Dzombak for their wisdom and patience while serving as committee members during my proposal and PhD defense.

Special thanks are due to Jeremy Manno, my industrial collaborator from Carrizo Oil & Gas, whose insight and experience with challenges that arise in practice have helped me to initiate the second part of the work, and whose enthusiasm and strong commitment to the project have made this thesis possible.

I would like to express my gratitude to Professor Meagan Mauter for very useful discussions and support on the work. Dr. David Miller and Dr. Robert Dilmore from the National Energy Technology Laboratory (NETL) have provided insightful suggestions and feedback on the work. I would also like to thank Raquel Salcedo-Diaz from University of Alicante and Mariano Martín for bringing their experience into the project.

I am very lucky to have met many friends from the PSE research groups as well as the visiting researchers, who have created both a positive work environment at CMU and many unforgettable memories in Pittsburgh. Among them, I would like to specially thank Francisco Trespalacios, Satyajith Amaran, German Oliveros Patino, Sumit Mitra, and Qi

Zhang for inspiration, encouragement, and friendship.

The financial support from NETL and the National Science Foundation under grants CBET-1437668 and CBET-0966524 is gratefully acknowledged.

Abstract

This thesis focuses on the optimization of an important natural resource, water, in chemical processes and shale gas production.

In the chemical industry, many unit operations require intensive use of water for processes such as synthesis, cleaning, cooling cycle, and steam production. The wastewater stream contains pollutants such as total dissolved solids (TDS) and organics that need to be removed prior to discharge into natural water bodies. With the increasingly stringent environmental regulations, freshwater and wastewater reuse allocation has become a major topic in process synthesis.

Chapter 2 presents an approach to perform simultaneous optimization of heat and water integration for a process flowsheet. As opposed to the sequential integration approach where heat and water integration are performed for flowsheets with fixed operating conditions, the simultaneous optimization method allows for variable stream qualities to account for potential trade-offs among raw material, investment cost, and utility and water consumption. Since detailed heat-exchange network and water network designs are generally formulated as nonconvex mixed-integer nonlinear programming and nonconvex nonlinear programming models, respectively, reducing complexities for these two networks is of utmost priority. We have developed a novel linear programming targeting model for minimizing freshwater consumption of multi-contaminants systems. This water targeting model, which is either exact or else predicts upper bounds, is incorporated along with the available heat targeting model into flowsheet optimization process to achieve the best operating conditions through the proposed simultaneous framework.

The conventional water network synthesis approach greatly simplifies wastewater treatment units by using fixed recoveries, creating a gap for their applicability to industrial processes. Chapter 3 describes a unifying approach combining various technologies capable of removing contaminants through the use of more realistic models. Unit-specific short-cut models are developed in place of the fixed contaminant removal model to describe contaminant mass transfer in reverse osmosis, ion exchange, sedimentation, ultrafiltration, activated sludge, and trickling filter. In addition, uncertainty in mass load of contaminant is considered to account for the range of operating conditions. Furthermore, the superstructure is modified to accommodate realistic potential structures. We also present a modified Lagrangean-based decomposition algorithm in order to effectively solve the resulting nonconvex mixed-integer nonlinear programming problem.

Management of water use in the rapidly developing shale gas industry has become a major challenge in recent years. Unlike most chemical processes that operate at steady-state conditions, hydraulic fracturing requires a large volume of water in a short period of time. In addition, there is a cost associated with each of the four key aspects, source water acquisition, wastewater production, reuse and recycle, and subsequent transportation, storage, and disposal. In chapter 4, water use life cycle is optimized for wellpads through a discrete-time two-stage stochastic mixed-integer linear programming model under uncertain availability of water. The objective is to minimize expected operating cost while accounting for the revenue from gas production.

As the number of producing wells increase, desalination options are evaluated since produced water management becomes an important economic driver. In chapter 5, we expand the operational model in chapter 4 to optimize capital investment decisions in water use for shale gas production. The goal is to determine the location and capacity of impoundment, the type of piping, treatment facility locations and removal capability, freshwater sources, as well as the frac schedule. In addition, we examine in several scenarios the impact of limiting truck hauling and increasing flowback volume on the solution.

Case studies in both Marcellus and Utica shale are presented to illustrate the application of the proposed formulations.

Contents

1	Introduction	1
1.1	Strategies for flowsheet optimization with heat and water integration . . .	1
1.2	Process water network optimization	4
1.3	Water management in shale gas production	6
1.4	Mathematical programming	11
1.5	Thesis outline	12
1.5.1	Chapter 2 - Water targeting model	13
1.5.2	Chapter 3 - Nonlinear models for water regeneration	13
1.5.3	Chapter 4 - Operational model for shale gas water management . .	14
1.5.4	Chapter 5 - Investment model for shale gas water management . .	15
1.5.5	Chapter 6 - Conclusion	15
2	Water Targeting Model for Water-Using Process Units	17
2.1	Introduction	17
2.2	Outline of proposed simultaneous optimization strategy	18
2.3	Water targeting for WN with process units only	20
2.3.1	NLP model for WN	21

2.3.2	Lower bound: McCormick relaxation	22
2.3.3	A novel LP target model	23
2.3.4	Non-isothermal water network targeting	28
2.4	Extension for treatment units	35
2.4.1	Motivating example	35
2.4.2	Addition of wastewater treatment unit	36
2.5	Simultaneous optimization	40
2.5.1	Procedure	40
2.5.2	Examples	40
2.6	Discussion	48
2.7	Conclusion	49
3	Wastewater Regeneration Models for Water Network Optimization	50
3.1	Introduction	50
3.2	Problem statement	52
3.2.1	Problem description	52
3.2.2	General model	53
3.2.3	Objective function	55
3.3	Illustrative example	56
3.4	Wastewater treatment unit short-cut models	57
3.4.1	Reverse osmosis	58
3.4.2	Ion exchange	60
3.4.3	Sedimentation	62
3.4.4	Ultrafiltration	63

3.4.5	Activated sludge	64
3.4.6	Trickling filter	66
3.4.7	Economics of treatment units	68
3.5	Computational strategies	71
3.5.1	Strategy for global optimal solution	71
3.5.2	Subproblem descriptions	72
3.5.3	Algorithm	74
3.6	Numerical examples	75
3.6.1	Example 1: illustrative example with short-cut treatment unit models	76
3.6.2	Example 2: metal finishing industry wastewater treatment	79
3.6.3	Example 3: petroleum refinery water use	81
3.7	Conclusion	84
4	Operational Model for Shale Gas Water Management	87
4.1	Introduction	87
4.2	Freshwater handling	88
4.2.1	Background	88
4.2.2	Problem I	89
4.2.3	Optimization model I	93
4.2.4	Example 1	96
4.3	Wastewater handling	100
4.3.1	Background	100
4.3.2	Problem statement II	102
4.3.3	Optimization model II	106

4.3.4	Example 2	108
4.4	Conclusion	110
5	Investment optimization model for freshwater acquisition and wastewater handling in shale gas production	114
5.1	Introduction	114
5.2	Treatment facility	115
5.2.1	Overview	115
5.2.2	Desalination methods	116
5.3	Problem statement	118
5.4	Problem formulation	121
5.4.1	Constraints	122
5.4.2	Objective	129
5.4.3	MILP approximation	131
5.5	Case study in Utica shale	132
5.5.1	Optimization model	132
5.5.2	Scenario description	136
5.5.3	Results and discussion	138
5.6	Conclusion	142
6	Conclusion	147
6.1	Summary of thesis	147
6.1.1	Water targeting model for water-using process units	147
6.1.2	Wastewater regeneration models for water network optimization	148
6.1.3	Operational model for shale gas water management	149

6.1.4	Investment optimization model for freshwater acquisition and wastewater handling in shale gas production	150
6.2	Research contribution	151
6.3	Future research directions	152
6.3.1	Process water network	152
6.3.2	Shale gas water management	153
A	LP Targeting Model for Single Contaminant System	156
B	Convex Envelopes	161

List of Tables

1.1	Best available techniques (BAT).	6
2.1	Additional problems using LP targeting formulation.	26
2.2	Example 1 from Wang and Smith.	27
2.3	Closeup on Mixer Unit 3.	27
2.4	Data for heat-integrated WN example.	31
2.5	Heat-integrated network example from Bogataj and Bagajewicz.	31
2.6	Data for heat-integrated WN example 3.	33
2.7	Water sources for heat-integrated WN example 3.	34
2.8	Result comparison: heat-integrated WN example 3.	35
2.9	Data for stagewise structure.	38
2.10	Stage-wise superstructure result comparison.	39
2.11	Utility data.	41
2.12	Result comparison for methanol synthesis example.	43
2.13	Formulation size comparison for bioethanol production.	46
2.14	Result comparison for bioethanol production.	46
3.1	Illustrative example data.	56
3.2	Illustrative example optimization results.	57
3.3	Computational statistics for illustrative example.	57
3.4	Characteristics of the FILMTEC™BW30-400 membrane element.	60
3.5	Typical values for the empirical constants at 20 °C.	63
3.6	Characteristics of a typical UF membrane.	64

3.7	AS kinetic parameters.	66
3.8	Typical cost correlation values.	69
3.9	Example 1 subproblem model statistics.	77
3.10	Example 1 recovery comparison.	79
3.11	Example 2 metal finishing data.	79
3.12	Example 3 petroleum refinery data.	83
4.1	Example 1 wellpad data.	96
4.2	Example 1 parameters and cost coefficients.	96
4.3	Example 1 solution comparison.	97
4.4	Example 2 parameters and cost coefficients.	109
4.5	Example 2 solution comparison.	109
5.1	Specifications of desalination technologies. ^{1,2}	116
5.2	Case study wellpad data.	133
5.3	Case study cost coefficient data. ^{3,2}	134
5.4	Computational statistics.	138
5.5	Summary of objective values.	138

List of Figures

1.1	Water network superstructure.	4
1.2	Water consumption per unit of energy generation comparison.	8
1.3	Wellpad development timeline.	9
1.4	Horizontal well hydraulic fracturing stages.	9
1.5	Overall picture of water use in shale gas ⁴	10
2.1	Simultaneous optimization framework.	18
2.2	WN superstructure for water-using PUs.	21
2.3	Network with minimum freshwater consumption.	28
2.4	Nonisothermal WN.	29
2.5	Non-isothermal WN targeting diagram.	29
2.6	Example 2 superstructure.	31
2.7	Heat-integrated water network obtained by Bogataj.	32
2.8	Stagewise superstructure for WN with wastewater treatment.	36
2.9	Methanol synthesis process flowsheet.	42
2.10	Methanol synthesis simultaneous optimization: (a) WN (b) HEN.	43
2.11	Methanol synthesis sequential optimization: (a) WN (b) HEN.	44
2.12	Bioethanol production process flowsheet.	45
2.13	Bioethanol production simultaneous optimization: (a) WN (b) HEN.	47
3.1	Superstructure with multiple treatment unit options.	52
3.2	Illustrative example result: (a) Worst case scenario (b) Three-scenario.	57
3.3	Reverse osmosis diagram.	59

3.4	Ion exchange unit (a) breakthrough curve, (b) ion exchange column configuration (i) loading cycle (ii) regeneration cycle ⁵	60
3.5	Horizontal flow sedimentation diagram.	62
3.6	Organics removal units schematics, (a) Activated sludge, (b) Two-stage trickling filter.	65
3.7	Organic treatment unit shortcut model comparison.	71
3.8	Decomposition scheme.	73
3.9	Example 1 network superstructure.	76
3.10	Example 1(a) short-cut model optimal solution (b) simplified model optimal solution.	78
3.11	Example 2 metal finishing wastewater treatment network superstructure.	80
3.12	Example 2 metal finishing water network configuration.	82
3.13	Example 3 refinery process water system superstructure.	83
3.14	Example 3 optimal network configuration for the refinery water system.	84
4.1	Water transportation through temporary piping.	89
4.2	River discharge statistics.	91
4.3	Problem I superstructure.	92
4.4	Daily freshwater requirement for a given wellpad.	94
4.5	Example 1 fracturing schedule from (a) heuristic method (b) MILP model.	98
4.6	Daily impoundment volume comparison.	98
4.7	Daily truck use comparison.	99
4.8	Example flowback volume vs. TDS profile ³	101
4.9	Wellpad impoundment and frac tank aerial view.	102
4.10	Well production decline curve.	103
4.11	Natural gas price profile averaged over the years 2009, 2010, and 2012.	104
4.12	Problem 2 superstructure.	105
4.13	Example 2 (a) flowback profile and (b) production profile.	108
4.14	Example 2 fracturing schedule from (a) heuristic method (b) MILP model.	110
5.1	Main elements in water supply chain for shale gas production.	120
5.2	Flow directions for wellpads, impoundments, rivers, and ponds.	123

5.3	Wastewater flows.	126
5.4	Layout of Utica case study.	133
5.5	Total gas production curve of each wellpad.	134
5.6	Flowback (a) flowrate profile and (b) TDS concentration.	135
5.7	Comparison between the optimal and heuristic schedule.	139
5.8	Freshwater cost comparison for all scenarios.	140
5.9	Scenario 3 freshwater availability and trucking use.	141
5.10	Wastewater cost comparison for all scenarios.	141
5.11	Frac fluid composition in the optimal scenario for (a) all wellpads averaged over time and (b) wellpad 3.	142
A.1	Schematic representation of a water network.	157
A.2	Precursor and receivers of a process.	158
A.3	PU2 stream parameters and variables obtained in (a) Model 1 and (b) Model 2.	159
A.4	PU3 stream parameters and variables obtained in Model 1 and Model 2.	159
A.5	Excluded structural connectivity in Model 1.	159
A.6	Representation of Model 1 using Model 2 superstructure.	159

Chapter 1

Introduction

With increasing costs, diminishing quality of supplies, and stricter environmental effluent standards set forth by the Environmental Protection Agency (EPA), water is becoming an important commodity. The focus of this dissertation is to optimize water use in both process industries and shale gas development. We introduce in section 1.1 the general strategies for performing flowsheet optimization with heat and water integration. The relevant background and procedures for water use optimization within the process flowsheets is described in section 1.2. Then section 1.3 motivates a systematic approach to managing water use at shale gas wellpads. Section 1.4 describes different types of mathematical programming models that represent these problems and optimization approaches to solve them. Finally, section 1.5 outlines this thesis.

1.1 Strategies for flowsheet optimization with heat and water integration

The primary water uses in process industries are process water, cooling water, and boiler feed water, with each use being emphasized by different industries. For example, the chemicals, petroleum refining, and metal sectors primarily use water for cooling, while

paper and pulp and food processing mostly use water for process use. In a study by Carbon Disclosure Projects of 137 companies with total assets over \$16 trillion, it has been reported that water has risen high on the corporate agenda⁶. Eighty nine percent of responding companies have developed specific water policies, strategies, and plans. Specifically, in the chemical sector, all ten companies surveyed recognize that there is a high growth potential for processes and products that support more efficient water use and water recycling. Thus, despite its relative low cost in most of the U.S., water reuse has received significant attention by the academic community.

In addition to water, energy is another important resource for the process industry. Systematic schemes for the reduction of energy use is a mature field where complex problems are analyzed and solved (e.g. pinch analysis^{7,8}, mathematical programming^{9,10}). Systematic methods for optimal WN synthesis with the objective of minimizing freshwater consumption can also be broadly categorized into pinch analysis^{11,12,13} and superstructure-based methods^{14,15,16,17}. Thorough reviews of insight-based methods are covered in Foo¹⁸, whereas mathematical optimization techniques can be found in Bagajewicz¹⁹, and more recent advancements are reviewed by Jeżowski²⁰.

Generally, the reduction of the consumption of heating utility can lead to the reduction of freshwater, and vice versa²¹. This coupling of the two process synthesis areas underlines the importance of performing simultaneous optimization, which solves the synthesis problem directly and accounts for complex trade-offs among raw materials, investment cost, and energy consumption, enabling the simultaneous approach to provide lower cost solutions with efficient use of energy and water²². Simultaneous process flowsheets and heat integration has been demonstrated to provide better solution.²³

The traditional procedure for large process synthesis designs relies on a sequential approach, which divides the problem into subproblems and solves them separately in their natural sequence. In the context of this work, the process flowsheet is optimized first, which determines operating conditions with the assumption that all of the heating, cooling, and water requirements will be satisfied by purchased utilities. Then, the resulting operating conditions and stream states are passed on to the heat-exchange network (HEN) synthesis^{24,25}, followed by the synthesis of the water network (WN)^{18,19,20}. The subprob-

lems are more attractive to solve since they are smaller in size. However, dividing a problem into subsystems forces important decision variables (e.g. temperature, flowrate) to be fixed, and since these parameters can have major impact on the cost of heat integration, the sequential approach may lead to suboptimal solutions.

Analogous to HEN pinch method, a pinch method for WN (consisting of water-using process units and/or wastewater treatment units) with a single contaminant has also been developed¹¹. However, whereas in heat integration a single quality, heat, is transferred, typical water integration involves the transfer of not only one but of multiple contaminants, which cannot be accounted for with water pinch analysis. Alternatively, a mathematical programming approach can be formulated by globally optimizing nonconvex NLP or MINLP problems based on superstructure optimization for handling multiple contaminants. Despite these efforts, a linear formulation for multicontaminants WN that can be easily embedded in simultaneous optimization has not yet been reported in the literature.

Flowsheet optimization problems can vary in difficulty depending on the level of model complexity (i.e. from shortcut models to fully nonlinear rigorous models²⁶). These problems usually take the form of nonconvex mixed-integer nonlinear programming (MINLP) models, where the nonconvexities arise from the concave cost terms in the objective function and the nonlinear equations describing the material and heat balances and design equations. In addition, formulations of HEN and WN synthesis are primarily characterized by MINLP problems and nonlinear programming (NLP) problems, respectively. Thus, the full simultaneous optimization of flowsheets, heat exchange networks, and water networks is very difficult and may incur expensive computational cost.

To overcome this drawback, a targeting approach, which determines ahead of detailed design the main design features (e.g. heating utility for HEN, freshwater consumption for WN), can be taken to simplify the simultaneous optimization problem. Although this approach neglects the investment costs of the HEN and WN, it can still capture the major trade-offs while keeping the problem dimensionality to a manageable size. Duran and Grossmann²⁷ have developed a targeting approach for HENS based on a set of linear and nonlinear constraints. The method can determine for variable stream heat capacity flowrates, inlet and outlet temperatures, the minimum heating and cooling utilities re-

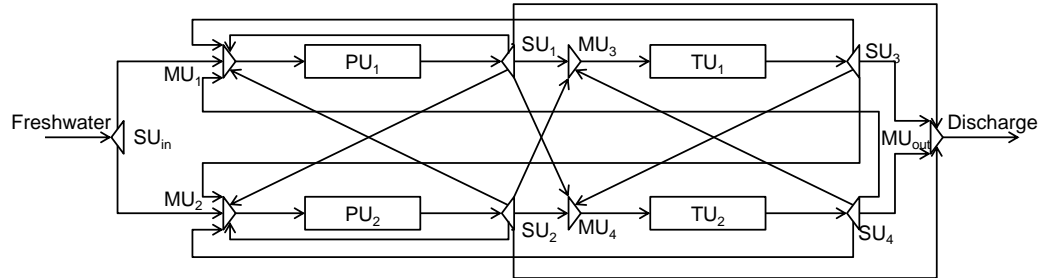


Figure 1.1: Water network superstructure.

quired without having to solve the detailed MINLP formulation for HENS. Due to the small size and linear nature of the model for fixed process stream conditions, this targeting formulation can be embedded much more easily than a detailed HEN superstructure within a process flowsheet optimization formulation. This work focuses on developing a strategy to perform simultaneous optimization using targeting formulations to minimize the computational requirement due to the integrated HEN and WN.

1.2 Process water network optimization

A mathematical programming approach can be formulated by globally optimizing nonconvex NLP or MINLP problems based on superstructure optimization for handling multiple contaminants. In a typical WN superstructure, water is supplied to water-using process units, and then wastewater streams generated from these processes are treated in various treatment units. Generally speaking, the standard formulation for a WN design problem consists of the following information. The process units in the water network are usually characterized by concentration limits of the entering stream and mass load of contaminants released from the unit, whereas the treatment units are characterized by fixed recoveries (i.e. $C_j^{out} = \beta_{tj} C_j^{in}$, where β_{tj} is the recovery of contaminant j in treatment unit t ; C_j^{in} and C_j^{out} are contaminant concentration levels at the inlet and the outlet of t).

This comprehensive superstructure (shown in Figure 1.1) considers systematic alternatives

for water reuse, recycle, and recycle-reuse to minimize freshwater consumption, or more generally, total network cost subject to a specified discharge limit^{16,28}. Variations of this superstructure have been considered in previous works for grassroots designs, namely, considering either only water-using process units²⁹, focusing only on wastewater treatment units³⁰, or on both^{14,15,31,16,28}. In addition, retrofit of industrial water systems has also been considered³². Many studies have been performed to integrate wastewater treatment systems in industrial plants using both insight-based and optimization approaches^{33,34}. These models greatly simplify the water network design, but create a gap for their applicability to industrial processes since more accurate treatment models should be considered in the optimization of these water networks.

The majority of the works related to WN optimization in the literature assume that the network operates at a nominal steady state. However, since conditions for a given process may change during the course of the operation, Karuppiah and Grossmann³⁵ presented a multiscenario nonconvex MINLP model that is a deterministic equivalent of a two-stage stochastic programming model with recourse. For each of the best, worst, and nominal scenarios, the uncertain parameters such as treatment unit removal ratios and mass load of contaminant in the process units can take on a different set of values.

In order to understand the different types of individual treatment units, it is useful to first consider the treatment procedures of a centralized wastewater treatment plants³⁶. In a typical plant, oil and grease are removed in the pretreatment stage. Primary treatment involves the use of physical and chemical operations to remove suspended particles. The next step is secondary treatment, where microorganisms are required to stabilize waste components. Finally, tertiary treatment further removes nitrogen, phosphorus, heavy metals, and bacteria.

Different types of contaminants present in the system are removed by considering the Best Available Techniques (BAT)³⁷. These provide the industrial standards for discharge of the major pollutant groups and recommendations for their treatment as listed in Table 1.1. Detailed models have been developed for some of these specific treatment technologies such as reverse osmosis (RO), which has been a major topic of interest as desalination capacity around the world has been growing steadily in response to water shortage problems. El-

Table 1.1: Best available techniques (BAT).

	Suspended Solids (TSS)	Heavy Metals (HM)	Inorganic Salt (TDS)	Organic Unsuitable for Bio. (ORG)	Unsuitable for Bio. Treat	Organic Suitable for Bio. Treat (BOD)
Sedimentation	✓	✓				
Flotation	✓	✓				
Filtration	✓	✓				
Ultrafiltration	✓					
Precipitation		✓				
Ion Exchange		✓	✓			
Reverse Osmosis	✓	✓	✓			
Evaporation				✓		✓
Oxidation				✓		
Adsorption				✓		
Anaerobic Treatment						✓
Aerobic Treatment						✓

Halwagi³⁸ presented an MINLP formulation using a state space representation for optimal RO system synthesis. Lu et al³⁹ addressed the optimal cost design of RO desalination system including membrane module cleaning and replacing using an MINLP model. Saif et al⁴⁰ designed a reverse osmosis network for the desalination application. Khor et al⁴¹ addressed the synthesis of a water regeneration network using nonlinear mechanistic models and applied it to a single-stage reverse osmosis network. Karuppiah et al⁴² use detailed modeling of spiral wound membrane in a superstructure-based optimization framework to perform RO-based water treatment network synthesis. A two-stage stochastic programming formulation is adopted to incorporate the uncertainty associated with membrane performance.

1.3 Water management in shale gas production

A dramatic change in the energy industry in the United States within the past decade is due to the emergence of large-scale shale gas production. With the advancement in directional drilling and hydraulic fracturing, shale gas is predicted to provide 46% of the United States natural gas supply by 2035⁴³. The number of wells drilled in Pennsylvania

alone has increased from 112 prior to 2008 to a total of 7281 by the end of 2013⁴⁴. One of the advantages of shale gas wells is that multiple wells can be drilled from a single wellpad, and this configuration limits environmental footprint and impact on the surface in comparison to having individual vertical wells with one well per pad.

This development has tremendous impact on promoting efficient water management strategies. Unlike the process industries where water cost is low, water use makes up approximately 10% of the overall shale gas drilling and completion costs. In addition, whereas process plants are generally built along freshwater sources, shale plays such as the Eagle Ford and Barnett shale are not necessarily located in water-rich regions. Even though the Marcellus Shale Play overlies a water-rich region, water availability is not guaranteed year-round. Another important difference from the process industry is that a large volume of water is required in a short-period of time during stimulation. On average, about 19,000-26,000 m³ of water is used to complete each well. Since each wellpad allows multiple wells to be drilled, and each wellpad could contain tens of wellpads, billions of gallons of water must be sourced in a well field development area. Approximately 5000 trucks are required to haul water for the wellpad. Despite the large requirement for water, the water use per unit energy generated is lower compared to other conventional and unconventional energy sources as shown in Figure 1.2⁴⁵. Furthermore, if shale gas is used to generate electricity in a combined-cycle power plant, the quantity of water consumed per unit of energy generated could be 80% less than that required by a conventional pulverized coal power plant.

Development of a wellpad involves site preparation, drilling, completion, and production as can be seen on the timeline shown in Figure 1.3, and water use is associated with each step of the drilling and production process. As indicated in the figure, water is first acquired over several months for a given well where it is used for stimulation. Over the next few weeks water from the well returns as flowback water and then as produced water over the lifetime of the well. Specifically, 90% of water used in shale gas production is for hydraulic fracturing, while the remaining is necessary during the drilling process. Each well is injected under high-pressure using a fluid consisting of water, sand, and chemicals to fracture the gas-holding subsurface rock formation. The horizontal portion of the well

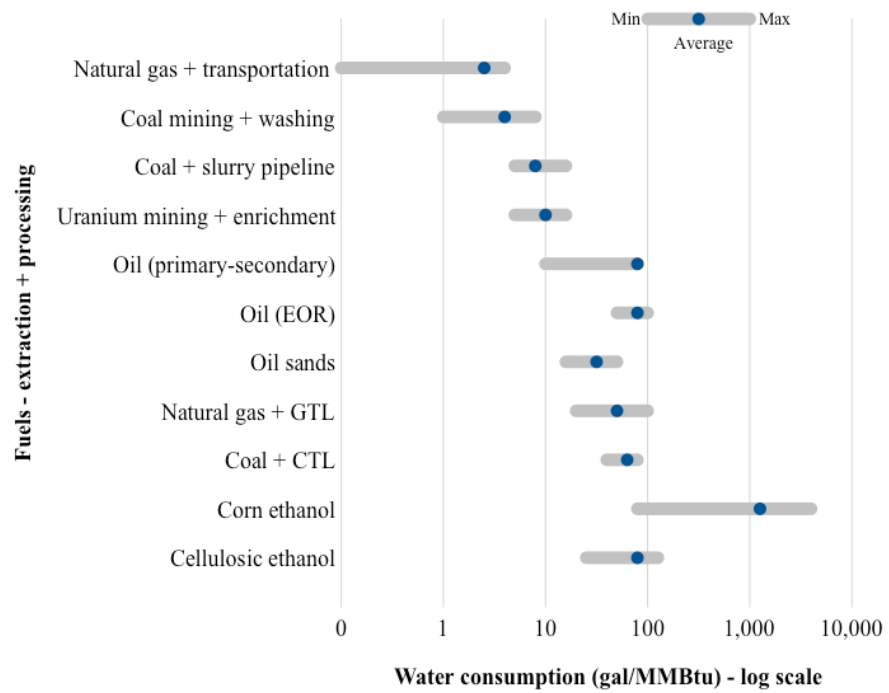


Figure 1.2: Water consumption per unit of energy generation comparison.

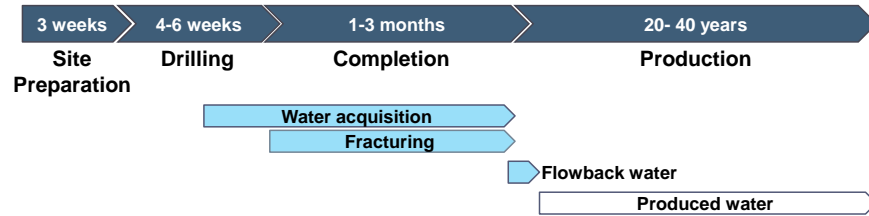


Figure 1.3: Wellpad development timeline.

is fractured, or stimulated, in a number of stages as shown in Figure 1.4. Each stage requires a fixed volume of water, which is acquired from freshwater sources and stored in freshwater impoundments. Then sand (8.96%) and chemical additives (0.44%) are added to the water to form the frac fluid⁴⁶. Stage 1, which is located near the end of the well, is stimulated first, then the stage is temporarily plugged to prevent flowback from stage 1. This is followed by stage 2, and the process is repeated along the full length of the horizontal portion of the well until the last stage is completed.

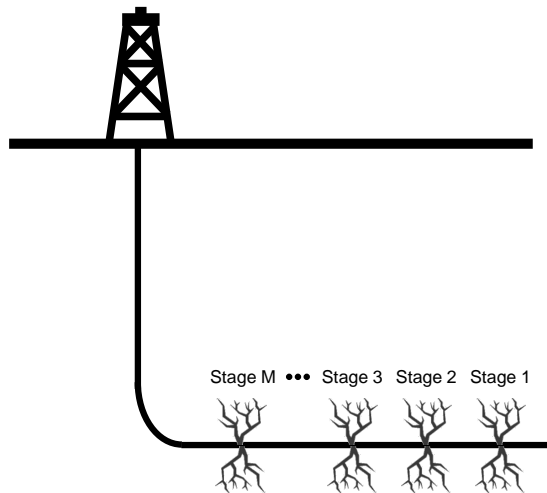


Figure 1.4: Horizontal well hydraulic fracturing stages.

Once all the stages are completed, the well plugs are drilled through and gas production begins. There is an initial period when water returns to the surface, which is referred to as flowback. This is followed by the well's production period of 20 to 40 years, during which

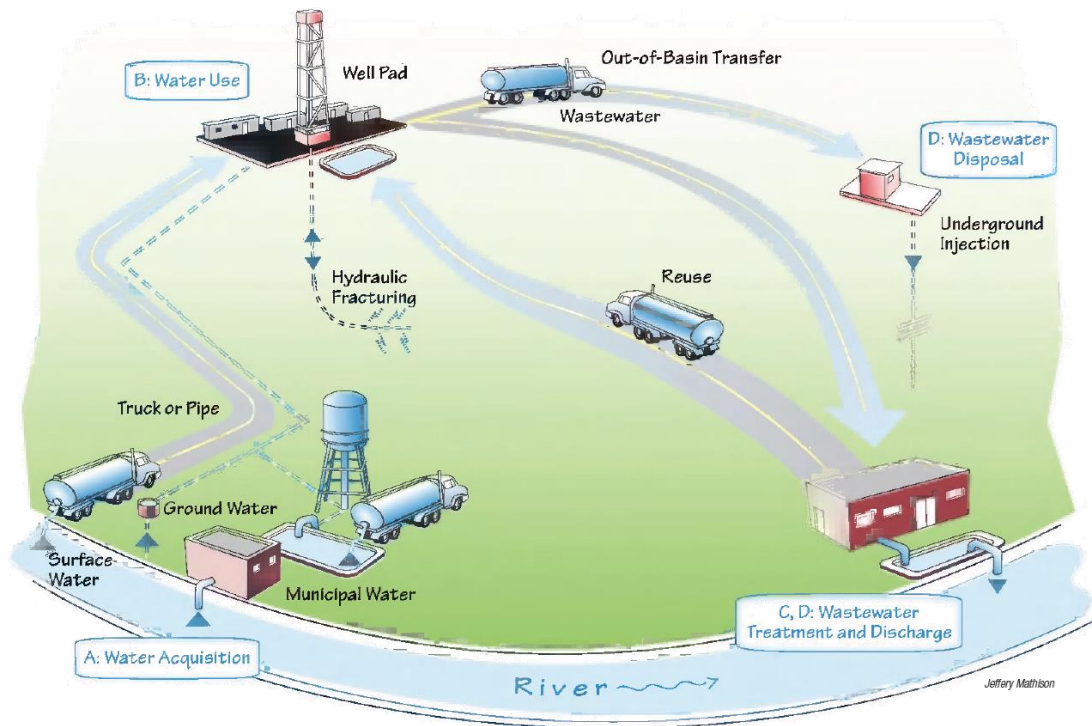


Figure 1.5: Overall picture of water use in shale gas⁴.

time there is a small amount of produced water that returns to the surface along with the gas produced. By regulations, wastewater cannot be stored in freshwater impoundments, but rather the stream is stored in frac tanks or specially constructed impoundments since flowback and produced water contain various contaminants. The stream can be treated in order to partially remove the impurities for recycling and reuse it at the next well. The cycle of water use in shale gas development is shown in Figure 1.5). A wastewater production forecast for the Marcellus play suggests that Pennsylvania wells will generate over 15 million m^3 per year by 2025⁴⁷.

The need for water treatment has increased significantly due to several factors. First, the performance of frac fluid has improved and become more tolerant of contaminants in the water, thereby encouraging more wastewater reuse. The disposal option of injecting wastewater in deep wells is not necessarily available in the Marcellus, since the geology of Pennsylvania is not conducive to injection wells. As a result, operators in the Marcellus

have to truck wastewater to Ohio for disposal, which drives up the cost. The Utica wells have more access to disposal wells. However, the regulatory constraints could potentially become more stringent due to its association with geological activities in the region. In addition, as the number of producing wells grows at each shale play, the total volume of produced water will quickly become substantial despite the low individual flowrate from each well.

One major limitation in wastewater handling is the high salt concentration. Among the alternative technologies, multistage flash distillation (MSF) and reverse osmosis are the most prevalent desalination processes⁴⁸. Although the cost of desalination processes have become more competitive over the past decades as a result of technological advances, it is not yet widely used in shale gas applications. These restrictions in shale play development pose considerable logistic challenges that demand sophisticated management and logistical strategies. Since shale gas production has been a relatively recent development, there are very few publications related to its water management issues.

1.4 Mathematical programming

Since in this thesis we apply mathematical programming techniques, we briefly describe the model types and solvers that are used to optimize the problems. The general formulation can be described as follows:

$$\begin{aligned} \min. \quad & z = f(x, y) \\ \text{s.t.} \quad & h(x, y) = 0 \\ & g(x, y) \leq 0 \\ & x \in X \\ & y \in \{0, 1\} \end{aligned} \tag{1.1}$$

where the objective function z is minimized subject to equality constraints h and inequality constraints g , x are continuous variables and y are binary variables.

In this work, the objective is typically to minimize cost and flow or maximize revenue.

The equality constraints represent physical operation model or mass balances in the problem, whereas the inequality constraints represent bounds and limitations. The continuous variables are used to represent flow, temperature, concentration which could take on a range of values, whereas the binary variables describe discrete decisions such as selecting equipment or performing a task in a given time intervals.

The formulation reduces to a linear programming (LP) formulation when the objective function and the constraints are linear and all variables are continuous. If the objective or any of the constraints is nonlinear, the formulation is categorized as nonlinear programming (NLP). Finally, mixed-integer linear programming (MILP) or MINLP formulations arise when the binary variables are present.

MILP problems are typically solved with branch and bound algorithms⁴⁹. Both LP and MILP formulations can be solved efficiently with solvers such as CPLEX and GUROBI. NLPs are typically solved through Newton's method, which makes them sensitive to initialization⁵⁰. CONOPT⁵¹, IPOPT⁵², SNOPT, and KNITRO are examples of the solvers used to solve NLP problems in this thesis. For nonconvex NLPs, global optimization solvers such as BARON⁵³, ANTIGONE, SCIP, are required to guarantee global optimality. For the MINLP model, decomposition algorithms are usually adapted where each iteration alternates between a MILP master problem and NLP subproblems for convergence. These algorithms include SBB, Generalized Benders Decomposition⁵⁴, Outer Approximation⁵⁵, and Extended Cutting Plane⁵⁶. DICOPT is used to solve convex MINLP problems, while BARON⁵³ is used to solve the nonconvex MINLP problems to global optimality in this work.

1.5 Thesis outline

This thesis deals with water use for both process industries (chapters 2 and 3) and unconventional natural gas industry (chapters 3 and 4).

1.5.1 Chapter 2 - Water targeting model

In chapter 2, we develop a targeting model for multi-contaminant WN with only water-using process units based on the superstructure proposed by Karuppiah and Grossmann¹⁶ and its extension by Ahmetović and Grossmann²⁸. The proposed LP formulation predicts the freshwater consumption target for the set of water-using process units, which can be easily incorporated in a simultaneous flowsheet, heat-exchange network, and water network optimization strategy. Since the proposed model is linear, significant computational savings can be achieved in comparison to nonlinear models, which are the typical formulations for multi-contaminant WNs. The simultaneous approach that allows for energy and water integration for the optimization of process flowsheets is presented and applied to two process design problems (methanol synthesis and bioethanol production).

In addition, we extend the model to address non-isothermal WN synthesis. So far, the reported works use NLP/MINLP formulations for HEN and WN synthesis to determine the optimal structure of a heat-integrated WN. Specifically, each inlet and outlet stream to the water-using process unit is also a stream in the HEN with its starting and ending temperatures. The LP targeting formulation can then complement the heat targeting formulation²⁷ to determine the minimum heating, cooling, as well as freshwater consumptions in heat-integrated WNs. This is discussed in detail and is illustrated with examples.

1.5.2 Chapter 3 - Nonlinear models for water regeneration

Chapter 3 focuses on the modeling of nonlinear wastewater treatment options with shortcut models in order to address the synthesis of integrated water networks. For a standard multi-contaminant WN superstructure with both water-using process units and wastewater treatment units, we make the following improvements. First, unit-specific shortcut models are developed in place of the fixed contaminant removal model to describe contaminant mass transfer in wastewater treatment units. Shortcut wastewater treatment cost functions are also incorporated into the model. By using shortcut models instead of simplified models for treatment units in the synthesis of WNs, we are able to gain a more accurate and

realistic water network designs. In addition, uncertainty in mass load of contaminants is considered to account for the range of operating conditions that can be achieved in process units as described by Karuppiah and Grossmann³⁵. This model then ensures that the final design solution is feasible and optimal over the set of all scenarios. This representation can effectively capture the wide range of operating conditions without overly complicating the formulation. Furthermore, the superstructure is modified to accommodate multiple treatment technologies for the removal of each contaminant to reflect realistic potential structures.

Since the resulting formulation is a nonconvex MINLP problem, it is computationally difficult to solve to global optimality. In order to solve the problem efficiently, we take advantage of the multiscenario representation and present a modified Lagrangean-based decomposition algorithm.

1.5.3 Chapter 4 - Operational model for shale gas water management

Since shale gas production has experienced rapid expansion relatively recently, there has been virtually no prior work that uses rigorous mathematical optimization approach to handle water management issues for shale plays. In chapter 4, we optimize water use life cycle for wellpads through a discrete-time two-stage stochastic MILP model under uncertain availability of water. The objective is to minimize expected transportation, treatment, storage, and disposal cost while accounting for the revenue from gas production. Assuming freshwater sources, river withdrawal data, location of wellpads and treatment facilities as given, the goal is to determine an optimal fracturing schedule in coordination with water transportation, and its treatment and reuse. The proposed models consider a long time horizon and multiple scenarios from historical data. The scheduling problem is formulated through a discrete-time model using as a basis the state-task network (STN) representation for batch scheduling⁵⁷. As will be demonstrated in the chapter, the formulation is efficient in handling the large number of binary variables in the formulation.

1.5.4 Chapter 5 - Investment model for shale gas water management

Chapter 5 builds upon the representation in chapter 4 and emphasizes investment decisions in the process. In addition to optimizing the frac schedule, maximizing revenue, and minimizing the operating cost, the goal is also to minimize freshwater source setup cost, impoundment capital cost, piping setup costs, and annualized centralized wastewater treatment facility (CWT) capital cost. In order to avoid heavy road use and negative environmental impact from hauling freshwater using trucks, this problem determines the optimal freshwater sources and piping connections to acquire freshwater for the given set of wellpads. In addition, despite increasing demands, desalination plants are not yet widely available for treating produced water due to its relatively high cost. We investigate wastewater desalination removal options that cater to the flowback and produced water characteristics of the Shale play region. A case study from the Utica shale is presented to illustrate the model.

1.5.5 Chapter 6 - Conclusion

Finally, chapter 6 summarizes the main findings of the thesis and lists its novel contributions. We also discuss additional future work directions that are worth investigating. This thesis had led to the following journal articles:

1. Yang, L.; Grossmann, I.E. Water Targeting Models for Simultaneous Flowsheet Optimization. *Industrial & Engineering Chemistry Research*. **2013**. 52 (9), 3209-3224.
2. Yang, L.; Salcedo-Diaz, R.; Grossmann, I.E. Water Network Optimization with Wastewater Regeneration Models. *Industrial & Engineering Chemistry Research*. **Just Accepted Manuscript**.
3. Yang, L.; Manno, J.; Grossmann, I.E. Optimization Models for Shale Gas Water Management. *AIChE Journal*. **2014**. 60 (10), 34903501.
4. Yang, L.; Manno, J.; Mauter, M.; Dilmore, R.; Grossmann, I.E. Investment Optimization Model for Freshwater Acquisition and Wastewater Handling in Shale Gas

Production. **In preparation.**

Chapter 2

Water Targeting Model for Water-Using Process Units

2.1 Introduction

In this chapter, a novel LP targeting model is first developed for the WN with only water-using process units based on the superstructure proposed by Karuppiah and Grossmann¹⁶ and its extension by Ahmetović and Grossmann²⁸. As will be shown, the proposed LP formulation predicts the exact freshwater consumption target under a specific assumption, and otherwise it predicts a tight upper bound for a set of water-using process units with multi-contaminants. This is discussed in detail and is illustrated with examples. In addition, this chapter will extend the LP targeting formulation to nonisothermal water networks. The LP formulation is expanded to isothermal WN that includes both water-using process units and wastewater treatment units. Finally, the simultaneous approach that allows for energy and water integration for the optimization of process flowsheets is presented and applied to two process design problems (methanol synthesis and bioethanol production).

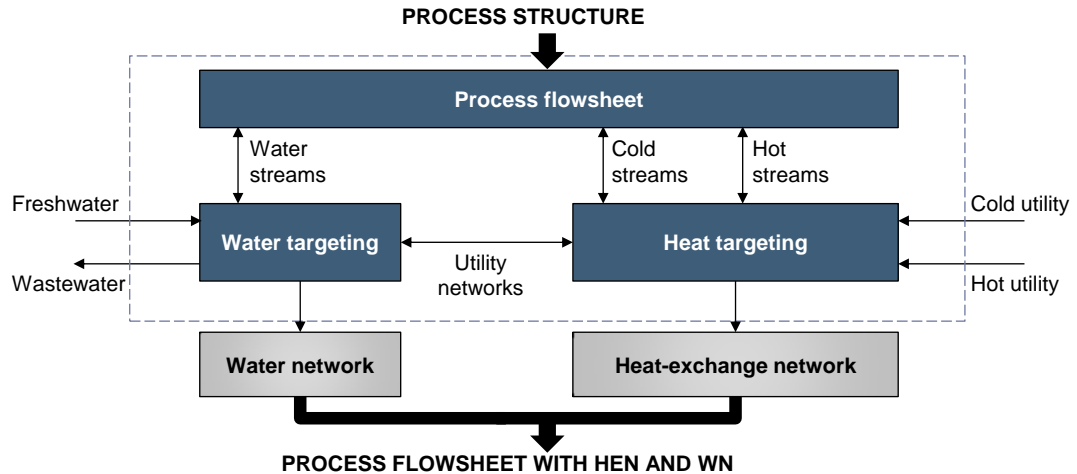


Figure 2.1: Simultaneous optimization framework.

2.2 Outline of proposed simultaneous optimization strategy

The proposed solution procedure for the simultaneous method involves two steps as seen in 2.1. The first step is to simultaneously optimize the economics of the flowsheet as well as the cost of HEN and WN targets subject to process constraints. The first step then fixes the operating conditions of the flowsheet. The second step is to determine the detailed HEN and WN structures and corresponding capital and utility costs using the fixed heat capacity flowrate, inlet and outlet temperatures, and water-using process unit flowrates. Note that the targets determined from step one are only used to estimate the heating and cooling costs, as well as the cost of the freshwater. The targets are not used in the synthesis of the network structures in the second step. This is done in order to allow readjustment of utility and water consumption so as to establish the proper trade-offs with the capital costs of the HEN and WN which are ignored in step one.

The formulation of the simultaneous optimization problem in step one is as follows,

$$\begin{aligned}
 \min. \quad & \phi = F(x, u, v) + c_H Q_H + c_C Q_C + c_{fw} FW \\
 \text{s.t.} \quad & h(x, u, v) = 0 \\
 & g^P(x, u, v) \leq 0 \\
 & g^{HEN}(u, Q_H, Q_C) \leq 0 \\
 & g^{WN}(v, FW) \leq 0 \\
 & x \in X, \quad u \in U, \quad v \in V
 \end{aligned} \tag{2.1}$$

where $F(x, u, v)$ and $h(x, u, v)$ are equations for the objective function and constraints of the flowsheet in terms of the variables x, u, v , where the u variables are involved in heat integration constraints, the variables v in the water integration constraints, x are the variables to model the cost of the process, Q_H and Q_C are the heating and cooling loads, and FW is the freshwater consumption. The extension of (2.1) to multiple heating and cooling utilities is trivial but not presented here for the sake of simplicity in the presentation.

Assuming non-isothermal process streams, the set of heat integration constraints g^{HEN} in (2.1) are given by (2.2)²⁷.

$$\begin{aligned}
 Q_H \geq & \sum_{js \in CS} fc_{js} [\max\{0, t_{js}^{out} - (T^p - \Delta T_m)\} - \max\{0, t_{js}^{in} - (T^p - \Delta T_m)\}] \\
 & - \sum_{is \in HS} FC_{is} [\max\{0, T_{is}^{in} - T^p\} - \max\{0, T_{is}^{out} - T^p\}]
 \end{aligned} \tag{2.2a}$$

$$\begin{aligned}
 Q_C = & Q_H + \sum_{is \in HS} FC_{is} (T_{is}^{in} - T_{is}^{out}) - \sum_{js \in CS} fc_{js} (t_{js}^{out} - t_{js}^{in}) \\
 T^p = & T_{is}^{in} \quad \forall p = is \in HS \\
 T^p = & (t_{js}^{in} + \Delta T_m) \quad \forall p = js \in CS
 \end{aligned} \tag{2.2b}$$

where Q_H, Q_C are the heating and cooling loads, FC_{is} and fc_{js} are the heat capacity flowrates of the hot and cold streams, $is \in HS, js \in CS, T_{is}^{in}, T_{js}^{in}$ are the inlet temperatures, $T_{is}^{out}, T_{js}^{out}$ are the outlet temperatures of the hot and cold streams, and T^p is the pinch temperature, and ΔT_m is the HRAT.

The constraints in (2.2) are linear when temperature and heat capacity flowrates are fixed, and as a result, the max operators are calculated a priori. For the case where temperatures are variables such as is the case in step one of the simultaneous optimization in 2.1, the max functions become non-differentiable functions. To circumvent this problem, they are approximated with the smooth approximation by⁵⁸,

$$\max\{0, f(x)\} = \frac{\sqrt{f(x)^2 + \varepsilon^2}}{2} + \frac{f(x)}{2} \quad (2.3)$$

where ε is a small parameter (typically $\varepsilon \approx 0.001$).

In this paper the formulation for g^{WN} will be presented first for the case of only process units, and second for the case when treatment units are also included. In addition, the problem of non-isothermal water networks is addressed for the former case. Various aspects of the simultaneous optimization framework in 2.1 are illustrated through two relevant examples - a methanol synthesis process that reflects the advantage of the simultaneous approach through improvement in the economic objective function, and a second example in bioethanol production whose result indicates the computational advantage of the proposed formulation, even though its result reduces to the sequential approach result.

2.3 Water targeting for WN with process units only

For the case of WN with only a single contaminant, Bagajewicz and Savelski⁵⁹ proved that the contaminant concentration at the outlet of each water-using process unit reaches its upper bound in optimal solutions. The linear mathematical formulation that follows from this result is presented in¹⁹, and is shown in Appendix A. Most WN problems, however, involve multiple contaminants which will be addressed below.

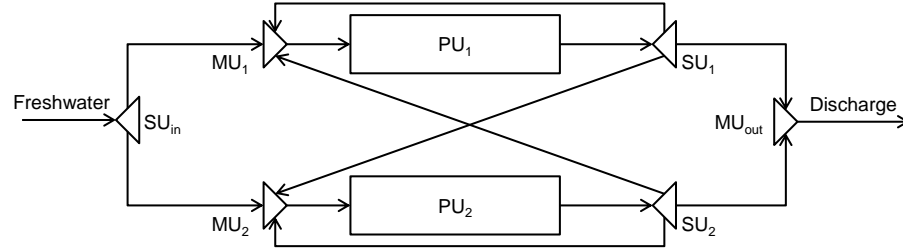


Figure 2.2: WN superstructure for water-using PUs.

2.3.1 NLP model for WN

We consider a typical WN problem with the information provided as follows. Given is a set of water-using process units PU (e.g. extraction, absorption) with water flowrates $P^p \quad \forall p \in PU$, maximum allowable inlet contaminant concentrations $C_j^{k,max} \quad \forall p \in PU, k \in p_{in}$, and maximum outlet allowable contaminant concentrations $C_j^{i,max} \quad \forall p \in PU, i \in p_{out}$ for those units. For simplicity, we assume that water is neither consumed nor produced in the water-using process units, i.e. $P_{in}^p = P_{out}^p = P^p \quad \forall p \in PU$. As seen in 2.2, each of the water-using process units is connected to other units through a mixer and a splitter, and local recycle is allowed for each unit as described in Ahmetović and Grossmann²⁸. We assume a given freshwater source without contaminants, although we can easily extend the formulation to accommodate a set of freshwater sources with different levels of contaminants. Also, the following assumptions are made: (a) the processes are isothermal, and (b) the loads of contaminants j in unit $p \in PU$, L_j^p , are known. The relevant formulation for minimizing freshwater consumption of the integrated water network superstructure is given by the formulation (NLP-1)¹⁶.

$$\begin{aligned}
 \text{min. } & FW \\
 \text{s.t. } & FW = \sum_{k \in SU_{in}} F^k \\
 & F^k = \sum_{i \in m_{in}} F^i \quad \forall m \in MU, k \in m_{out} \\
 & F^k C_j^k = \sum_{i \in m_{in}} F^i C_j^i \quad \forall j, \forall m \in MU, k \in m_{out} \\
 & F^k = \sum_{i \in s_{out}} F^i \quad \forall s \in SU, k \in s_{in} \\
 & C_j^i = C_j^k \quad \forall j, \forall s \in SU, i \in s_{out}, k \in s_{in} \\
 & P^p C_j^k + L_j^p = P^p C_j^i \quad \forall j, \forall p \in PU, k \in p_{in}, i \in p_{out} \\
 & F^{k,min} \leq F^k \leq F^{k,max} \quad \forall k \\
 & C_j^{k,min} \leq C_j^k \leq C_j^{k,max} \quad \forall j, \forall k
 \end{aligned} \tag{NLP-1}$$

where F^i and F^k are water flowrates, and C_j^i and C_j^k are concentration of contaminant j in stream i and k , respectively. The constraints consist of a set of contaminant mass balances in the mixer unit (MU), splitter units (SU), process units (PU), and treatment units (TU). The subscripts in , out , refer to the inlet and outlet streams of each of these units. Note that unlike water network design formulations, the aim here is to determine the minimum freshwater supply rate.

2.3.2 Lower bound: McCormick relaxation

The challenge with minimizing freshwater consumption in problem (NLP-1) is that there are bilinear terms (flowrate times concentration), which may lead to local optima or numerical singularities. The constraint that involves bilinear terms is the contaminant mass flowrate balance at the mixers,

$$F^k C_j^k = \sum_{i \in m_{in}} F^i C_j^i \quad \forall j, \forall m \in MU, k \in m_{out} \tag{2.4}$$

In order to circumvent the complexity of simultaneously optimizing the process flowsheet and the nonconvex NLP for the WN, we can determine a lower bound for the freshwa-

ter target by replacing (2.4) with the McCormick convex envelopes⁶⁰. The following LP model (LP-0) then predicts a lower bound for the minimum freshwater consumption required for the set of water-using process units.

$$\begin{aligned}
 \min. \quad & FW \\
 \text{s.t.} \quad & FW = \sum_{k \in SU_{in}} F^k \\
 & F^k = \sum_{i \in m_{in}} F^i \quad \forall m \in MU, k \in m_{out} \\
 & f_j^k = \sum_{i \in m_{in}} f_j^i \quad \forall j, \forall m \in MU, k \in m_{out} \\
 & F^k = \sum_{i \in s_{out}} F^i \quad \forall s \in SU, k \in s_{in} \\
 & C_j^i = C_j^k \quad \forall j, \forall s \in SU, i \in s_{out}, k \in s_{in} \\
 & f_j^k = \sum_{i \in s_{out}} f_j^i \quad \forall j, \forall s \in SU, k \in s_{in} \\
 & f_j^k = P^p C_j^k \quad \forall j, \forall p \in PU, k \in p_{in} \\
 & f_j^i = P^p C_j^i \quad \forall j, \forall p \in PU, i \in p_{out} \\
 & \left. \begin{aligned}
 f_j^i &\geq F^{i,min} C_j^i + C_j^{i,min} F^i - F^{i,min} C_j^{i,min} \\
 f_j^i &\geq F^{i,max} C_j^i + C_j^{i,max} F^i - F^{i,max} C_j^{i,max} \\
 f_j^i &\leq F^{i,min} C_j^i + C_j^{i,max} F^i - F^{i,min} C_j^{i,max} \\
 f_j^i &\leq F^{i,max} C_j^i + C_j^{i,min} F^i - F^{i,max} C_j^{i,min}
 \end{aligned} \right\} \forall j, \forall m \in MU, \forall i \in m_{in} \cup m_{out} \\
 & F^{k,min} \leq F^k \leq F^{k,max} \quad \forall k \\
 & C_j^{k,min} \leq C_j^k \leq C_j^{k,max} \quad \forall j, \forall k
 \end{aligned}
 \tag{LP-0}$$

2.3.3 A novel LP target model

Since the model (LP-0) may predict targets that are relatively weak lower bounds, we propose in this section a novel linear water targeting formulation that provides exact targets under some assumptions. Otherwise it predicts tight upper bounds.

Using as a basis the model (NLP-1) for WN, we apply the maximum driving force principle proposed by Wang and Smith¹¹ and necessary optimality conditions proven by Savelski and Bagajewicz⁶¹. Both indicate that at least one contaminant reaches its upper bound at the inlet of a process unit, that is,

$$C_j^k = C_j^{k,max} \quad \text{for some } j, \forall p \in PU, k \in p_{in} \quad (2.5)$$

Next, we can determine the direction of relaxation for the nonlinear constraint (2.4) by applying the Karush–Kuhn–Tucker (KKT). The following dual multipliers are assigned to each of the constraints containing $C_j^k \quad \forall p \in PU, k \in p_{in}$.

$$(\lambda_j^k) \quad F^k C_j^k = \sum_{i \in m_{in}} F^i C_j^i \quad \forall j, \forall m \in MU, k \in m_{out} \quad (2.6a)$$

$$(\nu_j^k) \quad P^p C_j^k + L_j^p = P^p C_j^i \quad \forall j, \forall p \in PU, \forall k \in p_{in}, i \in p_{out} \quad (2.6b)$$

$$(\mu_j^k) \quad C_j^k \leq C_j^{k,max} \quad \forall j, \forall k \in s_{out} \cup m_{out} \quad (2.6c)$$

Since (2.6c) is an inequality, the multipliers μ_j^k are non-negative. Constraint (2.6b) can easily be shown to relax as a \leq inequality, and therefore ν_j^k are also non-negative. The multipliers λ_j^k in (2.6a) are in principle unrestricted in sign but analysis of the KKT conditions reveals their sign. The stationary condition of the Lagrange function with respect to C_j^k is as follows,

$$\frac{\partial \mathcal{L}}{\partial C_j^k} = \lambda_j^k F^k + \mu_j^k + \nu_j^k P^p = 0 \quad (2.7)$$

We can see that in order to satisfy dual feasibility, since $\nu_j^k \geq 0$ and $\mu_j^k \geq 0$, $P^p > 0$, this implies that $\lambda_j^k \leq 0$. Therefore, (2.6a) relaxes as follows,

$$F^k C_j^k \geq \sum_{i \in m_{in}} F^i C_j^i \quad \forall j, \forall m \in MU, k \in m_{out} \quad (2.8)$$

If we make the assumption that when one contaminant j reaches its concentration upper bounds at a given unit $m \in MU$, it also reaches the upper bound at all other process units from which reuse streams have non-zero flowrate, we obtain the following linear

inequality,

$$F^k C_j^{k,max} \geq \sum_{i \in m_{in}} F^i C_j^{i,max} \quad \forall j, \forall m \in MU, k \in m_{out} \quad (2.9)$$

From (2.4), the active inequality is active for contaminant j . Therefore, we can replace the bilinear constraint (2.4) in model (NLP-1) to arrive at the following LP formulation (LP-1).

$$\begin{aligned} \min. \quad & FW \\ \text{s.t.} \quad & FW = \sum_{k \in SU_{in}} F^k \\ & F^k = \sum_{i \in m_{in}} F^i \quad \forall m \in MU, k \in m_{out} \\ & F^k C_j^{k,max} \geq \sum_{i \in m_{in}} F^i C_j^{i,max} \quad \forall j, \forall m \in MU, k \in m_{out} \\ & F^k = \sum_{i \in s_{out}} F^i \quad \forall s \in SU, k \in s_{in} \\ & C_j^i = C_j^k \quad \forall j, \forall s \in SU, \forall i \in s_{out}, k \in s_{in} \\ & P^p C_j^k + L_j^p = P^p C_j^i \quad \forall j, \forall p \in PU, \forall k \in p_{in}, i \in p_{out} \\ & F^{k,min} \leq F^k \leq F^{k,max} \quad \forall k \\ & C_j^{k,min} \leq C_j^k \leq C_j^{k,max} \quad \forall j, \forall k \end{aligned} \quad (LP-1)$$

The following proposition holds for (LP-1):

Proposition *The minimum freshwater consumption predicted by the LP model in (LP-1) is the same as the global minimum predicted by the NLP model (NLP-1) under the condition that at least one contaminant reaches its concentration upper bounds as well as at all other process units from which reuse streams have non-zero flowrate.*

The proof trivially follows from the derivation. The LP formulation (LP-1) can then be used to determine the freshwater flowrate target for a given set of water-using processes. The assumption in the above proposition is a sufficient condition for the proposition to hold. In the case where the assumption is not satisfied, the LP will yield an upper bound for the freshwater target. This follows from the fact that the inequality in (2.9) is a restriction of the inequality in (2.8). The upper bound from (LP-1) is nonetheless useful in the first

Table 2.1: Additional problems using LP targeting formulation.

Problem	$ PU $	$ j $	NLP-1	LP-0	LP-1
1	2	2	40	40	40
2	5	3	40	40	40
3	3	3	105.6	105.6	105.6
4	3	3	101	98.64	101
5	5	3	84.28	84.28	84.28
6	3	3	82.85	82.85	82.85
7	3	3	101.35	82.86	101.81
8	3	3	78.18	78.18	79.22
9	5	3	84.29	84.29	84.29
10	5	3	232.1	225.1	233.2

stage of the simultaneous optimization scheme in 2.1, since the overestimation is small as will be shown with the numerical results. It should also be noted that the quality of this upper bound can be evaluated by the lower bound predicted from (LP-0). In the event of a large gap between the two bounds, we could partition the feasible region through the use of piecewise McCormick relaxation to decrease the size of the gap¹⁶.

Numerical results

The results from the LP targeting formulation (LP-1) are compared against the results from NLP formulation (NLP-1) and from the lower bound McCormick (LP-0) in the ten examples shown in 2.1, which have been reported in previous work^{16,11,12}. As can be seen, (LP-1) provides exact targets for 7 problems (1-6,9), whereas the formulation predicts tight upper bounds (within 0.5-1.5%) for the NLP in the 3 other problems. Note that the model (LP-0) yields valid lower bounds that are also exact in 7 problems(1,2,3,5,6,8,9). However, in problems 4,7, and 10 the results predict- lower bounds for the NLP with 2.3, 18.2, and 3.0% gaps, respectively. Although the results indicate that model (LP-0) could also be used as a reasonable target, model (LP-1) generally predicts more accurate targets.

Table 2.2: Example 1 from Wang and Smith.

PU, p	P^p (ton/h)	j	L_j^p (kg/h)	$C_j^{pin,max}$ (ppm)	$C_j^{pout,max}$ (ppm)
Distillation	45	Hydrocarbon	0.675	0	15
		H ₂ S	18	0	400
		Salt	1.575	0	35
HDS	34	Hydrocarbon	3.4	20	120
		H ₂ S	414.8	300	12500
		Salt	4.59	45	180
Desalter	56	Hydrocarbon	5.6	120	220
		H ₂ S	1.4	20	45
		Salt	520.8	200	9500

Table 2.3: Closeup on Mixer Unit 3.

	from SUin		from SU1		from SU3		to Desalter		
	C_j	F	C_j	F	C_j	F	Avg C_j^k	C_j^{max}	F
HC	0		15		100		3	120	
H ₂ S*	0	52.1	400	2.7	25	1.2	20	20	56
Salt*	0		35		9500		200	200	

Example 1

We illustrate the application of the LP model in (LP-1) with a multi-contaminants example taken from Wang and Smith¹¹ with data given in 2.2. This problem, which corresponds to the third entry in 2.1, has 3 PUs and 3 contaminants. The configuration with no recycle and reuse requires 135 ton/hr of freshwater.

The NLP network model in (NLP-1) involves 90 variable and 81 constraints, and was globally optimized with BARON 9.3, requiring 0.09s. The solution yields a network requiring 105.6 ton/hr of freshwater that is to be supplied to the set of process units as shown in 2.3. The LP targeting formulation in (LP-1), which has the same problem size as (NLP-1), is solved with CPLEX 12 requiring 0.06s and yields the same amount of freshwater as one of the NLP formulation, 105.6 ton/hr. An examination of the result from the targeting formulation shows that indeed, each mixer placed prior to process unit has at least one

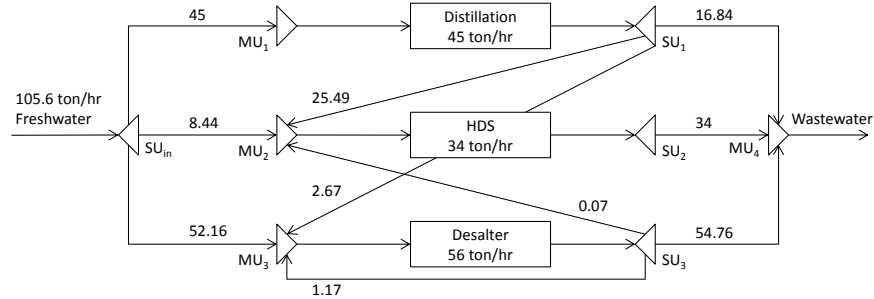


Figure 2.3: Network with minimum freshwater consumption.

contaminant reaching its maximum concentration. 2.3 shows a close-up on Mixer Unit 3 for the desalter, note that both H_2S and salt are at their limiting concentrations (indicated with asterisks), while the average concentration of HC at the inlet of the mixer is below the limit at the outlet of the mixer.

2.3.4 Non-isothermal water network targeting

In the previous section, we have assumed that the water network is isothermal. However, this may not be the case since the process units may operate at different temperatures. This means that different temperature values may be assigned to the streams in the superstructure of 2.2, giving rise to the possibility of heat recovery among the streams within the water network. Consequently, simultaneous optimization of heat integration within a water network should also be considered. Studies in this area are rather limited, with the more recent developments including works by Bogataj and Bagajewicz⁶², Dong et al⁶³, Savulescu and Smith⁶¹, Leewongtanawit and Kim⁶⁴, and Kim et al⁶⁵. Previous works have dealt with approaches for simultaneous integration where HEN and WN superstructures are combined into a single MINLP formulation. If the purpose is to perform the simultaneous optimization of a flowsheet with the HEN and nonisothermal WN, we can predict the utility and freshwater targets, circumventing in this way the MINLP formulation of the nonisothermal WN by using the water and heat targeting formulations given by (NLP-1) and (2.2). In this case, the streams that participate in heat integration are the ones

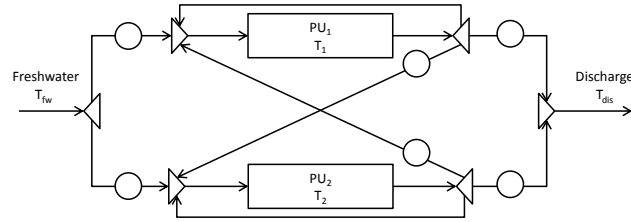


Figure 2.4: Nonisothermal WN.

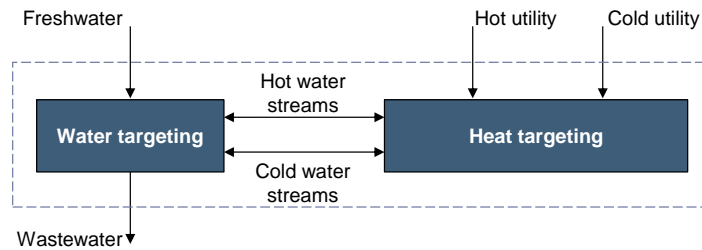


Figure 2.5: Non-isothermal WN targeting diagram.

that connect splitters and mixers. The placement for potential heaters and coolers for a two PU non-isothermal WN structure is shown in 2.4. As indicated in the figure, based on the supply and target temperatures, we specify each stream in the nonisothermal WN as either a hot stream or cold stream with constant heat capacity in heat integration. By considering the integration of targeting models as shown in 2.5, the resulting LP formulation (LP-2) consists of the objective function in (2.1), the heat targeting formulation (2.2) developed by Duran and Grossmann²⁷ as well as the LP water targeting formulation (LP-1).

$$\begin{aligned}
 \text{min.} \quad & \phi = c_H Q_H + c_C Q_C + c_{fw} FW \\
 \text{s.t.} \quad & Q_H \geq \sum_{js \in CS} f c_{js} [\max\{0, t_{js}^{out} - (T^p - \delta T_m)\} - \max\{0, t_{js}^{in} - (T^p - \delta T_m)\}] \\
 & \quad - \sum_{is \in HS} FC_{is} [\max\{0, T_{is}^{in} - T^p - \max\{0, T_{is}^{out} - T^p\}] \\
 & Q_C = Q_H + \sum_{is \in HS} FC_{is} (T_{is}^{in} - T_{is}^{out}) - \sum_{js \in CS} f c_{js} (t_{js}^{out} - T_{js}^{in}) \\
 & T^p = T_i^{in} \quad \forall p = i \in HS \\
 & T^p = (t_j^{in} + \Delta T_m) \quad \forall p = j \in CS \\
 & FW = F^k \quad k \in SU_{in} \\
 & F^k = \sum_{i \in m_{in}} F^i \quad \forall m \in MU, k \in m_{out} \\
 & F^k C_j^{k,max} \geq \sum_{i \in m_{in}} F^i C_j^{i,max} \quad \forall j, \forall m \in MU, k \in m_{out} \\
 & F^k = \sum_{i \in s_{out}} F^i \quad \forall s \in SU, k \in s_{in} \\
 & C_j^i = C_j^k \quad \forall j, \forall s \in SU, \forall i \in s_{out}, k \in s_{in} \\
 & P^p C_j^i + L_j^p = P^p C_j^k \quad \forall j, \forall p \in PU, \forall i \in p_{in}, k \in p_{out}
 \end{aligned}
 \tag{LP-2}$$

Example 2

An example from Bogataj and Bagajewicz⁶², proposed originally by Savulescu and Smith⁶⁶, is presented to illustrate the application of (LP-2). The superstructure is shown in 2.6. In this example, there are 4 water-using process units operating at the indicated temperatures. The system involves a single contaminant, with the data given in 2.4 and 2.5.

The original objective of this example is to minimize the annualized water network and heat-exchange network cost. 2.7 shows the optimal network structure obtained by Bogataj and Bagajewicz. The minimum heating utility is 3767 kW, there is no cooling utility required, and freshwater is supplied at a rate of 324 ton/hour. Employing the LP targeting

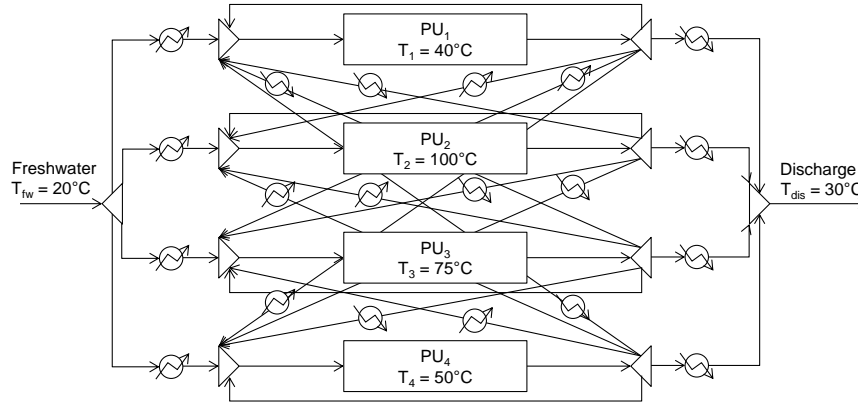


Figure 2.6: Example 2 superstructure.

Table 2.4: Data for heat-integrated WN example.

Parameter			
$C_{HU} (\$/ (kW a))$	260	$T_{HU}^{IN} (^\circ C)$	126
$C_{CU} (\$/ (kW a))$	150	$T_{HU}^{OUT} (^\circ C)$	126
$C_{FW} (\$/ t)$	2.5	$T_{CU}^{IN} (^\circ C)$	15
HRAT ($^\circ C$)	10	$T_{CU}^{OUT} (^\circ C)$	20

model (LP-2) to minimize the utility and freshwater costs for non-isothermal WN leads to the same solution as the MINLP optimization for the heating and cooling utility and freshwater consumption (3767 kW, 0 kW and 324 ton/hr). The reported problem size of the MINLP for HEN and WN superstructures in Bogataj and Bagajewicz⁶² has 749 continuous variables and 115 binary variables, the number of constraints was unspecified. This problem took 2.64 s on a 3.2 GHz PC machine with 1 GB RAM using DICOPT with

Table 2.5: Heat-integrated network example from Bogataj and Bagajewicz.

PU, p	$L^p (kg/h)$	$C_j^{p_{in}, max}$ (ppm)	$C_j^{p_{out}, max}$ (ppm)	$T_p (^\circ C)$
P1	7.2	0	100	40
P2	18.0	50	100	100
P3	108.0	50	800	75
P4	14.4	400	800	50

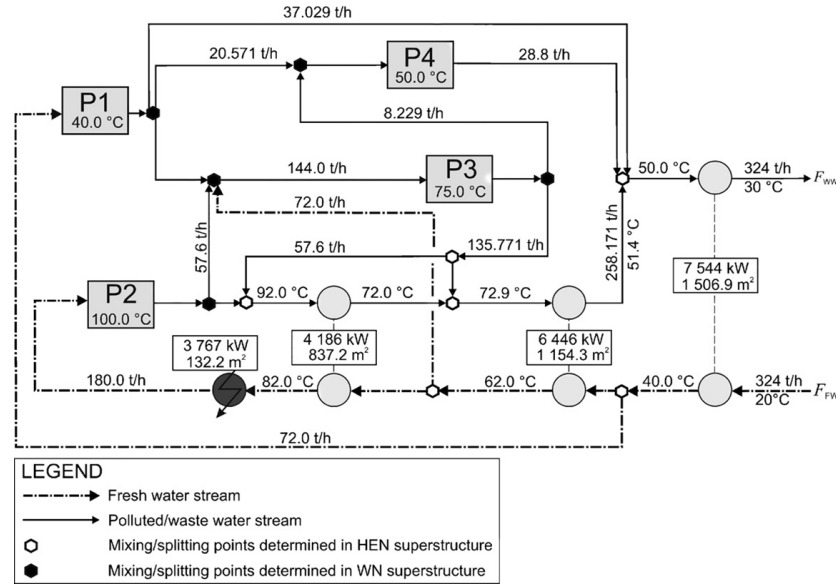


Figure 2.7: Heat-integrated water network obtained by Bogataj.

CPLEX as the MIP solver and SNOPT as the NLP solver. In comparison, the targeting formulation (LP-2) reduces to 206 continuous variables and 229 constraints, requiring 0.104 s to solve on a Intel 2.4 GHz PC machine with 4 GB memory. We should note that with DICOPT there is no guarantee of global optimality. Had the authors used BARON, the CPU time required would have been much higher.

Example 3

An industrial case study from⁶⁴ is also used to illustrate the heat-integrated water network targeting model(LP-2). The network is the largest we have considered so far and consists of 10 water-using operation units, 2 freshwater sources, and 4 contaminants (data is presented in 2.6 and 2.7). The plant is assumed to operate 8600 h/year, all water streams are assumed to have heat capacity of 4.2 kJ/(kg °C), and the minimum approach temperature (ΔT_{min}) is 10 °C. The authors of⁶⁴ determined the HEN and WN structure with the objective of minimizing total annualized cost of heat-exchangers, piping, and utilities.

Table 2.6: Data for heat-integrated WN example 3.

PU, p	Contaminant j	$C_j^{p_{in},max}$ (ppm)	$C_j^{p_{out},max}$ (ppm)	PP (t/h)	T_p (°C)
P1	A	200	25000	24.87	70
	B	500	20000		
	C	100	28500		
	D	1500	230000		
P2	A	350	8000	40.98	60
	B	3000	9000		
	C	500	24080		
	D	400	3000		
P3	A	200	3500	39.2	90
	B	500	2500		
	C	100	1500		
	D	1500	1500		
P4	A	350	15000	4.0	80
	B	450	5000		
	C	150	700		
	D	500	1500		
P5	A	800	2000	3.92	70
	B	650	7000		
	C	450	9000		
	D	300	10000		
P6	A	3000	12000	137.5	100
	B	2000	10000		
	C	100	8000		
	D	0	200		
P7	A	450	2000	290.96	40
	B	0	3000		
	C	250	1000		
	D	650	12000		
P8	A	100	3450	23.81	80
	B	250	4000		
	C	200	700		
	D	550	7000		
P9	A	150	1000	65.44	50
	B	450	1000		
	C	3000	4000		
	D	100	100		
P10	A	0	100	4	60
	B	0	100		
	C	0	100		
	D	0	100		

Table 2.7: Water sources for heat-integrated WN example 3.

Water sources s	Contaminant j	C_j^s (ppm)	T_p (°C)	Cost (\$/ton)
WS1	A	0	20	0.5
	B	0		
	C	0		
	D	0		
WS2	A	10	30	0.1
	B	10		
	C	10		
	D	10		

We have used model(LP-2) described earlier in this section to minimize the utility consumption of this network. The results are shown in Table 2.8, where the solution taken from literature is compared against that of the LP targeting formulation. “McCormick” indicates the case where heat targeting formulation (2.2) is combined with the WN formulation (LP-0) using the McCormick constraints. “NLP-2” represents the combination of the heat targeting formulation (2.2) and the formulation (NLP-1) for WN with only process units. This NLP is guaranteed to predict exact targets. Finally, “LP-2” is the LP model presented in this section. As can be seen in the table, the result reported in⁶⁴ incurs the highest utility cost, since its original objective include both capital cost and utility cost. As described in the previous section, McCormick provides a lower bound for freshwater flowrate, and LP-2 predicts an upper bound for the minimum freshwater consumption. Even though the targeting model does not predict the interconnections of the units, it is able to predict each of the utility consumption to within 5% of the NLP solution. Specifically, water source 1 is predicted exactly, water source 2 is over-estimated by 7.2%, and the heating and cooling utilities are overestimated by 1.9% and 7.2% (due to the higher water target predicted). However, note that the total cost is only overestimated by 1%.

The authors in⁶⁴ used CPLEX as the MILP solver and CONOPT2 as the NLP solver in their special purpose algorithm. The problem requires 12 min with an AMD 1.24 GHz PC to solve using their solution procedure, and the problem size was not reported. In comparison, the LP targeting formulation took 0.203 s to solve on a Intel 2.4 GHz PC machine with 4 GB memory.

Table 2.8: Result comparison: heat-integrated WN example 3.

	Literature	McCormick	NLP-2	LP-2
Cost (1000 \$/yr)	2,931	2,797	2,878	2,908
Water flowrate source 1 (t/hr)	432.46	418.71	432.46	432.46
Water flowrate source 2 (t/hr)	178.86	157.07	158.35	169.74
Heating Utility (\$/yr)	7,132	6,717	6,893	7,026
Cooling Utility (\$/yr)	2,087	1,832	1,847	1,980

2.4 Extension for treatment units

2.4.1 Motivating example

Consider the model (LP-1) with the addition of one wastewater treatment unit in example 1. The treatment unit is assumed to remove 99.9% of contaminant B.

The simplest option to extend the LP model in (LP-1) is to consider the following equations,

$$\begin{aligned} F^k &= F^i \quad \forall t \in TU, \forall i \in t_{out}, k \in t_{in} \\ C_j^i &= \beta_j^t C_j^k \quad \forall j, \forall t \in TU, \forall i \in t_{out}, k \in t_{in} \end{aligned} \quad (2.10)$$

where β_j^t is the recovery of contaminant j in treatment unit t . Recall from section 2.3.3, the upper bounds for contaminant concentrations in stream $F^k, k \in p_{out}, p \in PU$ are given.

In this case, the LP targeting formulation consisting of equations (LP-1) and (2.10) provides the same result as the NLP network formulation, 55.47 ton/hr. However, it is not generally the case that the addition of wastewater treatment units still allows (LP-1) to provide the exact freshwater consumption as explained below. The reason is that treatment units are defined by percent removal of contaminants β_j^t , and consequently, the upper bounds for contaminant concentrations in stream $F^k, t \in TU, k \in t_{in}$ are not given. Since each treatment unit has multiple inlets (at the corresponding MU), we can only obtain an approximate upper bound for contaminant concentrations, $\max C_j^{i,max}, \forall s \in SU, i \in s_{out}$. Exact upper bounds of contaminant concentration are provided for process units, which

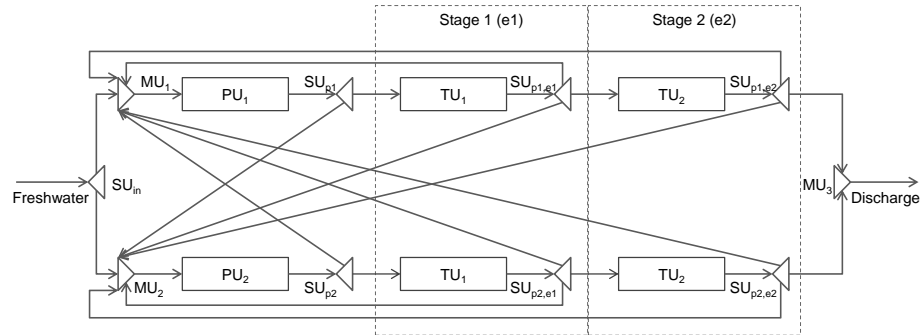


Figure 2.8: Stagewise superstructure for WN with wastewater treatment.

allow the simplifications in section 2.3.3. Since (LP-1) with the constraints in (2.10) cannot guarantee the exact target for water networks with treatment units, we next introduce a model that is based on a different network superstructure.

2.4.2 Addition of wastewater treatment unit

Yee and Grossmann⁹ presented a stage-wise structure for the case of heat integration. Compared to other superstructures reported, the advantage of the stage-wise superstructure is that the constraints can be kept in linear form by relying on the isothermal assumption for stream mixing. This quality of a stage-wise structure has motivated us to explore the modelling of multi-contaminant water networks with wastewater treatment units. In the method to be described below, we take advantage of the stage-wise structure to approximate the freshwater target for a WN.

In a targeting formulation, it is not essential to employ a realistic network structure since the purpose is not to determine the precise stream connectivities, but it is rather to predict a performance target. In this superstructure, as shown in 2.8, it is assumed that the outlet stream from each process unit is treated through all the treatment units in a predefined sequence, where the number of stages is equal to the number of treatment units available in the system. Specifically, there is no mixer place at the inlet of the treatment units

The stream connectivity involving any process unit remains unchanged from the network

superstructure approach, since the formulation is already linear as shown in section 2.3.3. On the other hand, the structure of the treatment units requires exploiting a special property in order to achieve linearity. It is observed that since the removal ratio, β_j^t , for each treatment unit is fixed, a tight upper bound for contaminant concentration at the outlet of the treatment unit can be calculated a priori. The complete formulation for this stage-wise structure is given by the following LP,

$$\begin{aligned}
 \min. \quad & FW \\
 \text{s.t.} \quad & FW = F^k \quad k \in SU_{in} \\
 & F^k = \sum_{i \in m_{in}} F^i \quad \forall m \in MU, k \in m_{out} \\
 & F^k C_j^{k,max} \geq \sum_{i \in m_{in}} F^i C_j^{i,max} \quad \forall j, \forall m \in MU, k \in m_{out} \\
 & F^k = \sum_{i \in s_{out}} F^i \quad \forall s \in SU_p, k \in s_{in} \\
 & C_j^i = C_j^k \quad \forall j, \forall s \in SU_p, \forall i \in s_{out}, k \in s_{in} \\
 & F^k = \sum_{i \in s_{out}} F^i \quad \forall s \in SU_{p,e}, k \in s_{in}, e \in ST \\
 & C_j^i = C_j^k \quad \forall j, \forall s \in SU_{p,e}, \forall i \in s_{out}, k \in s_{in}, e \in ST \\
 & P^p C_j^i + L_j^p = P^p C_j^k \quad \forall j, \forall p \in PU, \forall i \in p_{in}, k \in p_{out} \\
 & F^k = F^i \quad \forall t \in TU_{p,e}, \forall e \in t_{out}, k \in t_{in} \\
 & C_j^i = \beta_j^t C_j^k \quad \forall j, \forall t \in TU_{p,e}, \forall i \in t_{out}, k \in t_{in}, e \in ST \\
 & C_j^i \leq \beta_j^t C_j^{k,max} \quad \forall j, \forall t \in TU_{p,e}, \forall s \in SU_{p,e}, i \in s_{out}, k \in s_{in}, e \in ST \\
 & C_j^k \leq C_j^{k,max} \quad \forall j, \forall s \in SU_p, k \in s_{in}, e \in ST \\
 & F^{k,min} \leq F^k \leq F^{k,max} \quad \forall k \\
 & C_j^{k,min} \leq C_j^k \leq C_j^{k,max} \quad \forall j, \forall k
 \end{aligned} \tag{LP-3}$$

where SU_p is the set of splitters at the outlet of the process units p , $SU_{p,e}$ is the set of splitters at the outlet of the treatment unit $t \in TU$ following each process unit $p \in PU$ at stage $e \in ST$, $|TU| = |ST|$.

It should be noted that (LP-3) will not necessarily predict upper bounds because the stage-

Table 2.9: Data for stagewise structure.

	Problem 1		Problem 2		Problem 3		Problem 4		Problem 5		Problem 6		Problem 7		Problem 8		Problem 9		Problem 10	
PPD (ton/s)	40	80	45	45.8	45.8	45.8	45.8	45.8	45.8	45.8	45.8	45.8	45.8	45.8	45.8	45.8	45.8	45.8	45.8	45.8
PU1	50	70	34	32.7	32.7	32.7	32.7	32.7	32.7	32.7	32.7	32.7	32.7	32.7	32.7	32.7	32.7	32.7	32.7	32.7
PU2			56	56.5	56.5	56.5	56.5	56.5	56.5	56.5	56.5	56.5	56.5	56.5	56.5	56.5	56.5	56.5	56.5	56.5
PU3				32.7	32.7	32.7	32.7	32.7	32.7	32.7	32.7	32.7	32.7	32.7	32.7	32.7	32.7	32.7	32.7	32.7
PU4																				
PU5																				
$C_{j,issue}^{max}$ (ppm)	A	B	A	B	C	A	B	C	A	B	C	A	B	C	A	B	C	A	B	C
PU1	0	0	1	1	5	1	1	20	1	1	20	0	0	0	1	1	1	50	50	50
PU2	50	80	20	300	45	50	20	500	50	20	500	50	1	500	500	20	50	50	50	500
PU3			120	20	200	20	120	200	20	120	200	20	120	200	20	120	200	20	120	200
PU4																				
PU5																				
L_j (kg/s)	A	B	A	B	C	A	B	C	A	B	C	A	B	C	A	B	C	A	B	C
PU1	1	1.5	8	4	0.675	18	1.575	17.9	0.5	1.2	17.9	0.5	1.2	17.9	0.5	1.2	17.9	0.5	1.2	17.9
PU2	1	1	11.2	4.2	3.4	414.8	4.59	536	3.3	0.5	536	3.3	0.5	536	3.3	0.5	536	3.3	0.5	536
PU3			5.6	1.4	520.8	20	1.3	5.7	20	1.3	5.7	20	1.3	5.7	20	1.3	5.7	20	1.3	5.7
PU4																				
PU5																				
β_j	A	B	A	B	C	A	B	C	A	B	C	A	B	C	A	B	C	A	B	C
TU1	0.05	1	0.1	0.2	1	0.001	1	0.001	1	1	0.1	1	1	0.001	1	1	0.5	1	1	0.05
TU2	1	0.05	0.8	0.05	1	1	0.05	0.8	1	1	0.05	1	1	0.05	1	1	1	1	1	0.05
TU3																				

Table 2.10: Stage-wise superstructure result comparison.

Problem	Units			Superstructure		
	$ PU $	$ TU $	$ j $	NLP-3	LP-4	LP-3
1	2	2	2	40	40	40
2	2	2	2	79	79	79
3	3	2	3	49.34	42	44.09
4	3	2	3	25.7	0	21.01
5	3	3	3	14.15	0	14.82
6	3	3	3	59.17	48.55	48.55
7	3	3	3	45.8	45.8	45.8
8	5	3	3	36.2	33.6	36.92
9	5	3	3	60	0	60
10	5	3	3	40	40	40

wise superstructure does not include the mixer mass balances in the network superstructure. We demonstrate the application of this superstructure for targeting minimum freshwater assumption by considering ten problems. For comparison with model (LP-3), we consider the original NLP network superstructure formulation¹⁶ consisting of the model (NLP-1) and the equations (2.10), which will be referred to as “NLP-3”. In addition, “LP-4” corresponds to the LP relaxation of “NLP-3” using McCormick inequalities.

NLP-3 was solved to global optimality with BARON 9.3, whereas the LP’s are solved with CPLEX 12.3. Even though this superstructure will not always predict the exact target for freshwater flowrate supplied to the total water network, some improvements have been noted. As can be seen from 2.10, the stagewise structure predicted the exact target in 4 out of the 10 problems. In the 6 remaining ones the upper bounds are overestimated in the range of 2.0% to 18.2% of the actual targets. In contrast, the McCormick relaxation of the NLP network superstructure formulation predicts a significantly lower bound with a gap ranging between 0 and 100%. Note that in problems 4,5,9, the McCormick relaxation predicts zero freshwater flowrates, while (LP-3) predicts significantly better estimates.

2.5 Simultaneous optimization

2.5.1 Procedure

As was indicated in section 2.2, the simultaneous flowsheet, heat, and water optimization problem can be stated as follows. Given is a flowsheet with fixed structure, the process streams that need to be heated or cooled are identified for heat integration, water-using process units are specified with their maximum inlet and outlet concentrations, and percent of contaminant removal is provided for wastewater treatment units in water integration. The problem is then to simultaneously optimize the flowsheet with heat and water integration as given in model (2.1), using (2.2) for heat integration targets, and (LP-1) or (LP-3) for the WN target. The detailed HEN and WN structures are synthesized using superstructure-based methods^{9,16} in a second step without incorporating the targets.

2.5.2 Examples

The proposed procedure has been applied to two process flowsheet optimization problems. For heat integration, we used cost values found in the original example in the literature^{21,27}. For the case of the methanol plant, we only considered process units for the water target. In the case of the bioethanol process, we included the treatment units, where we estimated the presence of various contaminants and upper contaminant concentration tolerated by process unit as shown in 2.11.

Methanol synthesis

We consider the methanol flowsheet example taken from Duran and Grossmann²⁷ and Turkey and Grossmann⁶⁷ shown in 2.9. This problem requires 90% pure methanol to be produced at a flowrate of 1300 kmol/day. Syngas (65% H₂, 30% CO, and 5% CH₄) is the feed which is compressed in a two-stage compression with interstage cooling. The feed is combined with the recycle stream and preheated before entering the methanol reactor,

Table 2.11: Utility data.

$C_j^{in,max}$ (ppm)	TSS	TDS	ORG
Boiler Loop	2	100	10
Cooling Cycle	10	500	10
β_j^t	TSS	TDS	ORG
Settling Tank	0.05	1	1
Reverse Osmosis	1	0.1	1
Anaerobic Tank	1	1	0.01

where the exothermic reaction occurs and steam is raised. The pressure of the stream leaving the reactor is reduced and the stream is cooled down before entering the flash unit, which then separates the product stream from the recycle stream. Part of the vapor stream from the flash is purged and sold as byproduct. In order to incorporate the effect of water integration, the cooling tower cycle and the steam system are also embedded in this process. Water requirements in those units are make-up water and blowdown. The conventional values for maximum contaminant concentration present in the utility cycles are taken from the literature²¹ and shown in 2.11. Also, no wastewater treatment is considered for this case.

The WN is assumed to be isothermal, which means that the WN itself will not be heat-integrated in the simultaneous step, where the heat and water targeting equations are added. The NLP for the flowsheet optimization has 161 constraints and 163 continuous variables, while the NLP for the simultaneous method, which includes the equations in (2.1) with (LP-1) as g^{WN} has 237 equations and 244 continuous variables. The problems are first optimized using CONOPT 3 to provide an initial local optimum, then they are furthered optimized using BARON 9.3 to ensure a global optimal solution. The solution time was 5575 CPU s for the simultaneous case and 4332 CPU s for the sequential optimization.

The major design parameters and the optimal profit for both methods are shown in 2.12. The important observation here is that the sequential approach uses the expansion valve to cool the stream, thus saving cooling utility before the stream needs to be cooled even further entering the flash. However, the lower pressure from the expansion led to a less effective separation of product from the recycle stream in the flash unit. Consequently, the

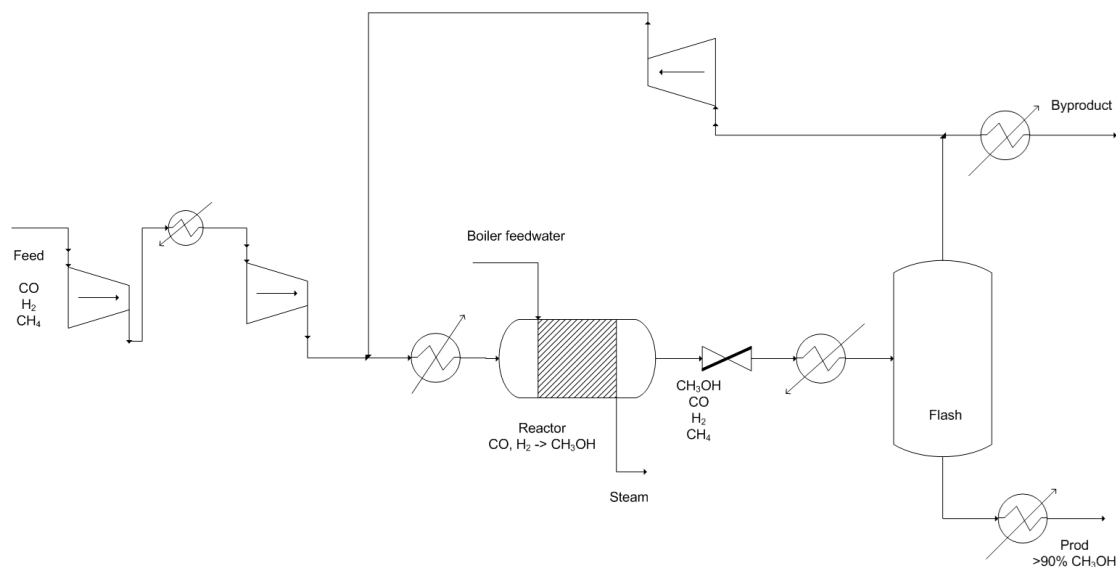


Figure 2.9: Methanol synthesis process flowsheet.

sequential solution has a lower overall conversion (68% vs 88%), and it requires a much higher compression power (6.59 vs 1.84 kW) in the recycle compressor. In contrast, in the simultaneous approach, heating and cooling are integrated with significantly different operating conditions (higher pressure, 2.6 MPa vs 1.3 MPa, in the flash unit and lower compression ratio, 1.03 vs 1.26, in the recycle compressor). Furthermore, note that the simultaneous approach requires no heating and 20% less consumption of freshwater (29.25 kg/s vs 36.43 kg/s), although it requires more cooling water. Overall, the resulting flowsheet from the simultaneous optimization improves the profit from 62.7MM\$ to 73.4MM\$ per year, a 17% increase.

Applying the second step, the resulting WN is shown in 2.10a and HEN is shown in 2.10b, in which the total cost, investment and utilities were optimized. It is interesting to note that in this example, the freshwater consumption of 29.25 kg/s predicted by the targeting formulation (LP-1) is exact. In the optimal HEN design, the utilities required (no heating utility and 72.67×10^9 kJ/yr cooling utility) coincide with the minimum targets predicted in step one of the simultaneous optimization procedure. Also, in the WN design the consumption of freshwater was 29.25 kg/s, the same as predicted by the target. In comparison,

Table 2.12: Result comparison for methanol synthesis example.

	SEQUENTIAL	SIMULTANEOUS
Profit (1000 \$/yr)	62,695	73,416
Investment Cost (1000 \$)	1891	1174
Operating costs and parameters		
Electricity (kW)	6.59	1.84
Freshwater (kg/s)	36.43	29.25
Heating utility (10^9 kJ/yr)	0.293	0
Cooling utility (10^9 kJ/yr)	67.33	72.67
Steam generation (10^9 kJ/yr)	2448	1965
Flowrate (10^6 kmol/yr)		
Feedstock	48.04	37.13
Product	10.89	10.89
Byproduct	9.95	4.41
Overall conversion	0.68	0.88

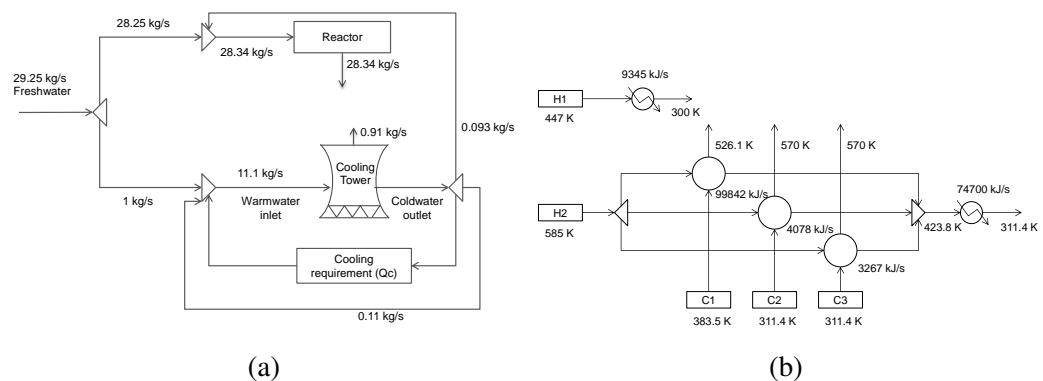


Figure 2.10: Methanol synthesis simultaneous optimization: (a) WN (b) HEN.

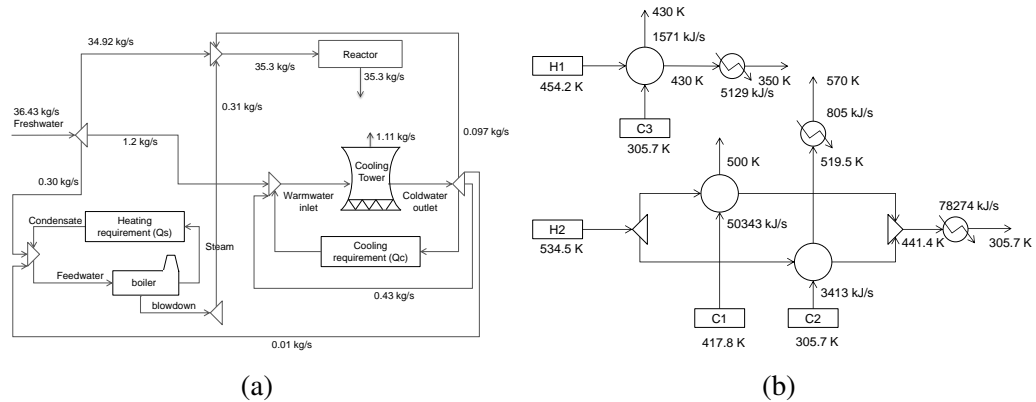


Figure 2.11: Methanol synthesis sequential optimization: (a) WN (b) HEN.

the resulting WN and HEN for the sequential optimization approach are shown in 2.11a and 2.11b. The major difference between the results is that the simultaneous approach yields a solution that does not have any heating requirement, therefore, the boiler loop that is present in WN from sequential optimization is not needed for the WN from simultaneous optimization, hence both HEN and WN designs are influenced. It is worth noting that not until the price of water increases by ten fold does the methanol flowsheet take on different operating conditions under the simultaneous approach.

Bioethanol production from corn

A second example shown in 2.12 involves optimizing a corn-based bioethanol plant taken from Karupiah et al²¹. Corn is processed through a series of process units - washing, cooking, fermentation, solid separation, and liquid separation - to produce 61.3 MMgal ethanol per year. The authors in the original example determined the flows and operating conditions in the flowsheet such that production cost for a fixed ethanol production rate is minimized through a sequential optimization approach. In this chapter, we make improvements upon the initial design by performing simultaneous heat and water integration on the optimally configured network. In addition, multieffect columns are modeled and embedded in the flowsheet using short-cut equations to further reduce energy consumption. This example assumes fixed raw material consumption and production rates. Thus,

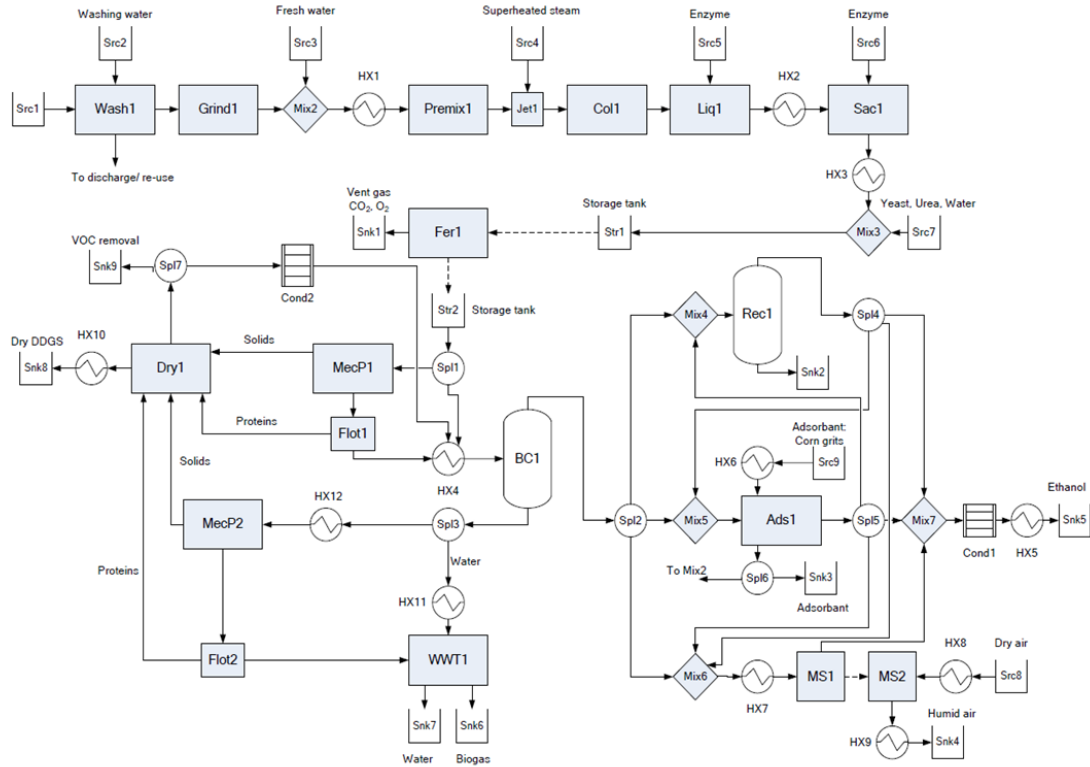


Figure 2.12: Bioethanol production process flowsheet.

the objective function is to minimize heating utility, cooling utility, and freshwater cost.

In case 1 we solved a modified version of the original example (NLP formulation), then we solved for its subsequent heat integration (MINLP) and water integration (NLP). In case 2, we replaced the single beer column and rectifying column by two multi-effect distillation columns, and performed sequential heat and water integration. Finally, in case 3, we performed simultaneous integration (with multi-effect columns) using model (2.1) with the constraints in (LP-3) for g^{WN} .

In this example, in addition to the water-using or water-producing process units, cooling loop and boiler cycle are taken into account for completeness. The empirical correlations for the two cycles are taken from Ahmetović et al⁶⁸. The contaminants taken into consid-

Table 2.13: Formulation size comparison for bioethanol production.

	Base Case	Case 1	Case 2	Case 3
CPU(s)	387	387	470	563
# eqns	2,232	2,232	3,213	5,221
# cont var	2,921	2,921	3,914	5,392

Table 2.14: Result comparison for bioethanol production.

	Base Case	Case 1	Case 2	Case 3
Cost (MM\$/yr)	14.91	11.77	8.57	8.57
Cooling water use (kg/s)	2895.6	1998.3	1127.3	1124.8
freshwater use (kg/s)	40.8	127.6	90.0	90.0
Steam use (kg/s)	35.1	28.3	21.3	21.3

eration are total suspended solids(TSS), total dissolved solids (TDS), and organics (ORG), treated by settling tank, reverse osmosis, and anaerobic tank, respectively.

The problem was implemented using GAMS 23.7⁶⁹ and solved on an Intel 2.4 GHz machine with 4 GB memory. CPLEX 12 was used for solving the LP and MILP subproblems; CONOPT 3 was used to solve the NLP subproblems; finally, both DICOPT and BARON were employed to solve the MINLP problems. The problem size and solution time are shown in 2.13. The total CPU time indicated for the simultaneous approach includes the solution time of the simultaneous flowsheet and targeting formulation only. The solution time for the subsequent HEN and WN problem are not included in the total solution time.

As we can see from the results in Table 2.14, the addition of multieffect columns contributes to 36% savings in energy consumption. However, there is no improvement in the solution quality under the simultaneous approach. This can be attributed to two reasons: first, the yield for this process is fixed; second, unlike the methanol synthesis example, this example does not involve recycle streams. Furthermore, the acyclic nature of the flowsheet does not lend itself to improved integration with the simultaneous optimization. However, comparing the problem size and solution time of these approaches, we can see that even though the simultaneous formulation is larger in size compared to the sequential approach, the solution time for both approaches are similar. This is largely due to the small size of

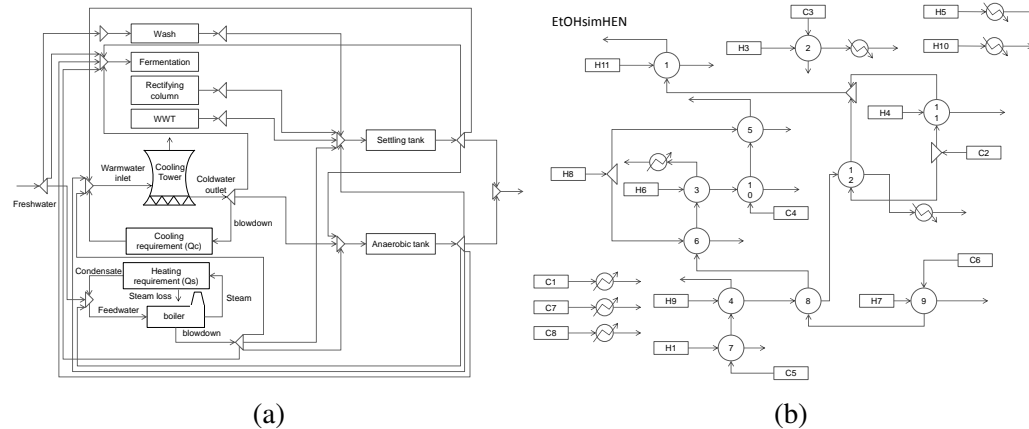


Figure 2.13: Bioethanol production simultaneous optimization: (a) WN (b) HEN.

the targeting formulations. Thus, our result indicates that the addition of heat targeting and water targeting formulations does not contribute significantly to the computational burden of flowsheet optimization, and that such an approach should be considered when energy usage and water usage are of primary concern in a process where possible trade-offs are in place. In this example, the freshwater consumption predicted by the targeting formulation (LP-1) in step 1 of the simultaneous optimization procedure is 15% greater than the actual target (103.4 kg/s vs 90.0 kg/s). In terms of cost, however, the impact is only of the order of 0.24%.

By applying the second step and solving the corresponding NLP and MINLP synthesis models, the water network for case 2 and case 3 is shown in 2.13a while the HEN is shown in 2.13b. The freshwater consumption is 90.0 kg/s (same as the actual target), and the optimal HEN design consumes the same level of hot and cold utilities as the minimum targets (1124.8 kg/s cooling water and 21.3 kg/s steam) predicted in step 1 of the simultaneous optimization strategy.

2.6 Discussion

Based on the examples presented, we have shown the advantage of performing simultaneous process flowsheet, heat, and water integration. Using the water targeting formulations developed in this chapter allows trade-offs to take place among the flowsheet, heat recovery, and freshwater use. Due to the linear nature of the formulations (LP-1 and LP-3 for isothermal networks) for fixed flows, they do not add much to the computational complexity of the flowsheet. Two points regarding this approach are discussed below.

First, the success of performing simultaneous optimization strategy greatly depends on the structure of the flowsheet. As shown in the methanol example, the simultaneous approach takes advantage of the recycle structure and relatively low conversion per pass, which allows for a higher overall conversion, and thus, less raw material consumption. The trade-off is that since the conversion per pass is low, this increases the flows in the recycle stream. However, the increased utility consumption due to the increased recycle stream can be mitigated by energy and water integration within the flowsheet. Thus, it is shown that the operating conditions should be chosen given the possibilities for heat and water integration. Furthermore, the impact of the simultaneous optimization will be larger if the process exhibits low conversion per pass²². In contrast, the bioethanol example has an acyclic structure and fairly few degrees of freedom. This prevents major economic trade-offs among capital cost, raw material consumption, and energy and water consumption be established. As a result, the simultaneous optimization approach has low potential in these systems.

The second point is that the synthesis of the WN is independent of the freshwater target predicted in step one of the simultaneous approach. As indicated in section 2.2, the target determined in the first step is not used as a constraint in WN synthesis, even though this could be done if the target was exact and if the user was only interested in the structure that requires minimum freshwater consumption. It is actually better to allow the readjustment of freshwater consumption in the second step since capital costs are included in the synthesis models. Thus, there are no feasibility issues when performing simultaneous

optimization using the water targeting formulations presented in this chapter, even if the exact target is not guaranteed as is the use of models (LP-1), (LP-2), and (LP-3). Finally, since the price of water is low (1 - 2.5 \$/ton), the target predicted in step one does not contribute greatly to the total cost of the process flowsheet.

2.7 Conclusion

Simultaneous optimization accounts for complex trade-offs among raw materials, investment cost, and energy consumption in a process flowsheet, which leads to lower cost solutions with efficient use of energy and water. We have proposed a solution methodology for simultaneous optimization of process flowsheet, HEN, and WN. As part of the solution procedure, simplified targeting formulation that can predict the minimum freshwater consumption is required. To this end, several LP formulations for freshwater targeting have been developed, which are the main contribution of this work. The formulation (LP-1) for multi-contaminants WN problems with only water-using process units has been shown to be exact under a certain assumption, and the formulation yields a tight upper bound in cases where the assumption does not hold true. This formulation is also combined with heat targeting model to determine the minimum utility and water requirement for non-isothermal WN. In addition, the LP targeting model has been extended to (LP-3) to include wastewater treatment units through the use of the stage-wise superstructure, although in this case exact target are not obtained. We then applied these targeting formulations to two examples using simultaneous optimization strategy and demonstrated the effectiveness of the simultaneous approach in improving both the quality and computational effort of the solution.

Chapter 3

Wastewater Regeneration Models for Water Network Optimization

3.1 Introduction

In contrast to chapter 2, the objective of this chapter is to more accurately predict the performance of the treatment units and gain a more thorough understanding of the trade-offs between the removal efficiency and the cost of the treatment units (reverse osmosis, ion exchange, sedimentation, ultrafiltration, activated sludge, and trickling filter), as well as their impact on the WN design. This work combines various technologies capable of removing the three major types of contaminants, namely, TDS, TSS, and ORG, through the use realistic treatment unit models. A number of features are considered in order to achieve this goal and they are described below.

First, unit-specific short-cut models based on the literature are developed to replace the fixed recovery model to more accurately describe contaminant mass transfer in wastewater treatment units. Even though short-cut models have been used in the context of wastewater treatment optimization problem, they usually pertain to specific treatment technologies. For example, Saif et al⁴⁰ designed a reverse osmosis network for desalination processes.

In contrast, in this work we consider multiple types of treatment units for general processes. To this end, appropriate modeling equations that can satisfactorily predict unit performance with reasonable computational complexity are presented.

Short-cut wastewater treatment cost functions (operating cost and investment cost) in the form of nonlinear functions are incorporated into the model. The conventional network cost function usually consists of a linear operating cost term and a concave capital cost term. The use of a more complex objective in this more rigorous model enables the design of WNs that allow for trade-offs that better meet the need of their respective decision criteria.

In addition, since conditions for a given process may change during the course of the operation, we account for the uncertain parameters through the use of a three-scenario model. This method was demonstrated by Karuppiah and Grossmann³⁵, where the authors present a multiscenario nonconvex MINLP model that is a deterministic equivalent of a two-stage stochastic programming model with recourse. For each of the best, worst, and nominal scenarios, the uncertain parameters can take on a different set of values. This model then ensures that the final design solution is feasible and optimal over the set of all three scenarios. This representation can effectively capture the wide range of operating conditions without overly complicating the formulation.

Furthermore, the topology of the superstructure is modified to accommodate realistic potential structures. Faria and Bagajewicz⁷⁰ explored the impact various topologies among the subsystems has on freshwater consumption of the overall water network. Different types of contaminants present in the system are removed by considering the Best Available Techniques (BAT)³⁷. These provide industrial standards for discharge of the major pollutant groups and recommendations for their treatment as listed in Table 1.1. Since there are multiple treatment technologies for the removal of each type of pollutants, the modified superstructure (Figure 3.1) allows for the selection of a subset of BAT treatment technology through the use of disjunctions in the generalized disjunctive programming (GDP) formulation¹⁶.

The resulting multiscenario GDP formulation associated with the WN synthesis problem

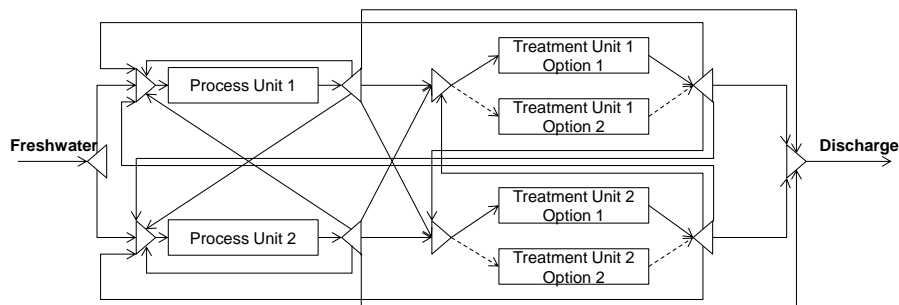


Figure 3.1: Superstructure with multiple treatment unit options.

is computationally expensive to solve to global optimality. Various methods have been proposed to address the issue of bilinear terms (products of flowrates and contaminant concentrations) and concave cost functions in the standard water network synthesis problems^{71,28,16}. The short-cut models presented in this chapter introduce additional nonlinear and nonconvex terms. To overcome the difficulty, we first reformulate the GDP problem into a nonconvex MINLP problem. We then present a modified Lagrangean-based decomposition algorithm in order to solve the resulting MINLP problem effectively. The formulation and the effectiveness of the algorithm are then illustrated through applications in metal finishing and petroleum refining industries.

3.2 Problem statement

3.2.1 Problem description

In this manuscript we consider an integrated multi-contaminant WN with a given set of process units (PU , e.g. scrubber, cooling tower), a set of treatment units (TU , e.g. reverse osmosis, sedimentation), freshwater sources (e.g. lake, municipal treatment plant, water from process separations), and wastewater discharge sinks (e.g. river, centralized wastewater treatment plant, cooling tower). These units are interconnected using mixer units (MU) and splitter units (SU) to form the superstructure, and are shown in Figure

1.1. Freshwater sources that vary in maximum flowrate and pollutant levels are supplied to one or more of the process units. Once the streams are treated, they are recycled to the process units or sent to wastewater discharge sinks that must satisfy limits on either the pollutant discharge concentration or on the discharge flowrate.

Each process unit has a fixed water flowrate requirement, upper limits on the inlet concentration level, and mass load of contaminants released into the water stream. The mass load of contaminant is the uncertain parameter that can take a range of values during process operation. We define its upper bound as the worst case scenario, its lower bound as the best case scenario, and the average as the nominal scenario. In comparison to a single steady state scenario design, the proposed model is defined over the three scenarios $n \in N$ that account for the uncertainties in the loads by introducing flexibility to the network design. This network flexibility can be achieved by increasing pipe capacity, piping connections, or treatment unit capacity and removal efficiency.

The standard wastewater treatment units considered in this work include the following: sedimentation, ultrafiltration, ion exchange, reverse osmosis, activated sludge, and trickling filter. By substituting the simplified models with short-cut models more accurate design can be obtained. The goal is to select a subset of technologies that best fit the treatment applications of the receiving wastewater streams.

3.2.2 General model

The general problem formulation (**GDP-1**) is an extension of earlier works by Karuppiah and Grossmann and Ahmetović and Grossmann^{16,35,28}. The main difference here is that the fixed recovery treatment units are replaced by short-cut models presented in section

3.4. The model (GDP-1) based on the superstructure in Figure (1.1) is as follows:

$$\begin{aligned}
 \min. \quad & Cost^{total} = AR \sum_{t \in TU} IC_t^{TU} + AR \left[\sum_{i \in Pipe} (C_i^{Pipe} y_i + IC_i^{Pipe} (\hat{F}_i)^\delta) \right] \\
 \text{s.t.} \quad & F_{kn} = \sum_{i \in m_{in}} F_{in} \quad \forall m \in MU, k \in m_{out}, \forall n \in N \\
 & F_{kn} C_{kjn} = \sum_{i \in m_{in}} F_{in} C_{ijn} \quad \forall j, \forall m \in MU, k \in m_{out}, \forall n \in N \\
 & F_{kn} = \sum_{i \in s_{out}} F_{in} \quad \forall s \in SU, k \in s_{in}, \forall n \in N \\
 & C_{ijn} = C_{kjn} \quad \forall j, \forall s \in SU, i \in s_{out}, k \in s_{in}, \forall n \in N \\
 & F_{kn} = F_{in} = P_p^{PU} \quad \forall p \in PU, i \in p_{in}, k \in p_{out}, \forall n \in N \\
 & P_p^{PU} C_{kjn} + L_{pjn} \times 10^3 = P_p^{PU} C_{ijn} \quad \forall j, \forall p \in PU, k \in p_{in}, i \in p_{out}, \forall n \in N \\
 & \bigvee_{r=1, \dots, RT_t} \left[\begin{array}{c} Y_{rt} \\ h_n(d_{rt}, F_{in}, C_{ijn}) = 0 \\ g_n(d_{rt}, F_{in}, C_{ijn}) \leq 0 \\ IC_t^{TU} = f_1(d_{rt}) \\ OC_{in}^{TU} = f_2(d_{rt}, F_{in}, C_{ijn}) \end{array} \right] \quad \forall j, \forall t \in TU, i \in t_{in} \cup t_{out}, \forall n \in N \\
 & Y_{rt} \in \{True, False\} \\
 & \hat{F}_i \geq F_{in} \quad \forall i, \forall n \in N \\
 & y_i \in \{0, 1\} \quad \forall i \\
 & F_i^{MIN} y_i \leq \hat{F}_i \leq F_i^{MAX} y_i \quad \forall i \\
 & F_i^{MIN} \leq F_{in} \leq F_i^{MAX} \quad \forall i, \forall n \in N \\
 & C_{ij}^{MIN} \leq C_{ijn} \leq C_{ij}^{MAX} \quad \forall j, \forall i, \forall n \in N
 \end{aligned} \tag{GDP-1}$$

where y_i are binary variables to indicate existence of piping connection i ; F_{in} and F_{kn} are flowrates (t/h) of any stream i and k in the superstructure respectively, in scenario n ; \hat{F}_i is the maximum flowrate capacity of pipe i , C_{ijn} and C_{kjn} are concentrations (ppm) of contaminant j , P_p^{PU} are the process unit water flowrates, L_{pjn} are the mass load of contaminant j in unit p in scenario n (kg/h). In the disjunctive formulation, Y_{rt} indicates if technology r is chosen for unit t , d_{rt} is the design variable associated with r and t . The constraints consist of a set of contaminant mass balances in the mixer units, splitter units, process units, and treatment units ($h_n(\cdot)$, $g_n(\cdot)$). Note that for the set of splitters SU , there

is a subset of initial splitters SU^w for which $F_{kn}^w = FW_n^w$, $w \in W$, where W is set of freshwater sources.

3.2.3 Objective function

The objective function of the problem is to minimize the total cost of the network ($Cost^{total}$). It consists of the annualized investment cost and the expected operating cost. The investment cost is scenario independent and is given by the sum of treatment unit capital costs (IC_t^{TU}) and pipe investment costs (the second term in the objective function). C_i^{Pipe} are the fixed charge cost coefficients (\$) associated with pipe existence, and IC_i^{Pipe} are the investment cost coefficients of pipes, and δ is the associated cost exponent. The expected operating cost of the network represents the operating cost for the selected a network design over all three scenarios, each with a given probability p_n . The term includes freshwater cost, pumping cost, and treatment unit operating cost. $OC^{FW,w}$ are the cost coefficients of freshwater sources (\$/t), OC^{Pipe} is the pumping cost coefficient (\$/t), and OC_{tn}^{TU} is the treatment unit operating cost. H is the operating hours in a year (hr/year), and AR is the annualized factor for investment cost ($year^{-1}$).

Treatment unit cost equations are greatly simplified in previous works on WN optimization. Specifically, the treatment unit capital costs are usually modeled as a concave function of the inlet flow, and the operating cost as a linear function of the inlet flowrate as shown in Equation 3.1.

$$\begin{aligned} IC_t &= CIC_t(F_i)^\alpha \\ OC_t &= COC_t F_i \end{aligned} \tag{3.1}$$

where CIC_t and COC_t are cost coefficients for investment cost and operating cost, respectively. In this work, we incorporate treatment unit cost correlations that are function of design variables such as area or volume of the unit to reduce the gap between the true total cost of the network and the objective obtained from the simplified optimization model.

3.3 Illustrative example

In order to demonstrate the advantage of performing multi-scenario optimization, we present an illustrative example with two process unit/two sets of treatment units (two options each)/two contaminants system with data given in Table 3.1. We solve the example using the worst case scenario model (i) and the three-scenario model (iii). The worst case scenario model optimizes over scenario (n1) only. To obtain an accurate comparison between the two solutions, we solve an additional three-scenario model (ii) subject to piping connectivity and flowrate capacity bound obtained from the worst case scenario model (i).

Table 3.1: Illustrative example data.

(a) Process units										(b) Treatment units								
Flowrate (ton/h)	Discharge Load (kg/h)						C_{in}^{max} (ppm)		Options	Removal Ratio (%)			IC(\$)	CO(\$/ton)				
	n1		n2		n3		A	B		A	B	A			B			
	A	B	A	B	A	B										A	B	
PU1	40	1.1	1.7	1	1.5	0.8	1.3	0	TU1	OP1	90	0	95	0	99	0	16800	1
PU2	50	2	2	1.7	1.8	1.5	1.6	50		OP2	80	0	90	0	98	0	4800	0.5
									TU2	OP1	0	80	0	90	0	95	12600	0.0067
										OP2	0	90	0	95	0	99	36000	0.067

The resulting network costs are presented in Table 3.2, where it can be seen that the worst case design (i) operating in the 3 scenarios (ii) is \$22,820 more expensive than the design that was optimized for the 3 scenarios (iii). As shown in Figure 3.2, both cases (i) and (iii) select Option 2 for TU1 and Option 1 for TU2. The difference lies in the number of piping connections –8 removable pipes in the superstructure are determined by model (i) vs 12 removable pipes in model (iii). A removable pipe is a piping connection between a mixer unit and a splitter unit. As a result, case (iii) allows for additional flexibility. Specifically, it allows for the bypass stream (PU1, discharge mixer unit) in the best scenario (n3). The bypass stream is not selected in the worst-scenario model. Thus, the flow is redirected to PU2 and treatment units, increasing the treatment cost.

The example was solved with BARON⁵³ and the computational statistics are presented in

Table 3.2: Illustrative example optimization results.

	(i) Worst case	(ii) Comparison with three-scenario	(iii) Three-scenario
# of removable pipes	8	8	12
Annualized IC (\$/yr)	39,426.50	39,430.60	39,821.43
Operating cost (\$/yr)	634,742.00	526,398.20	503,187.22
Total cost (\$/yr)	674,161.40	565,828.80	543,008.65

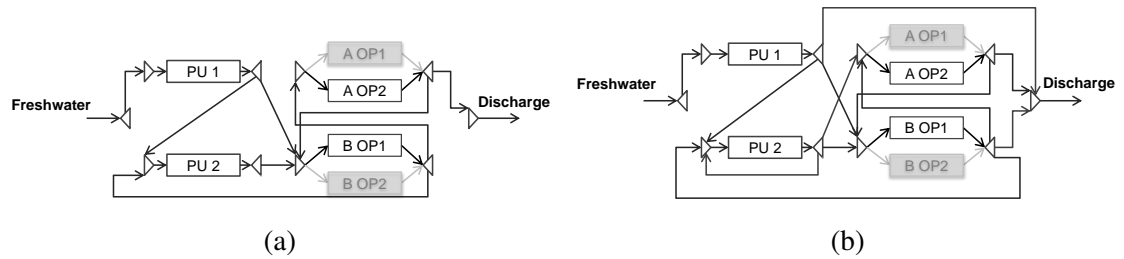


Figure 3.2: Illustrative example result: (a) Worst case scenario (b) Three-scenario.

Table 3.3. The large CPU time required in the three scenario case clearly indicates that a suitable decomposition scheme is required for these problems.

Table 3.3: Computational statistics for illustrative example.

	(i) Worst case	(iii) Three-scenario
# of constraints	229	575
# of continuous vars	161	431
# of integer vars	24	24
CPU time (s)	25	1800*
Optimality gap (%)	4.98	15.6

*Time limit

3.4 Wastewater treatment unit short-cut models

The purpose of this section is to describe a set of common treatment units mentioned previously, and to consider their performance as well as important design considerations. Treatment unit models with various levels of detail have been reported in literature. The models

reported here aim to describe each unit adequately while minimizing computational complexity. To the knowledge of the authors these models have not been incorporated into WN superstructure optimization. A list that summarizes the unit-specific variable names is presented in nomenclature.

For the sake of clarity, in this section we denote treatment unit inlet flowrate by Q_0 (m³/day), outlet flowrate by Q (m³/day), inlet contaminant concentration by S_0^j (ppm), treated outlet contaminant concentration by S^j (ppm), contaminant j removal ratio by Rc^j , and flow recovery ratio by Rr . The recovery Rr is assumed to be 1 for sedimentation, ion exchange, and trickling filter. They are related as follows.,

$$\begin{aligned} Q &= RrQ_0 \\ S^j &= (1 - Rc^j)S_0^j \end{aligned} \tag{3.2}$$

3.4.1 Reverse osmosis

Reverse osmosis is a pressure-driven membrane treatment process mainly used in seawater and brackish desalination applications. A high-pressure feed stream flows across the surface of a semi-permeable material. Due to a pressure differential between the feed and permeate sides of the membrane, a portion of the feed stream passes through the membrane. The permeate stream exits at nearly atmospheric pressure, while the concentrate remains at nearly the feed pressure. The salt rejection coefficient (Rc^{TDS}) limits the membrane performance and its value is fixed for a specific membrane. The value of the recovery ratio (Rr) usually lies between 0.5 and 0.9. A scheme of the RO process is shown in Figure 3.3.

The performance of the system depends mainly on two parameters in the RO process design, they are the transmembrane pressure ΔP and the membrane area A_{memb} . The selected type of membrane element is the spiral bound FILMTEC BW30-400 (DOW) that offers high flow and rejection. The membrane properties are specified by the manufacturer and they are shown in Table 3.4.

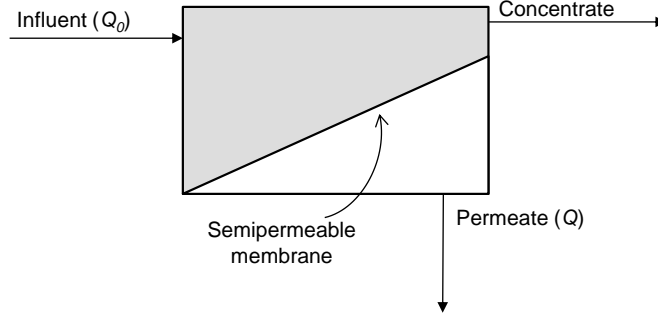


Figure 3.3: Reverse osmosis diagram.

Mass transfer in RO involves a diffusive mechanism such that separation efficiency is dependent on influent solute concentration, pressure, and water flowrate. The permeate flowrate across the membrane is determined by the osmotic pressure law (3.3),

$$Q = A_{memb} N k_m (\Delta P - \Delta \pi) \quad (3.3)$$

The transmembrane pressure (ΔP) is calculated as in (3.4)⁷²,

$$\Delta P = P_f - P_p - \frac{\Delta P_{drop}}{2} \quad (3.4)$$

where P_f is the feed stream pressure, P_p is the permeate stream pressure.

Assuming the feed stream is a dilute solution of salts, the osmotic pressure π can be approximated by the Van't Hoff equation in (3.5),

$$\Delta \pi = \frac{\phi RT}{M} (S_0^{TDS} - S^{TDS}) \quad (3.5)$$

It is also assumed that the concentration polarization is negligible so that the concentration at the membrane surface is considered to be equal to the concentration at the inlet of the RO treatment (C_f).

Table 3.4: Characteristics of the FILMTEC™BW30-400 membrane element.

Parameter	Symbol	Unit	Value
Membrane rejection coefficient	Rc		0.98
Membrane water permeability	k_m	t/(day m ² Pa)	6.48×10^{-7}
Membrane area	A	m ²	37
Gas constant	R	kJ/(kmol K)	8.31
Max pressure drop in vessel	ΔP_{drop}	bar	3.4
Number of ions in solution	ϕ		2
Molar mass of the dissolved solids	M	g/mol	58.44

3.4.2 Ion exchange

Ion exchange (IX) is a reversible reaction in which a charged ion in solution is exchanged for a similarly charged ion electrostatically attached to an immobile solid particle. In practice the raw water is commonly passed through a bed of resin. When the bed becomes saturated with the exchanged ion, it is shut down and regenerated by passing a concentrated solution of the presaturant ion back through the bed. The saturation of the resin is shown in the breakthrough curve (Figure 3.4a). At the break point, the effluent concentration exceeds the design criteria and the column needs to be regenerated. Figure 3.4b shows a scheme of a typical IX column configuration.

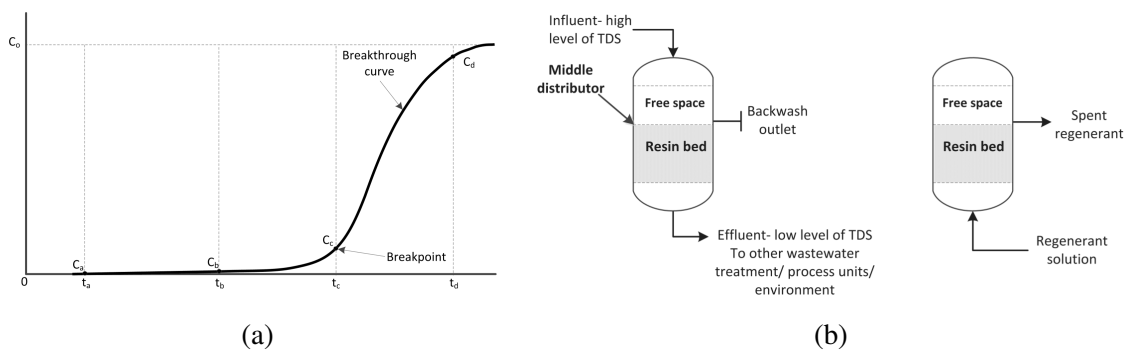


Figure 3.4: Ion exchange unit (a) breakthrough curve, (b) ion exchange column configuration (i) loading cycle (ii) regeneration cycle⁵.

For the complete removal of ions the water stream must pass through cationic and anionic

resins in series or through a unique column containing a mixture of both. The performance of the system depends on many parameters such as the operating capacity (q), the service flow rate (SFR) or the surface loading rate (SLR), which determines the pressure drop in the resin. BV is the volume of water treated per volume of resin, and it relates the concentration gradient with the capacity of the resin bed,

$$BV = 1000 \frac{q}{S^{TDS} - S_0^{TDS}} (X_{IX} MW_{ca} + (1 - X) MW_{an}) \quad (3.6)$$

where X_{IX} is the mass fraction in inlet water of ion to be removed, MW_{ca} is the molar mass of the cation, and MW_{an} is the molar mass of the anion.

SFR is determined from the following equation, and the typical SFR ranges from 8 to 40 bed volume per hour (BV/h).

$$SFR = \frac{BV}{CT} \quad (3.7)$$

where CT is the contact time.

The process design variables can be modeled with the equations in (3.8),

$$V_{IX} = \frac{Q_0}{SFR} \quad (3.8a)$$

$$V_{ww} = \frac{q}{S_0 - S} \quad (3.8b)$$

$$A_{IX} = \frac{Q_0}{SLR} \quad (3.8c)$$

where V_{IX} is the resin volume, V_{ww} is the volume of wastewater treated, and A_{IX} is the resin cross-sectional area.

Some design considerations for determining model parameters are as follows³⁶. The pressure drop in the bed should be kept in the range of 35-70 kPa, with a maximum value of 135 kPa. This results in a maximum SLR of 880 m/day, depending on the resin. Regarding the operating parameters, SFR should be kept in the range of 8 to 40 BV/h to ensure

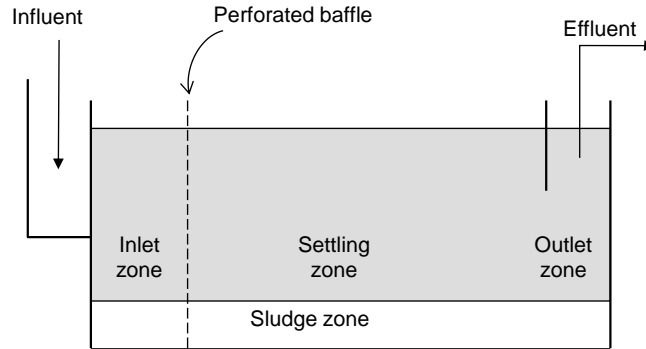


Figure 3.5: Horizontal flow sedimentation diagram.

an adequate contact time and to avoid an early breakthrough.

3.4.3 Sedimentation

Sedimentation is used as a preliminary step to reduce TSS level in wastewater streams. Typically, 50 to 70% of TSS and 25 to 40% of BOD can be removed using primary sedimentation tanks³⁶. The standard sedimentation tanks are of circular or rectangular design, whose selection is determined by a number of factors. Figure 3.5 is a schematic drawing of a horizontal flow tank.

The efficiency of sedimentation tanks is affected by a number of factors including eddy currents formed by the inertia of the incoming fluid, thermal convection currents, and density currents caused by cold or warm water along the bottom of the tank and warm water flowing across the top of the tank.

Typical removal performance (Rc^j) of a rectangular tank can be modeled by a hyperbolic function (3.9) of the detention time (t) and contaminant (j)⁷³.

$$Rc^j = 1 - \frac{t}{a_j + b_j t} \quad (3.9)$$

where a, b are empirical constants presented in Table 3.5.

Table 3.5: Typical values for the empirical constants at 20 °C.

Contaminant	a	b
BOD	0.018	0.020
TSS	0.0075	0.014

The design of the rectangular tank can be calculated by the following equations,

$$\begin{aligned}
 A_{SE} &= Q/OR_{SE} \\
 D_{SE} &= tQ/A_{SE} \\
 NC &= \frac{A_{SE}}{LW}
 \end{aligned}
 \tag{3.10}$$

where OR_{SE} is the overflow rate, A_{SE} is the area, D_{SE} is the depth, and NC is the number of clarifiers required.

3.4.4 Ultrafiltration

Ultrafiltration (UF) is a pressure driven membrane filtration process. The feed stream is a suspension, or two-phase system, in which the dispersed solid phase to be separated may include sediment, algae, bacteria, protozoa, viruses, or colloids. The primary goal of membrane filtration is to produce a product stream (water) from which the targeted solids have been almost completely removed. The predominant removal mechanism in UF is size exclusion so the process can theoretically achieve perfect exclusion of particles regardless of operational parameters such as influent concentration and pressure. UF membranes cover a wide range of molecular weight cut-offs (MWCOs) and pore sizes. Operational pressures range from 70 to 700 kPa, depending on the application³⁶.

The UF process shares some common features with the RO process. The material balances must be satisfied and the feed and permeate concentration are related through the rejection coefficient (3.2). The recovery ratio is assumed to lie between 0.5 and 0.9. Pure water transport across a clean porous membrane is directly proportional to the transmembrane pressure (ΔP). The number of units (N) required is based on the permeate flowrate (Q)

Table 3.6: Characteristics of a typical UF membrane.

Parameter	Symbol	Unit	Value
Membrane water permeability	k_m	t/(day m ² Pa)	1.3704×10^{-5}
Active area of membrane element	A	m ²	33
Max pressure drop in vessel	ΔP	bar	0.4-1.5

as shown in equation (3.11),

$$Q = N\Delta P k_M A_{memb} \quad (3.11)$$

Fouling of the membrane may occur during the filtration, which implies an additional resistance to the water flux through the membrane. For the sake of simplicity, we do not consider membrane fouling in the mathematical model. Typical UF membrane characteristics⁵ are shown in Table 3.6.

3.4.5 Activated sludge

Activated sludge (AS) is an aerobic slurry commonly used in wastewater treatment for the removal of soluble organic matters. Microorganisms in the wastewater convert organic matter to biomass and other components in the complete-mix suspended growth reactor. Once the stream exits the reactor, the suspended solids (sludge) are partially removed in a clarifier, while the rest is recycled to the reactor. The removed sludge then goes through a series of sludge treatment to be discharged to the environment. This process is shown in Figure 3.6a.

An important parameter that determines the system performance is the solid retention time (*SRT*), which is used to characterize the average time the activated-sludge solids remain in the system⁷³. The effluent soluble substrate concentrations in (3.12), S , is only a function of the *SRT* and kinetic coefficients, and is neither a function of the influent soluble substrate concentration nor the sizes of the reactor. However, the size of the reactor

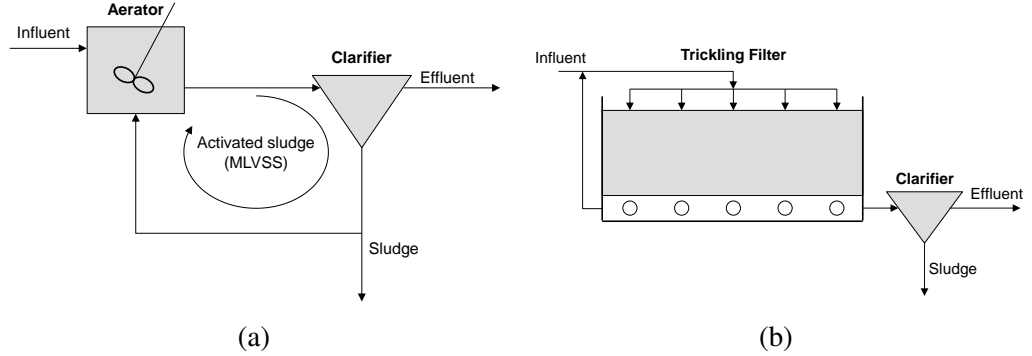


Figure 3.6: Organics removal units schematics, (a) Activated sludge, (b) Two-stage trickling filter.

needs to scale with SRT in order to avoid system upsets.

$$S = \frac{K_s[1 + (k_d)SRT]}{SRT(Yk - k_d) - 1} \quad (3.12)$$

where K_s, k_d, Y, k , and f_d are kinetic parameters and their values are given in Table 3.7. The process can be modeled with the equations in (3.13),

$$\begin{aligned} X_{AS} &= \left(\frac{SRT}{\tau}\right) \left[\frac{Y(S_0 - S)}{1 + (k_d)SRT}\right] \\ X_T &= \left(\frac{SRT}{\tau}\right) \left[\frac{Y(S_0 - S)}{1 + (k_d)SRT}\right] + (f_d)(k_d)XSRT + \frac{(X_{0,i})SRT}{\tau} \\ P_{X_T, VSS} &= \frac{X_T V}{SRT} \\ P_{X, bio} &= P_{X_T, VSS} - QX_{0,i} \end{aligned} \quad (3.13)$$

where X_{AS} is the biomass concentration in the aeration tank, X_T is MLVSS concentration, $X_{0,i}$ is the influent nbVSS concentration, $P_{x, bio}$ is biomass wasted, and $P_{X_T, VSS}$ is total sludge wasted daily.

In general, the operating cost of the AS is higher than the cost of other secondary treatment processes primarily because of the need to supply molecular oxygen using mechanical aerator, which can be energy-intensive. The oxygen consumption (RO_{AS}) is given by the

Table 3.7: AS kinetic parameters.

Symbol	Unit	Value
K_s	g COD/m ³	10
k_d	g VSS/(g VSS day)	0.1
Y	g VSS/g COD	0.4
k	g VSS/(g VSS day)	12.5
f_d	g VSS/g VSS	0.15

following correlation:

$$R_{O_{AS}} = Q(S_0 - S) - 1.42P_{x,bio} \quad (3.14)$$

The sizing of the unit is modeled as follows,

$$\begin{aligned} V_{AS} &= \tau Q \\ Acl_{AS} &= \frac{QX_T}{SLR} \end{aligned} \quad (3.15)$$

where V_{AS} is the reactor volume, τ is the residence time, and Acl_{AS} is the clarifier area.

3.4.6 Trickling filter

Trickling filter (TF) is a circular packed bed of media covered with a biological film of microorganisms, which operates using attached-growth process. Liquid wastewater is distributed over the top of the unit by a rotary distributor. Oxygen diffuses into the media, and treatment of the wastewater stream is accomplished by the biofilm in the filter. Organic removal rate is related to the available surface area and contact time of the wastewater with the surface³⁶.

A two-stage trickling filter system is the most typical process used that improves the performance of the unit. The second stage provides additional contact between the organics and the microorganisms on the filter media. The two stages could have different media as shown in Figure 3.6b. The organic removal ratio (Rc^{ORG}) can be related to the removal

efficiency of stage one (E_1) and stage two (E_2) as follows,

$$Rc^{ORG} \times 100 = E_1 + E_2 \left(1 - \frac{E_1}{100}\right) \quad (3.16)$$

The empirical design equations for BOD removal were developed for rock trickling filters based on the performance at 34 plants at military installations treating domestic wastewater⁵. For a single-stage filter or the first stage of a two-stage rock filter, the efficiency at 20°C is,

$$E_1 = \frac{100}{\left(1 + 0.4432 \sqrt{\frac{W_1}{VF}}\right)} \quad (3.17)$$

$$W_1 = Q S_0 \frac{1kg}{1000g}$$

where W_1 is BOD loading applied to the first-stage filter. For the purpose of this work, we ignore the effect of wastewater temperature on the BOD removal efficiency.

The recirculation factor F represents the average number of passes of the raw wastewater BOD through the filter. The 0.1 factor accounts for the empirical correlation of the decreasing biodegradability with increasing number of passes⁽³⁶⁾. The recycle ratio R_{rcy} is typically between 0 and 2.

$$F = \frac{1 + R_{rcy}}{(1 + 0.1R_{rcy})^2} \quad (3.18)$$

The second stage efficiency is given as follows:

$$E_2 = \frac{100}{\left(1 + \frac{0.4432}{1 - E_1/100} \sqrt{\frac{W_2}{VF}}\right)} \quad (3.19)$$

$$W_2 = (1 - E_1)W_1$$

where W_2 is BOD loading applied to the second-stage filter.

As with all aerobic treatment operations, an adequate supply of air is crucial to provide efficient treatment of the wastewater stream. The formulation (3.20) has been developed by

Dow Chemical to estimate oxygen consumption (RO_{TF}) for trickling filter applications⁷³,

$$\begin{aligned} RO_{TF} &= 20(0.8e^{-9L_B} + 1.2e^{-0.17L_B}) \\ L_B &= QS_0/V_{TF} \end{aligned} \quad (3.20)$$

where L_B is BOD loading to filter.

Important design variables include the volume of the filter media and the area of the clarifier. The depth, D_{TF} , of each filter is typically within 3 - 11.4 m. Other design parameters include,

$$\begin{aligned} OR &= -0.0556D_{TF}^2 + 0.7056D_{TF} - 0.7889 \\ A_{TF} &= Q/OR_{TF} \\ V_{TF} &= A_{TF}D_{TF} \\ Acl_{TF} &= Q/19.92 \end{aligned} \quad (3.21)$$

where OR_{TF} is overflow rate, Acl_{TF} is the clarifier area, and A_{TF} , D_{TF} , V_{TF} are area, depth, and volume of the filter media, respectively.

3.4.7 Economics of treatment units

The cost correlations for standard wastewater treatment units can be found in several sources^{74,75}. In addition, we have derived cost equations as functions of unit sizes using the software Superpro Designer⁷⁶ through curve fitting. Superpro features end-of-pipe treatment process units for pollution prevention studies.

The investment cost terms IC_t are functions of equipment sizing such as area and volume, whereas operating cost OC_t include unit throughput, electricity (c_e , \$0.0981/kWh), material replacement, oxygen consumption (c_{O_2} , \$0.02/kg) and waste disposal cost (c_d , \$0.0001/kg). N_t represent the number of units required to achieve the separation. The equations for the various units are presented below, and their corresponding cost coefficients, c^t , and cost exponents, α^t , for the various units are collectively presented in Table 3.8. H is the number of working hours in a year.

Table 3.8: Typical cost correlation values.

	c_1	c_2	c_3	c_4	c_5	c_6	α_1	α_2
Reverse Osmosis	121.35	7802.6	830					
Ion Exchange	8400.7	1e-13	-2e-7	0.1517	39162		0.3474	
Sedimentation	8483.8	1.69	11376				0.6	
Ultrafiltration	138.9	303.47	400					
Activated Sludge	241.17	8485.9	4.58	36295	3.32	5842	0.6416	0.6
Trickling Filter	-2.4234	1731.6	69391	8485.9	3.3445	43678	0.6	

Reverse osmosis The capital cost is a function of the membrane area, A_{RO} , and the operating cost consists of membrane replacement cost, pumping electricity cost, and disposal cost. LT_m is the membrane element lifetime (5 years), η_p is the pump efficiency (0.8), and ρ^{RO} is the feed density (1000 kg/m^3). The operating cost of the RO unit is high due to the energy consumption of the high pressure pump.

$$\begin{aligned}
 IC_{RO} &= (c_1^{RO} A_{RO} + c_2^{RO}) N_{RO} \\
 OC_{RO} &= \frac{c_3^{RO} N_{RO}}{LT_m} + \frac{c_e H \Delta P F_{in}}{\eta_p \rho^{RO}} + c_d^{TDS} H F W^{RO}
 \end{aligned} \tag{3.22}$$

Ion exchange The capital cost is a function of the resin volume, V_{IX} , needed for the treatment. The operating cost includes the regenerating cycle (chemicals, brine disposal), which is a polynomial function of the throughput.

$$\begin{aligned}
 IC_{IX} &= c_1^{IX} (V_{IX})^{\alpha_1^{IX}} \\
 OC_{IX} &= c_2^{IX} (F_{in})^3 - c_3^{IX} F_{in}^2 + c_4^{IX} F_{in} + c_5^{IX}
 \end{aligned} \tag{3.23}$$

Sedimentation The capital cost is a function of the area, A_{SE} , and the operating cost is a function of throughput and the number of rectangular clarifiers NC_{SE} .

$$\begin{aligned}
 IC_{SE} &= c_1^{SE} A_{SE}^{\alpha_1^{SE}} \\
 OC_{SE} &= NC_{SE} \left(\frac{c_2^{SE} F_{in}}{OR_{SE}} + c_3^{SE} \right)
 \end{aligned} \tag{3.24}$$

Ultrafiltration The capital cost mainly depends on the membrane area, A_{UF} , needed for

the separation. The operating cost include membrane replacement cost, electricity cost, and disposal cost. Since the transmembrane pressure in UF is not so high as in RO, the operational cost is less dependent of the electricity consumption.

$$\begin{aligned} IC_{UF} &= (c_1^{UF} A_{UF} + c_2^{UF}) N_{UF} \\ OC_{UF} &= \frac{c_3^{UF} N_{UF}}{LTm} + \frac{c_e H \Delta P F_{in}}{\eta_p \rho_{UF}} + c_d^{TSS} H F w_{UF} \end{aligned} \quad (3.25)$$

Activated sludge The capital cost is a function of aeration basin volume V_{AS} and clarifier area Acl_{AS} . The operating cost has three terms: maintenance cost as a function of throughput, oxygen consumption, and sludge disposal cost.

$$\begin{aligned} IC_{AS} &= c_1^{AS} (V_{AS})^{\alpha_1^{AS}} + c_2^{AS} (Acl_{AS})^{\alpha_2^{AS}} \\ OC_{AS} &= (c_3^{AS} F_{in} + c_4^{AS} + c_5^{AS} F_{in} + c_6) + c_{O_2}^{AS} Ro_{AS} + c_d^{ORG} P_{X_T, VSS} \end{aligned} \quad (3.26)$$

Trickling filter The capital cost is a function of filter area A_{TF} and clarifier area Acl_{TF} . Similar to the activated sludge, the operating cost has three terms: maintenance cost as a function of throughput, oxygen consumption, and sludge disposal cost.

$$\begin{aligned} IC_{TF} &= 2(c_1^{TF} A_{TF}^2 + c_2^{TF} A_{TF} + c_3^{TF}) + c_4^{TF} Acl_{TF}^{\alpha_1^{TF}} \\ OC_{TF} &= (c_5^{TF} F_{in} + c_6^{TF}) + c_{O_2}^{TF} Ro_{TF} (C_{in} - C_{out}) F_{in} + c_d^{ORG} (C_{in} - C_{out}) F_{in} \end{aligned} \quad (3.27)$$

As can be seen from these equations, the correlations (3.22)–(3.27) include bilinear and concave terms that are nonlinear and nonconvex. The cost model gains in accuracy despite the computational complexities compared to the simple equations in (3.1). To see this difference more clearly, we can compare the performance of activated sludge and trickling filter for the removal of organic contaminants shown in Figure 3.7. The investment cost as a function of inlet concentration for activated sludge under fixed operating parameters is shown in Figure 3.7a. It is clear that there is a significant increase in investment cost (9.89%) over the range of concentration considered. Figure 3.7b shows that trickling filter removal efficiency is also a function of inlet concentration when the recycle ratio is fixed

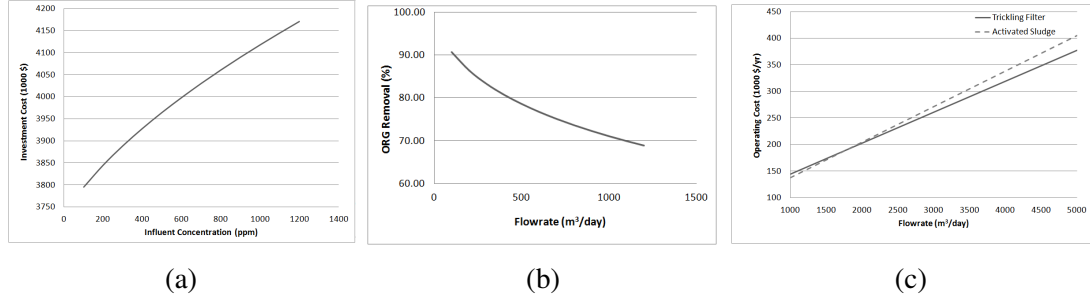


Figure 3.7: Organic treatment unit shortcut model comparison.

to 0.2. Finally, in Figure 3.7c we compare the operating costs of activated sludge and trickling filter as functions of flowrate only. The figure shows that there exists a crossover point between the two curves, which indicates that it is incorrect to estimate the operating cost as a linear function of the flowrate. As a result, the simplified model, which is only dependent on the flowrate across the treatment unit, may lead to suboptimal, and possibly to solutions with the incorrect selection of treatment technology.

3.5 Computational strategies

3.5.1 Strategy for global optimal solution

The resulting multi-scenario GDP problem (GDP-s) is given by the model in (GDP-1), where $h_n(\cdot)$ and $g_n(\cdot)$ are replaced by the short-cut equations in (3.2)-(3.21), and $f_1(\cdot)$ and $f_2(\cdot)$ are defined by the cost equations (3.22)-(3.27). Due to the presence of nonconvexities, sub-optimal solutions may be obtained if local solvers are used. Finding efficiently the global optimal solution in the proposed multi-scenario model would allow to solve the more accurate short-cut formulation.

The multi-scenario model (GDP-s) gives rise to a block diagonal structure, in which the design variables (d_{rt}) are complicating variables in that they need to be accounted for in all scenarios. By defining the copy variables d_{rt}^m , \hat{F}_i^n , y_i^n , for each scenario, the problem

can be reformulated as one with complicating constraints as shown in equation (3.28).

$$\begin{aligned}
 d_{rt}^n &= d_{rt}^{n+1} \quad \forall t \in TU, r = 1, \dots, RT_t, \forall n \in N, n < |N| \\
 \hat{F}_i^n &= \hat{F}_i^{n+1} \quad \forall i, \forall n \in N, n < |N| \\
 y_i^n &= y_i^{n+1} \quad \forall i, \forall n \in N, n < |N|
 \end{aligned} \tag{3.28}$$

This allows the application of the Lagrangean decomposition algorithm⁷⁷.

The proposed algorithm shown in Figure 3.8 involves an outer problem and an inner problem. The outer problem determines a global lower bound from a special relaxation problem (RP) and fixes the selection of treatment unit options. The inner problem is then constructed for a fixed set of treatment unit technologies. The inner loop is solved with the Lagrangean decomposition algorithm and iterates between a lower bounding problem (SP_1)-(SP_N) and an upper bounding problem (P''). Since the predicted lower bounds are rigorous but exhibit dual gaps in the inner problem, global optimality can only be guaranteed within the predicted global upper and lower bounds after a maximum number of iterations.

3.5.2 Subproblem descriptions

Problem (P) is a nonconvex MINLP that results from applying the hull reformulation⁷⁸ to (GDP-s). The MINLP relaxation problem (RP) is obtained by replacing all the nonconvex terms present in (P) with linear or convex underestimators so as to yield a valid lower bound. See Appendix B for a summary of relevant nonconvex terms and their convex estimators. Problem (SP_n) are MINLPs obtained by decomposing (P) into $|N|$ scenarios using Lagrangean decomposition to obtain subproblems(SP_1)-($SP_{|N|}$). The complicating design variables d_{rt}, F_i^n, IC_t^{TU} are replaced by their copy variables $d_{rt}^n, \hat{F}_i^n, IC_{tn}^{TU}$, respectively, as in constraints (3.28). The linking constraints (3.28) are dualized and transferred

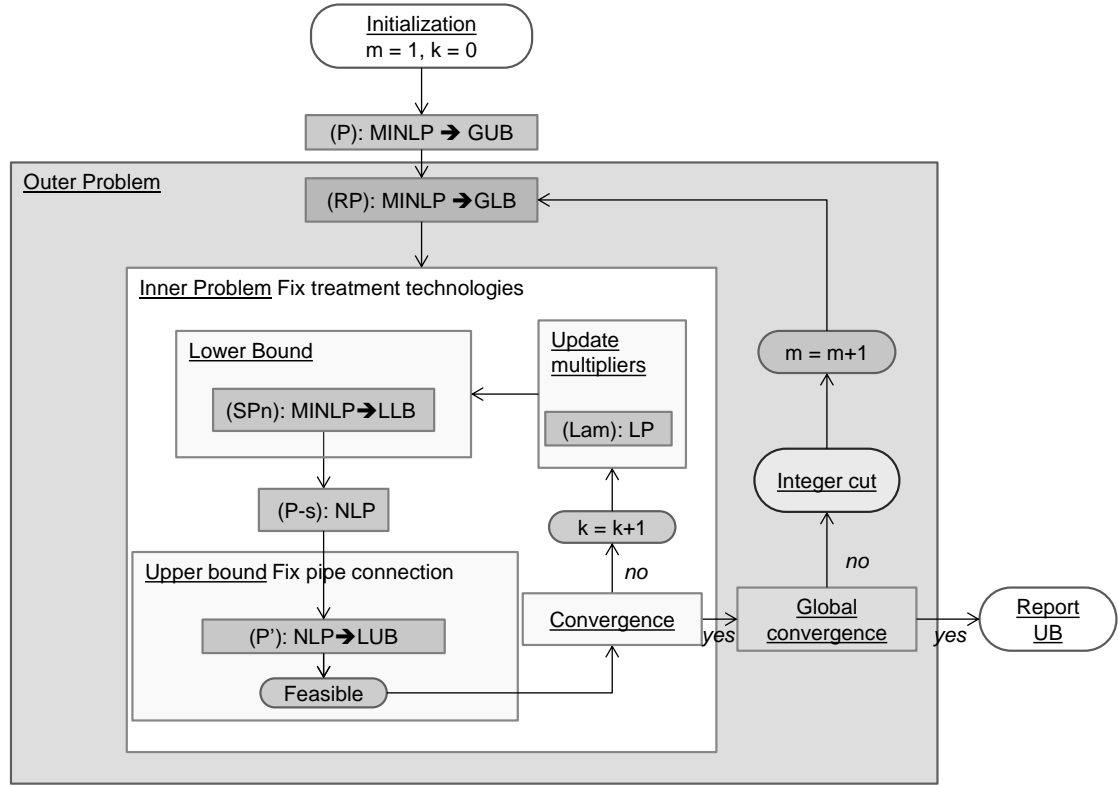


Figure 3.8: Decomposition scheme.

to the objective function as shown in equation (3.29).

$$\begin{aligned}
 \min. \quad z_n = p_n AR & \left[\sum_{t \in TU} IC_{tn}^{TU} + \sum_{i \in Pipe} (C_i^{Pipe} y_i^n + IC_i^{Pipe} (\hat{F}_i^n)^\delta) \right] \\
 & + H p_n OC^{FW} FW_n + H p_n \sum_{i \in Pipe} OC^{Pipe} F_{in} + p_n OC_{tn}^{TU} \\
 & + \sum_i (\lambda_{in}^f - \lambda_{i(n-1)}^f) \hat{F}_i^n + \sum_i (\lambda_{in}^y - \lambda_{i(n-1)}^y) y_i^n \\
 & + \sum_i (\lambda_{rtn}^d - \lambda_{rt(n-1)}^d) d_{rt}^n + \sum_{t \in TU} (\lambda_{tn}^{IC} - \lambda_{t(n-1)}^{IC}) IC_{tn}^{TU} \\
 n = 1, \dots, |N|
 \end{aligned} \tag{3.29}$$

Problem (P-s) can help to improve the solution quality of the upper bounding problem

(P'). ($P-s$) is an NLP that represents the simplified multi-scenario model. It applies effective contaminant removal ratios β_{tj}^n and flow recovery ratios Rr_t^n from the subproblems (SP_n), where $F_{out} = Rr_t F_{in}$. Problem (P') is the NLP upper bounding problem in the inner iteration resulted from fixing all the integer variables in the original problem (P). In problem (Lam) the Lagrangean multipliers are updated using a hybrid algorithm based on the combination of cutting-plane and subgradient strategies described in Oliveira et al⁷⁹.

3.5.3 Algorithm

The steps of the proposed algorithm are as follows:

- 0. Initialization** Determine bounds on variables d_{rt} and \hat{F}_i based on the numerical data provided in each water network. Set all multipliers $\lambda_{in}^f, \lambda_{in}^y$, and λ_{rtn}^d to zero. Set outer iteration count $m = 1$, inner iteration count $k = 0$.
- 1. Global Upper Bound** Fix all binary variables y_i to 1, and solve the MINLP problem (P) in terms of the binary variables Y_{rt} for the treatment units using non-global MINLP solvers such as DICOPT or a global solver such as BARON and LINDOGlobal with a large optimality gap (e.g. 70%). If the time limit is exceeded, fix the binary variable Y_{rt} to 1 for a subset of treatment technologies and solve problem (P) again.
- 2. Global Lower Bound** Solve the MINLP problem (RP) to determine the global lower bound. Once the solution is obtained, fix the binary variables, Y_{rt} , for the inner problem.
- 3. Inner Problem** Set $k = 1$.
 - i.** Solve the MINLP (SP_n) for each scenario $n \in N$ to global optimality for the fixed treatment selection. Three potential situations could result from this step. First, if all the subproblems are feasible and are solved to ε_1 -tolerance within time limit, then we obtain for the selected treatment units a lower bound solution Z^{LLB} by taking the sum of the subproblems' objective values z_n^* . If

the problem is not solved within ε_1 -tolerance in the specified time limit, then we convexify the subproblem as in problem (RP) to form (rSP_n) , which can then be solved using a non-global MINLP solver. The third situation arises when any of the sub-problems is found to be infeasible, in which case the set of treatment selection is eliminated.

- ii.(optional) Solve $(P-s)$ to local optimality.
 - iii. The binary variables y_i in subproblem (P') are fixed to zero if the flowrate capacity, \hat{F}_i , for a given pipe i takes a value of zero in $(P-s)$. Solve the upper bounding problem (P') to local optimality. Update Z^{LUB} .
 - iv. Check for convergence of the inner problem. If $Z^{LUB} < Z^{GUB}$, then update $Z^{GUB} = Z^{LUB}$. If $(Z^{LUB} - Z^{LLB})/Z^{LUB} < \varepsilon_2$ or if $Z^{LLB} > Z^{GUB}$, end inner loop.
 - v. Update the Lagrangean multipliers in (Lam) . $k = k + 1$ as described in ⁷⁹.
- 4. Convergence** Check global convergence criteria $(Z^{GUB} - Z^{GLB})/Z^{GUB} < \varepsilon$, if the algorithm does not meet the ε -convergence criterion, add an integer cut (3.30) to (RP) to eliminate the current set of Y_{rt} . Reset all multipliers to 0. $m = m + 1$.

$$\sum_{(r,t) \in B^m} (1 - Y_{rt}) + \sum_{(r,t) \in N^m} Y_{rt} \geq 1 \quad \forall m = 1, \dots, M \quad (3.30)$$

$$B_{rt}^m = \{(r, t) | Y_{rt}^m = 1\} \quad N_{rt}^m = \{(r, t) | Y_{rt}^m = 0\}$$

3.6 Numerical examples

Three water network examples are provided to demonstrate the formulation and decomposition algorithm. Problem (GDP-1) was automatically reformulated as an MINLP using GAMS/EMP (Extended Mathematical Programming)⁸⁰, which is a modeling framework for automated mathematical reformulation. The MINLP models are formulated using GAMS 24.0 and solved on an Intel Core i7 2.93 GHz machine with 4.00 GB memory.

CPLEX was used for the MILP problems, and DICOPT⁸¹, LINDOGlobal⁸² and BARON 11.1⁵³ are used to solve the MINLP problems. Note that while DICOPT is a non-global solver, LINDOGlobal and BARON are global optimization solvers.

3.6.1 Example 1: illustrative example with short-cut treatment unit models

In this example, we consider the problem structure presented in the illustrative example in section 3.3. The process unit data are the same, but we now incorporate short-cut models of treatment units for TSS and TDS removal. TU1 involves as choices reverse osmosis and ion exchange for the removal of TDS, and TU2 involves sedimentation and ultrafiltration for the removal of TSS. The superstructure is shown in Figure 3.9.

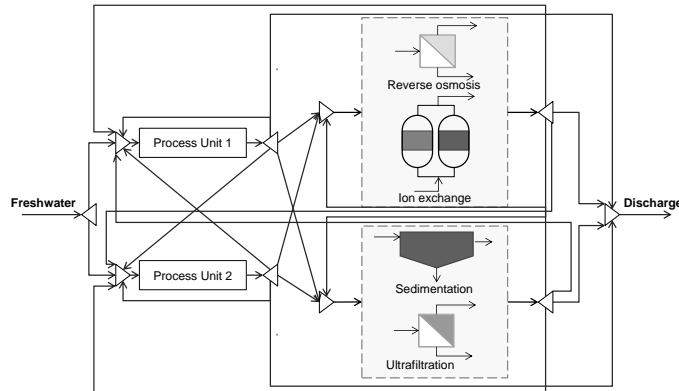


Figure 3.9: Example 1 network superstructure.

The full problem and the decomposition algorithm subproblems' model statistics are shown in Table 3.9. The full MINLP, which is obtained with the hull reformulation (GDP-s)⁸³ problem is solved using BARON to arrive at the solution of \$434,164.59 in 2,132 CPUs with a 5% optimality gap. Then the problem is solved using the decomposition algorithm to global optimality. The first step is to obtain a good initial solution from problem (P). This is accomplished by using LINDOGlobal terminating the search as soon as a feasible

Table 3.9: Example 1 subproblem model statistics.

Subproblem	Formulation Type	UB/LB	Solution Type	# Binary Vars	# Cont Vars	# Constraints	# Non-convex Terms
(P)	MINLP	UB	Global	24	465	610	198
(SP_n)	MINLP	LB	Global	20	203	206	86
$(P-s)$	NLP	-	Local	-	373	547	144
(P')	NLP	UB	Local	-	435	430	198

solution is found. The global upper bound \$462,712.88 is obtained in 93 CPUs. The convex MILP relaxation (RP) provided a global lower bound of \$352,346.66. Ion exchange is chosen to remove TDS and ultrafiltration to remove TSS. For these choices the MINLP subproblems (SP_n) is each solved with BARON with a 5% optimality tolerance. They each yield an objective value of \$146,711.84, \$142,964.20, and \$142,619.09. Summing the values from the three scenarios yields a lower bound of \$432,295.12. We then solve the NLP optional step ($P-s$) to reach a solution of \$381,083.40, a lower bound for this configuration. The objective value of this problem is not crucial to the algorithm since the treatment units are simplified, instead, we use this step to obtain stream connectivities for the NLP problem (P') with that fixed configuration to obtain an upper bound. The NLP problem (P') yields a solution of \$433,173.72 (shown in Figure 3.10a), which is a new upper bound. Since the lower bound (\$352,346.66) lies below this upper bound, we add an integer cut to the convex MILP relaxation (RP). Since this problem is infeasible within the updated global upper bound, the search is terminated in a total of 471 CPUs. Thus, the decomposition algorithm is able to reduce the computational effort by almost a factor of five (471 CPUs vs. 2,132 CPUs).

In order to demonstrate the advantage of using short-cut models, we can compare its optimal solution with the result from the simplified model. To make the comparison on the same basis, the first step is to optimize the WN with simplified model, then in the second step, the WN with short-cut model is optimized with fixed network structure from step one. The optimized WN structure obtained using simplified models is shown in Figure 3.10b. As can be seen, the main difference is that the treatment unit chosen for TDS removal is reverse osmosis for the simplified model WN and ion exchange for the short-cut model WN. There are also two piping connections that are different in the result, namely, from PU1 to TU1 and from TU1 to PU2. The cost of the network increased from \$430,157

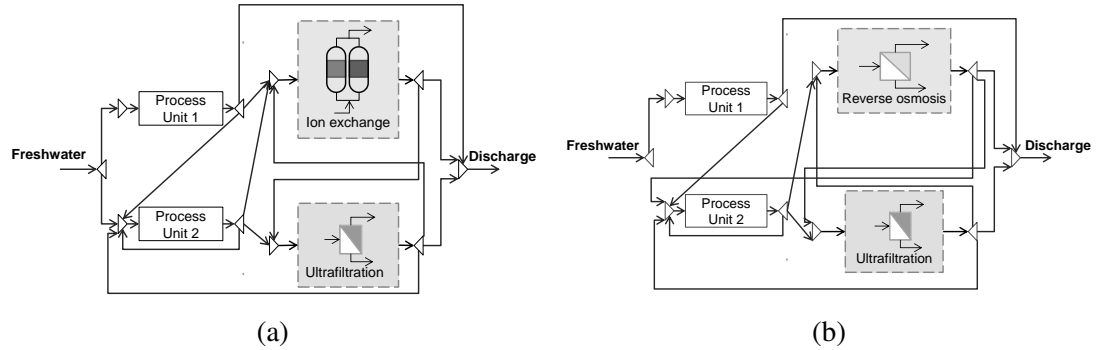


Figure 3.10: Example 1(a) short-cut model optimal solution (b) simplified model optimal solution.

for configuration in Figure 3.10a to \$440,884 for configuration in Figure 3.10b. Note that the problem is optimized to within 1% optimality gap instead of 5% in order to ensure the validity of the comparison. Hence the short-cut WN has a cost of \$430,157 instead of \$433,174 as presented in the detailed decomposition algorithm steps where a 5% tolerance was used.

Furthermore, the recoveries have a direct impact on treatment cost in practice. Thus, the purpose of using short-cut models is to calculate the wastewater treatment recoveries through optimization, whereas simplified models assume that they are fixed. Both specified recoveries in the simplified models and the calculated recoveries in the short-cut models are presented in Table 3.10. Column S1 represents the removal ratios specified in the simplified WN; S2 shows the calculated recoveries from optimizing short-cut WN with the fixed configuration in Figure 3.10b; and S3 represents the recoveries from directly optimizing short-cut WN. From the table, we can see that the removal ratio upper bounds are reached (90% for IX and 99% for UF) or nearly reached (99% for RO) for the selected units, which is due to the specification for the water discharge (10 ppm TDS and 20 ppm TSS).

Table 3.10: Example 1 recovery comparison.

Treatment Unit		n1			n2			n3		
		S1	S2	S3	S1	S2	S3	S1	S2	S3
TDS Removal	RO	80	98	-	90	98	-	99	98	-
	IX	70	-	90	80	-	90	90	-	90
TSS Removal	SE	50	-	-	60	-	-	70	-	-
	UF	70	99	99	85	99	99	99	99	99

Table 3.11: Example 2 metal finishing data.

Stream	Flowrate (ton/h)	Concentration (ppm)											
		TSS			HM			TDS			BOD		
		n1	n2	n3	n1	n2	n3	n1	n2	n3	n1	n2	n3
Metal Containing	5.25	195	150	105	96.59	74.3	52.01	2405	1850	1295	78	60	42
Oily	5.084	546	420	294	0	0	0	3250	2500	1750	260	200	140
General Waters	3.96	39	30	21	14.3	11	7.7	1690	1300	910	58.5	45	31.5
Dye Containing	3.3	136.5	105	73.5	6.5	5	3.5	6890	5300	3710	1950	1500	1050
Discharge Limit			120			30			300			80	

3.6.2 Example 2: metal finishing industry wastewater treatment

The next example comes from a metal finishing industry located in Turkey³⁰. Steel wheel production, tractor production, engine assembly shop, and spring production are the four main production lines that are involved. Each process results in a wastewater stream with various levels of TSS, heavy metal (HM), TDS, and BOD. The worst, nominal, and best scenario concentration values are given in Table 3.11. This example considers only wastewater treatment network (no PU included) whose superstructure is shown in Figure 3.11. We apply the short-cut treatment models for the removal of TSS, TDS, and BOD. For HM removal we assume fixed recoveries. Note that TDS has the highest average concentration among the four groups of contaminant, thus it gives rise to the most difficult removal. On the contrary, HM is the easiest contaminant to remove.

The corresponding MINLP using the hull reformulation⁸³ has 1,229 equations, 47 discrete variables, and 961 continuous variables. Solving (P) directly does not yield a feasible solution using standard solvers such as DICOPT, KNITRO, or SBB. To facilitate computation, we fix all y_i to 1 (i.e. all piping connections exist) and Y_{rt} to 1 for ultrafiltration,

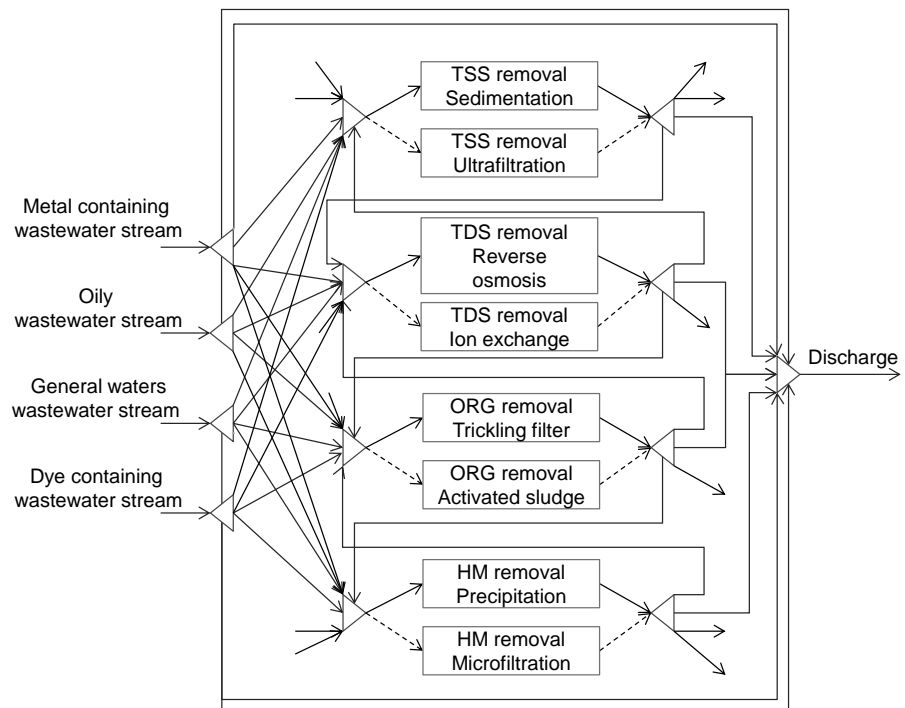


Figure 3.11: Example 2 metal finishing wastewater treatment network superstructure.

reverse osmosis, activated sludge, and microfiltration. With these fixed values, we can obtain a global upper bound with an objective value of \$304,405 in 27.6 CPUs using LINDOGlobal with a 70% optimality tolerance. Problem (RP) is solved subsequently and a global lower bound with an objective value of \$98,790 is obtained in 12.6 CPUs. The lower bound solution fixes ultrafiltration, ion exchange, activated sludge, and microfiltration as the technology selections for the inner iteration. In the operating range of this example, ion exchange has a higher capital cost and a worse removal performance. However, its operating cost is lower than that of the reverse osmosis. In addition, both technologies are capable of meeting the discharge limit. Thus, it is possible that the selections from the lower bound outperform the initial technologies chosen for (P). For the new choices the MINLP subproblems (SP_n) is each solved with BARON with a 10% optimality tolerance. They yield an objective value of \$131,690, \$52,954, and \$46,226. Summing the values from the three scenarios yields a lower bound of \$230,870. We then solve the NLP optional step ($P-s$) to obtain the stream connectivities. Based on the configuration, the NLP problem (P') yields an upper bound of \$234,820. With the integer cut to eliminate the current configuration, the subsequent outer problem (RP) is found to be infeasible; thus, we have reached the global optimum. The entire algorithm requires 2,308.5 CPUs, where 1,608.0 CPUs is used to solve the lower bounding problem. In comparison, the original problem (P) cannot be solved to optimality in the resource limit (7200 CPUs) with LINDOGlobal and BARON.

The resulting configuration is shown in Figure 3.12. Note that the recovery ratio in the ion exchange unit is chosen to be the lower bound 0.5, which implies that it is cheaper to dispose rather than to treat the stream. Also, since the HM concentration in all the wastewater streams are lower than the discharge limit, no HM removal is required.

3.6.3 Example 3: petroleum refinery water use

We consider a modified refinery case study as the final example^{15,84} and the units involved are shown in Figure 3.13. The primary water sources are freshwater and purified water. In addition, crude oil often carries emulsified water, and can be considered as a third process

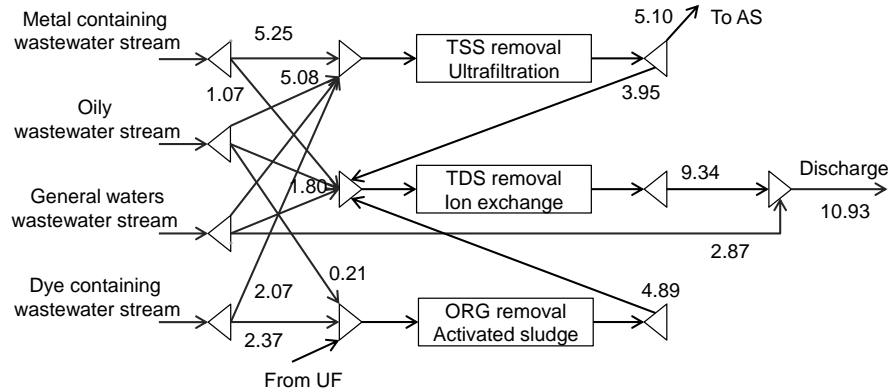


Figure 3.12: Example 2 metal finishing water network configuration.

water source. Two sinks are considered for discharge, a centralized wastewater treatment facility on site and the nearby river. Five water-using process units are considered in this study. They are desalination, column condensation, steam generation, cooling water, and general consumption. The water quality and flowrate requirement of these processes are summarized in Table 3.12. The third water source, crude oil train, has a maximum flowrate of 15 ton/h, and the wastewater treatment plant can accept a maximum of 360 ton/h of wastewater. Reverse osmosis and ion exchange remove salt from the streams, and trickling filter and activated sludge are used to remove organic content of the streams.

The resulting MINLP has 1,768 equations, 1,331 continuous variables, and 85 binary variables. Note that the problem size is larger than that of Example 2. However, solving the problem directly using LINDOGlobal yields an optimal solution of \$1,906,264 with 5% optimality gap in 209 CPU s. The reason that the problem can be solved effectively without the decomposition algorithm can be seen in the resulting network configuration as shown in Figure 3.14. Trickling filter is chosen to remove ORG, and the highest removal ratio, $R_c^{ORG} = 90\%$, is selected. The consumption of freshwater is 360.5 t/h, and the consumption of purified water is 47.5 t/h, which is a 734.5 t/h reduction had reusing and recycling not been performed. First, the wastewater streams are reused and recycled within the network instead of being discharged to the wastewater sinks. Also, no salt-removal unit is selected in this configuration, which is due to the high TDS tolerance level

CHAPTER 3. WASTEWATER REGENERATION MODELS FOR WATER NETWORK OPTIMIZATION

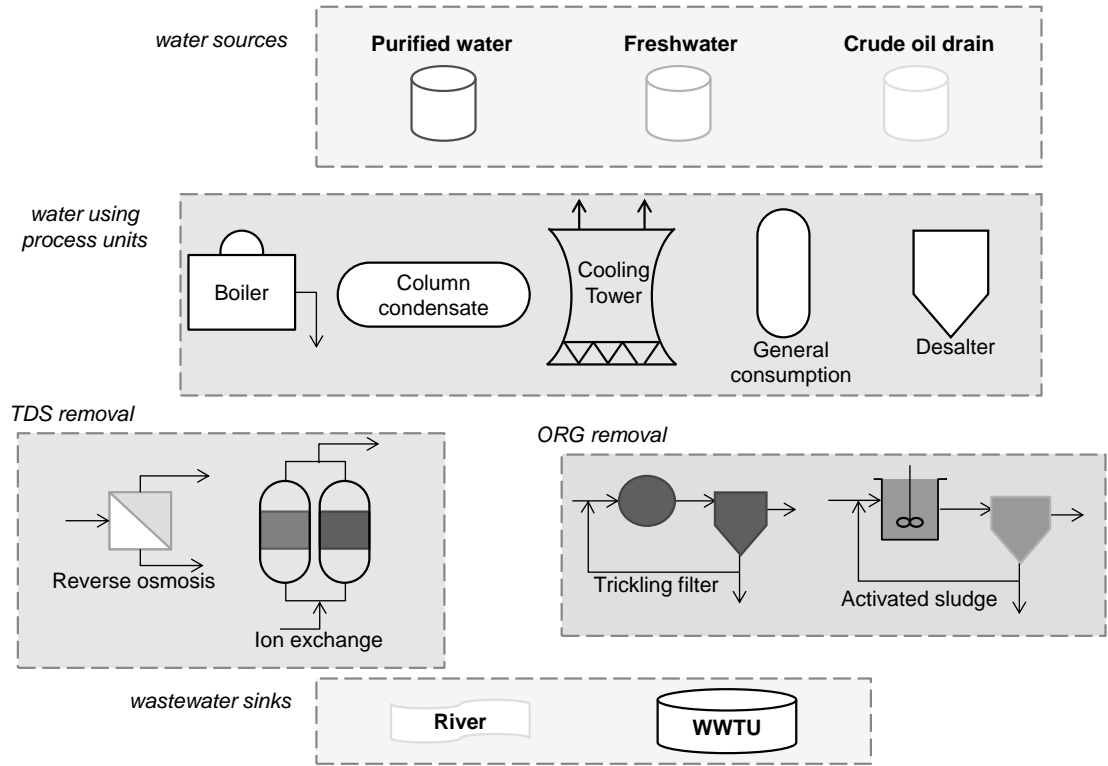


Figure 3.13: Example 3 refinery process water system superstructure.

Table 3.12: Example 3 petroleum refinery data.

(a) Process units

	Flowrate (ton/h)	Loss (ton/h)	Discharge Load (kg/h)						C_{in}^{max} (ppm)	
			n1		n2		n3		TDS	ORG
			TDS	ORG	TDS	ORG	TDS	ORG		
Boiler	25	18	3.5	1.21	2.07	1.10	0.64	0.99	10	1
Condensate	22.5	0	4.28	146.23	3.94	125.55	3.6	104.87	10	1
Cooling tower	1000	405	615	219	310.9	110	6.8	1	2500	220
General consumption	10	0	9.5	70	8.29	61.1	7.08	52.19	300	50
Desalter	85	0	153	544	136.07	510.31	119.14	476.63	200	100

(b) Concentration limit (ppm)

	Sources			Discharge sinks	
	Fresh water	Purified water	Crude oil train	River	Wastewater treatment plant
TDS	50	10	135	50	364
ORG	15	0	45	200	759

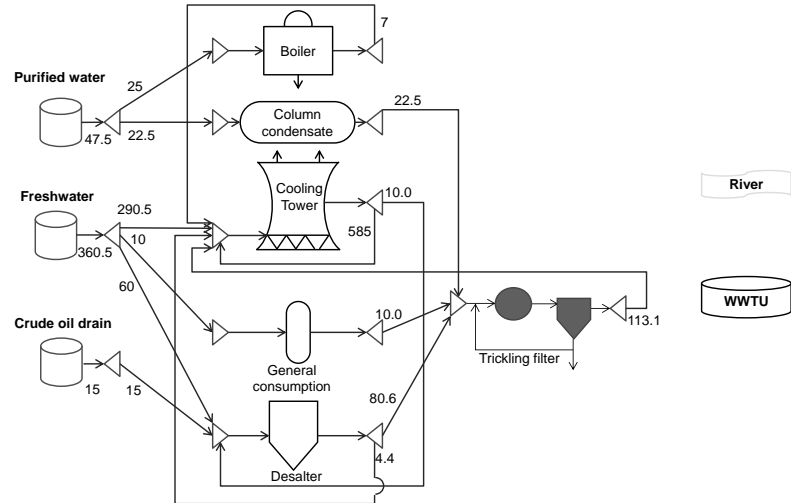


Figure 3.14: Example 3 optimal network configuration for the refinery water system.

at the inlet stream of the cooling tower, as well as the high rate of evaporation loss in the cooling tower. The cooling tower then reuses most of its outlet stream, leading to a cooling loop that is more efficient than a once-through design.

3.7 Conclusion

By considering the use of short-cut models for treatment units that remove TDS, TSS, and organics, we are able to exploit the trade-offs between treatment cost and removal efficiency of the units. The model (GDP-1) is developed to accommodate the modifications in the architecture and formulation of the treatment units. In order to solve the resulting formulation to global optimality, we have presented a Lagrangean-based decomposition algorithm that is tailored to the water network problem. Several examples are presented to demonstrate the effectiveness of the algorithm in improving the quality and computation effort of the solution.

Nomenclature

Reverse osmosis

ΔP_{drop}	Pressure drop along the membrane channel, Pa
$\Delta\pi$	Osmotic pressure difference across the membrane, Pa
P_f	Pressure at the feed side of the membrane, Pa
P_p	Pressure at the permeate side of the membrane, Pa
N	Number of membranes

Ion exchange

X^{IX}	Mass fraction in inlet water of ion wanted to be removed
q	Operating capacity of the resin, $eq/Lresin$
MW_{ca}	Molar mass of cation, $kg/kmol$
MW_{an}	Molar mass of anion, $kg/kmol$
SLR	Surface loading rate, m/h
SFR	Service flow rate, $m^3water/(m^3resinh)$
BV	Volume of water treated per volume of resin, $Lwater/Lresin$
CT	Contact time, h
V_{IX}	Resin volume, m^3
V_{ww}	Volume of waste water treated
A_{IX}	Resin cross-sectional area, m^2

Ultrafiltration

k_M	membrane resistance coefficient
μ	dynamic viscosity of water
ΔP	Transmembrane pressure
A_{memb}	Membrane area

Sedimentation

t	Nominal detention time, h
OR_{SE}	Overflow rate, m^3/m^2day
A_{SE}	Area of the filter media, m^2

NC	Volume of the filter media, m^2
D_{SE}	Depth, m
Activated sludge	
SRT	Solid retention time, day
X_{AS}	Biomass concentration in the aeration tank, g/m^3
τ	Residence time, day
X_T	MLVSS concentration, g/m^3
$X_{0,i}$	Influent nbVSS concentration, g/m^3
$P_{x,bio}$	Biomass wasted, g/day
$P_{X_T,VSS}$	Total sludge wasted daily, g/day
Ro_{AS}	Oxygen consumption, g/day
V_{AS}	Aerator volume, m^3
Acl_{AS}	Clarifier area, m^2
Trickling filter	
R_{rcy}	Recirculation ratio
F	Recirculation factor
W_1	BOD loading applied to the first-stage filter, kg/d
W_2	BOD loading applied to the second-stage filter, kg/d
E_1	Fraction of BOD removal for first stage
E_2	Fraction of BOD removal for second stage
L_B	BOD loading to filter, $kg\ BOD/m^3d$
Ro_{TF}	Oxygen consumption, $kg\ O_2/kg\ BOD\ applied$
OR_{TF}	Overflow rate, m/hr
A_{TF}	Area of the filter media, m^2
D_{TF}	Depth, m
V_{TF}	volume of filter media, m^3
Acl_{TF}	Clarifier area, m^2

Chapter 4

Operational Model for Shale Gas Water Management

4.1 Introduction

In this chapter we develop a model that optimizes water-use life cycle for wellpads through a MILP discrete-time representation. The objective is to minimize the cost of transportation, treatment, storage, and disposal while also accounting for the revenue of gas production within the specified time horizon. This time horizon must be at least one year to capture the seasonal availability of water. Assuming that freshwater sources, river withdrawal data, location of wellpads and treatment facilities are given, the goal is to determine an optimal fracturing schedule and recycling ratio. Since this is a difficult problem to model and solve, we intend to consider as a first step freshwater acquisition.

The chapter is organized as follows. The freshwater handling section accounts for the trade-off between water availability and freshwater transportation cost, as well as environmental implications of transportation. We next address in the wastewater handling section the problem that considers the entire economic optimization, including water treatment, storage, disposal, and income from gas production. In each section, relevant background

is introduced first, followed by a general problem statement, its optimization formulation, and an example to illustrate the application of the optimization model. We focus on applications in the Marcellus shale play although the proposed models can be used in other shale gas formations.

4.2 Freshwater handling

4.2.1 Background

The conventional sources for water used in hydraulic fracturing includes surface water, ground water, treated wastewater, and cooling water. The most common one is surface water such as lakes or rivers, which typically costs about \$1.76-3.52/m³ in the state of Pennsylvania. On the other hand, some operators are exploring the possibility of using acid mine drainage (AMD) which is present in large volume in the Marcellus region. In addition, natural gas liquid (NGL) is also being used by some as frac fluid. The issues commonly faced by water acquisition include seasonal variation in water availability, permitting complexity, and access near the drilling site. In Pennsylvania, the Susquehanna River Basin Commission (SRBC) has incorporated minimum "stream pass-by flows" into water withdrawal permits. This rule is meant to ensure that enough water remains flowing downstream.

Freshwater is transported to the wellpad by truck or by pipeline (Figure 4.1). Transportation costs are often the primary economic driver influencing water management decisions. Approximately 4,000-6,500 one-way truck trips are required for the completion of a typical wellpad. While trucks allow for a more flexible operation, it causes burden to the local community in terms of noise and road damage. The operators are responsible for maintaining both paved and unpaved roads through "bonding". In addition, all operators that share a portion of the road are responsible for damage caused by the heavy trucking traffic. Thus, the combination of expensive trucking cost and the costs associated with road deterioration encourages operators to use pipelines that are more economical by drawing water

from nearby sources. However, many are temporary pipe networks given the relatively short duration of the fracturing process of the wells.



Figure 4.1: Water transportation through temporary piping.

Once water is transported to the wellpad, frac fluid is prepared. Note that chemical additives make up approximately 0.5% of this fluid⁴⁷. Frac fluid quality is the key driver for water requirement because contaminants can interfere with its performance. For example, sulfates cause scaling and the presence of TSS can decrease biocide effectiveness and plug wells. In addition, water compatibility with the different types of frac fluid designs governs treatment requirements. The different fluid designs include slickwater, linear gel, and crosslink gel. As a result, operators need to exercise proper caution when preparing the frac fluid. Yet the exact criterion for fluid composition is not well-defined. Many operators use a "copy-and-paste" approach to determine the treatment requirement for the frac fluid. This lack of exact criteria is partially due to the unclear correlation between frac fluid composition and operational issues.

4.2.2 Problem I

Motivated by the logistics of water distribution shown in Figure 1.5, the first specific problem that we address is as follows. We assume we are given a number of freshwater sources,

freshwater withdrawal data, location of wellpads, and location of treatment facilities for removing suspended solids. Also, given is the total number of frac stages for each wellpad, date restrictions for hydraulic fracturing, and the number of frac crews available. The goal is to determine the fracturing schedule of the wellpads, the rate that each wellpad is stimulated, as well as the starting date for the frac holiday. The frac holiday is a flexible period of time when the frac crew take time off, usually due to low water availability. The objective is to minimize the expected trucking and pumping cost of the water required to complete all the wellpads. The scenarios considered for the uncertain availability of water are the years of historical stream data for which equal probability is assigned to each of them.

The main opportunity for optimization is the trade-off between the cost of trucks and pipelines for freshwater transportation, while accounting for water availability in the water sources. There are two types of freshwater sources under consideration. The first one, an "uninterruptible" source, is a large body of water (e.g. large river or lake) that provides water year-round. However, the source is usually located remotely so that trucking is required for transporting freshwater from the source to the wellpads. Alternatively, there are interruptible water sources (e.g. small river or creek) that can be piped to the wellpads, but with an uncertain water supply throughout the year. Typically, the interruptible water source is dry in the summer to early fall, and its withdrawal is only allowed when a minimum flowrate requirement has been met. Historical flowrate data (shown in Figure 4.2⁸⁵) can be used to estimate water availability and guide decision-making for the fracturing schedules. Specifically, if the water source flowrate is above the withdrawal criterion, then the operators are allowed to pump water from the source to their impoundment; otherwise, pumping is not allowed. There are two options on how to use these historical data to account for uncertainty in the water supply. The first option is to determine for each day of the year the mean value of the water flowrate over the number of years, R . Alternatively, we can treat data from each calendar year as a scenario, each with equal probability, $1/R$, and formulate the problem as a two-stage stochastic programming problem⁸⁶. The first stage decisions determine the dates to fracture each wellpad and number of stages to stimulate per day, and the second stage decisions determine the amount of water for pumping

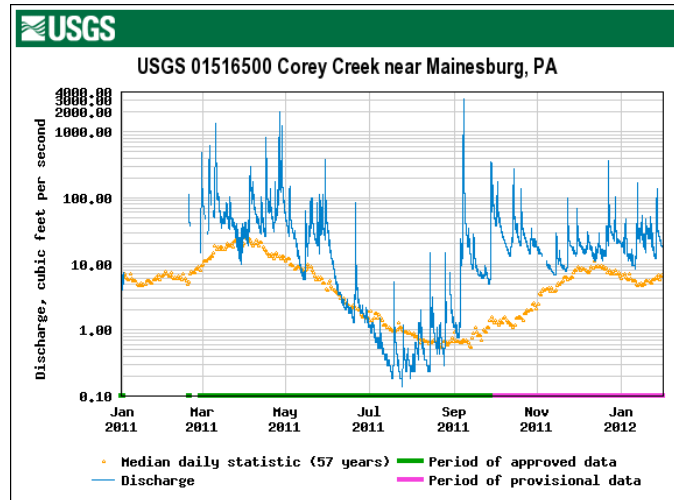


Figure 4.2: River discharge statistics.

and trucking from the water sources to their respective impoundments on each day. In this chapter, we consider the second approach.

The scheduling problem can be formulated through a discrete-time model using as a basis the state-task network (STN) representation for batch scheduling⁵⁷. The STN representation consists of three major elements: states, tasks, and equipment. Similar to STN-based batch processing models, the processing tasks in the context of this work correspond to the fracturing of the wells on each wellpad. These tasks require the assignment of frac crews and then drilling equipment to the wellpads as shown in the superstructure in Figure 4.3. The states correspond to the water sources and impoundments that feed into the wellpads. The flowback water is not shown in Figure 4.3 since we do not consider water treatment and reuse as will be done later in problem II.

The assumptions made in the formulation of the model are as follows:

1. Each of the interruptible sources is connected through piping to an impoundment that serves as a buffer tank for the storage of freshwater. The combination of an interruptible source and its impoundment is defined by t .
2. Each wellpad is connected to exactly one of the impoundments through piping.

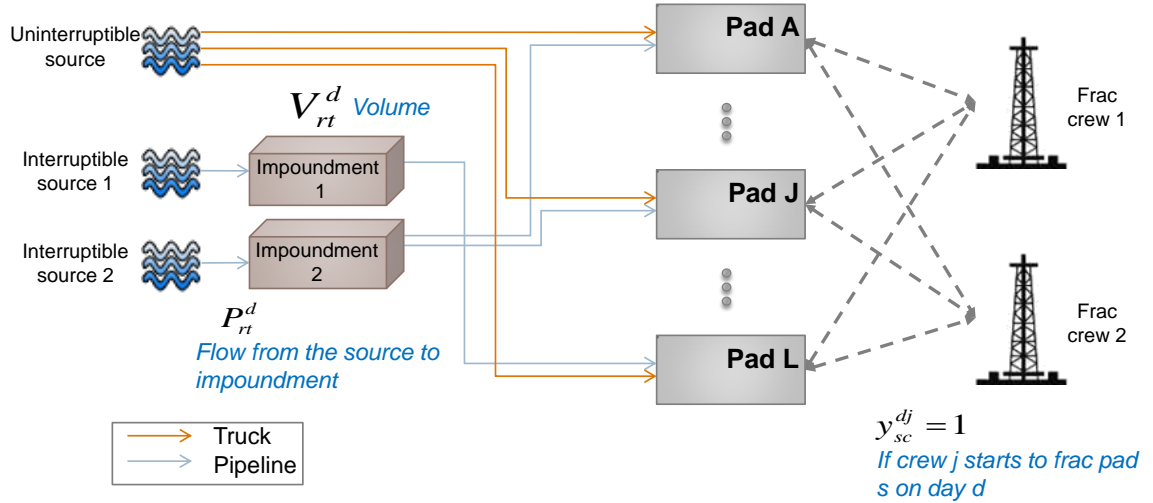


Figure 4.3: Problem I superstructure.

3. The pumps can only operate from the impoundment at the maximum rate, or they do not pump at all.
4. The wells in each wellpad are aggregated (i.e. each well has a fixed number of stages, and the wellpad is characterized by the total number of stages of the wells on the pad). All wells on the same wellpad are completed before the frac crew is transferred to another wellpad.
5. A fixed percentage of freshwater is supplied for frac fluid from the uninterrupted and interruptible sources.
6. Only existing water pipelines are considered.
7. Since the distance between the uninterrupted source and the wellpads is significantly further than the distance among wellpads, trucking cost is assumed to be volume-dependent only.
8. A fixed time horizon consisting of days d as time intervals is considered.

4.2.3 Optimization model I

Problem I can be formulated as a two-stage multi-period MILP model under uncertain availability of interruptible water that includes the following elements: allocation constraints, material balances, date restrictions, and an objective function. The main decision variables are as follows. y_{sc}^{dj} is a stage-one binary variable that indicates the starting date d for stimulating wellpad s with frac crew j . P_{rt}^d is a stage-two continuous variable indicating volume pumped from the interruptible source to the corresponding impoundment on day d use as scenario historical water flowrate value in year r . D_{rt}^d , the water requirement deficit, is the volume supplied by truck hauling instead of pumping.

Allocation constraints. Constraint (4.1) specifies that each wellpad s has to be fractured exactly once at a given date d , for a number of stages to frac per day c , and by crew j .

$$\sum_c \sum_d \sum_j y_{sc}^{dj} = 1 \quad \forall s \quad (4.1)$$

Constraint (4.2) represents a backward aggregation constraint from the STN model⁸⁷ that ensures there is no overlap between different wellpad operations for each frac crew j ,

$$\sum_s \sum_c \sum_{d'=d-fD_{sc}-CT_s^{s'}+1}^d y_{sc}^{d'j} \leq 1 \quad \forall d, \forall j \quad (4.2)$$

where D_{sc} represents the duration of the hydraulic fracturing, $CT_s^{s'}$ represents the transition time required to move the frac crew from wellpad s to wellpad s' .

Material balances. The freshwater use is modeled with the following mass balances. The volume of water used for each stage, dy_{sc}^{fw} , is fixed. However, the fracturing rate for each wellpad, indicated by the index c , is determined by the optimization problem. This rate is limited between 2 to 4 stages per day. Constraint (4.3) determines the daily freshwater use for each wellpad. All but the last day require the same volume of water dy_{sc}^{fw} since the rate is fixed. The volume of water required on the last day ds_{sc}^{fw} , is determined by the stages left for completion as shown in Figure 4.4.

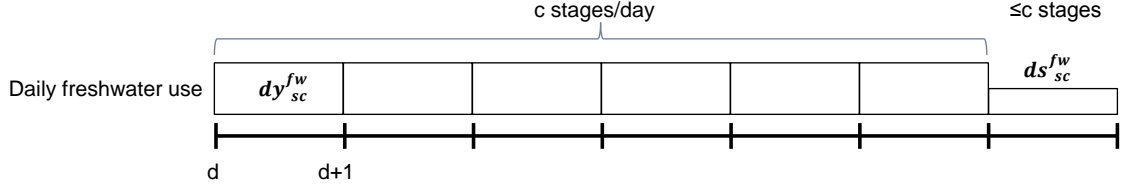


Figure 4.4: Daily freshwater requirement for a given wellpad.

$$da_s^{fw,d} = \sum_c \sum_j \left(\sum_{d'=d-fD_{sc}+2}^d dy_{sc}^{fw} y_{sc}^{d'j} + \sum_{d'=d-fD_{sc}+1} ds_{sc}^{fw} y_{sc}^{d'j} \right) \quad \forall d, \forall s \quad (4.3)$$

Constraint (4.4) describes the total daily freshwater use from each impoundment $to_t^{fw,d}$, given the piping connections TP_{st} between the impoundments t and the wellpads s .

$$to_t^{fw,d} = \sum_{s \in TP_{st}} da_s^{fw,d} \quad \forall d, \forall t \quad (4.4)$$

The daily impoundment level V_{rt}^d for a given scenario year r is tracked by the following mass balance (4.5).

$$V_{rt}^d = V_{rt}^{d-1} + P_{rt}^d - to_t^{fw,d} + D_{rt}^d \quad \forall d, \forall r, \forall t \quad (4.5)$$

where the volume on a given day, V_{rt}^d , is determined by: i) the volume in the previous day, ii) plus water pumped from the interruptible source, iii) minus total freshwater used from the impoundment, iv) and plus water transported by trucks.

Date restrictions. The dates for fracturing each wellpad are limited by several factors. For example, stimulation cannot start until two weeks after drilling is completed due to the time needed to remove the rig and to prepare the well for completions. Since temporary water pipelines have to be connected between the impoundments and the wellpads, stimulation cannot begin until the pipelines are secured. In addition, gas pipelines have to be installed before the frac is completed. These can be enforced by setting the binary variable y_{sc}^{dj} to zero for the durations of restricted time period.

In addition, constraint (4.6) ensures that a target number of stages T is completed by a given date E within the time horizon, and where fD_{sc} is the time it take to fracture a wellpad s with c stages. The total number of stages for a given wellpad s is denoted by sgT_s .

$$\sum_s sgT_s \sum_c \sum_j \sum_{d=1}^{E-fD_{sc}} y_{sc}^{dj} \geq T \quad (4.6)$$

A frac holiday of length hD can be incorporated in the model by constraints (4.7) and (4.8). (4.7) is a big-M constraint that disallows operation during the holiday period. Constraint (4.8) indicates that only one frac holiday is allowed.

$$\sum_c \sum_j \sum_s \sum_{d'=d}^{d+hD} y_{sc}^{d'j} \leq |s|(1 - z^d) \quad \forall d \quad (4.7)$$

$$\sum_d^{|d|-hD} z^d = 1 \quad (4.8)$$

where z^d indicates the starting date for the frac holiday.

In addition, each wellpad s has to be completed before the end of the time horizon. In constraint (4.9), we ensure that a wellpad cannot start stimulating after fD_{sc} days prior to the last day of the time horizon.

$$\sum_c \sum_j \sum_{d>|d|-fD_{sc}} y_{sc}^{dj} = 0 \quad \forall s \quad (4.9)$$

Objective. Finally, the objective function (4.10) minimizes the expected transportation cost from trucking and pumping, which is defined for the scenarios given by the R years of historical data.

$$\text{Expected cost} = \sum_s OC_s^{truck, fw} \sum_d \sum_r \sum_{t \in TP_{st}} \frac{D_{rt}^d}{R} + \sum_s OC_s^{pump, fw} \sum_d \sum_r \sum_{t \in TP_{st}} \frac{P_{rt}^d}{R} \quad (4.10)$$

The MILP model given by Eqs. (4.3) – (4.10), defines then the formulation for the freshwater acquisition problem I. It is a two-stage programming problem where the stage-one decisions correspond to the variables y_{sc}^{dj} , z^d , $da_s^{fw,d}$, and $to_t^{fw,d}$, while the stage-two decisions for each scenario r correspond to P_{rt}^d , V_{rt}^d and D_{rt}^d .

4.2.4 Example 1

We consider an example with 14 wellpads, 540 days discretized at one day per time period, one uninterruptible freshwater source, two interruptible sources connected to impoundments, and one frac crew. The data are given in Tables 4.1 and 4.2. Historical data for the two interruptible sources are given over a total of 30 years. They are not shown here for space limitations but they can be found in USGS Water-Quality Daily Data⁸⁵.

Table 4.1: Example 1 wellpad data.

	A	B	C	D	E	F	G	H	I	J	K	L	M	N
Match with takepoints, TP_{st}	t2	t1	t1	t1	t1	t2	t2	t2	t2	t2	t2	t1	t1	t2
Earliest frac day	1	1	1	1	1	39	1	273	273	273	396	379	379	1
Latest frac day	540	540	540	540	540	540	540	462	462	462	472	540	540	540
# of stages, sgT_s	57	61	54	55	64	26	97	88	86	76	63	100	100	87

Table 4.2: Example 1 parameters and cost coefficients.

Parameter	Symbol	Value
Crew transition time (day)	$CT_s^{s'}$	5
Volume of frac fluid used per stage (m^3)		950
Freshwater used (%)		85
Max pumping rate of $t1$ (m^3)		8176
Max pumping rate of $t2$ (m^3)		2725
Frac holiday (day)	hD	50
Freshwater pumping cost ($\$/m^3$)	$OC_s^{pump, fw}$	15.93
Freshwater trucking cost ($\$/m^3$)	$OC_s^{truck, fw}$	29.35

The two-stage MILP model, which consists of 540 time periods and is defined over 30 scenarios, has 19,552 binary variables, 151,201 continuous variables, and 42,149 constraints. The model is solved using GAMS 24.0/CPLEX 12.5 on an Intel 2.93 GHz Core i7 CPU

Table 4.3: Example 1 solution comparison.

	Heuristic schedule	MILP schedule
Frac holiday (days)	90	171
Trucking cost (\$)	5,886,743	568,827
Water trucked (1,000 m ³)	267.3	25.7
Pumping cost (\$)	9,905,219	12,792,088
Water pumped (1,000 m ³)	829.0	1,070.5
Total cost (\$)	15,791,963	13,360,915

machine with 4GB of memory. The model was solved to a 2.8% optimality gap in 351 CPUs.

The result is compared against a heuristic schedule shown in Table 4.3. The heuristic schedule considers all 30 years of historical water withdrawal data on a daily basis. The total expected cost is reduced by \$2.4 million (from \$15,791,963 to \$13,360,915). Note that the total amount water consumed in both schedules is the same, 1.1 million m³. However, the trucking cost is reduced from \$5.9 million to \$569,000, which is one order of magnitude improvement. This is an important result since it means that instead of requiring approximately 14,010 one-way truck trips, the 14 wellpads can be fractured using only 1,350 truck trips, representing only 2.4% of the overall water requirement. This also means that the CO₂ emissions from trucking are reduced from 630 metric tons down to 60 metric tons. Thus, both cost and environmental benefits can be achieved through more efficient use of the water available in the interruptible sources. The reason behind the improvement can be explained through a comparison between the optimized schedule against the heuristic schedule of the 14 wellpads as shown in Figures 4.5 and 4.6. As can be seen in Figure 4.5, the schedules are quite different as they involve different sequences and number of stages. For example, wellpad H requires 2 stages per day in the heuristic schedule, while the optimal MILP schedule involves 4 stages per day, and therefore it is completed in half the time. In Figure 4.6, the average daily impoundment storage levels between the heuristic schedule and the optimized schedule are compared. Note that the curve representing the optimized schedule generally lies on top of the heuristic curve, which indicates that the optimized schedule manages to obtain higher water availability from the interruptible

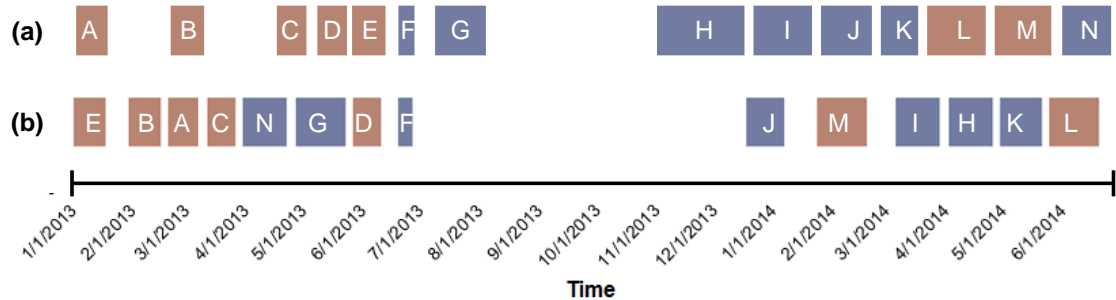


Figure 4.5: Example 1 fracturing schedule from (a) heuristic method (b) MILP model.

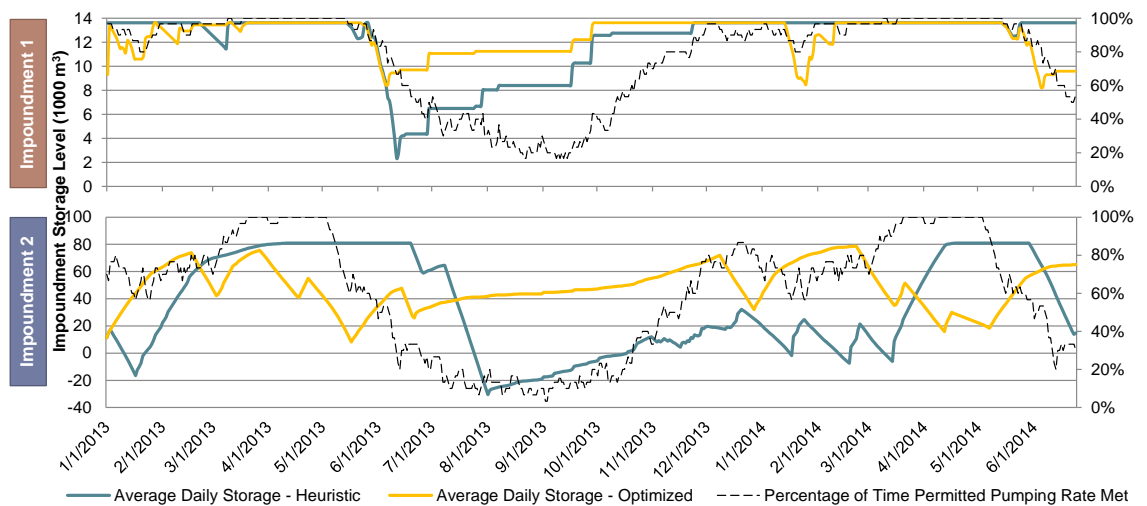


Figure 4.6: Daily impoundment volume comparison.

sources. As a result, less trucking is required, the infrastructure investments are better utilized, and savings in transportation cost can be achieved.

In addition, the choice of transportation affects the rate at which the wellpads are stimulated. Figure 4.7 shows the daily truck use for the two schedules. Clearly the heuristic schedule requires significantly more trucking. Wellpad H is fractured in early fall when there is less water available in the impoundment since a large volume is required to be trucked to H at the beginning of the period. Due to the higher cost of trucking, the heuristic schedule chooses to fracture H at the slowest rate possible (2 stages per day). In contrast,

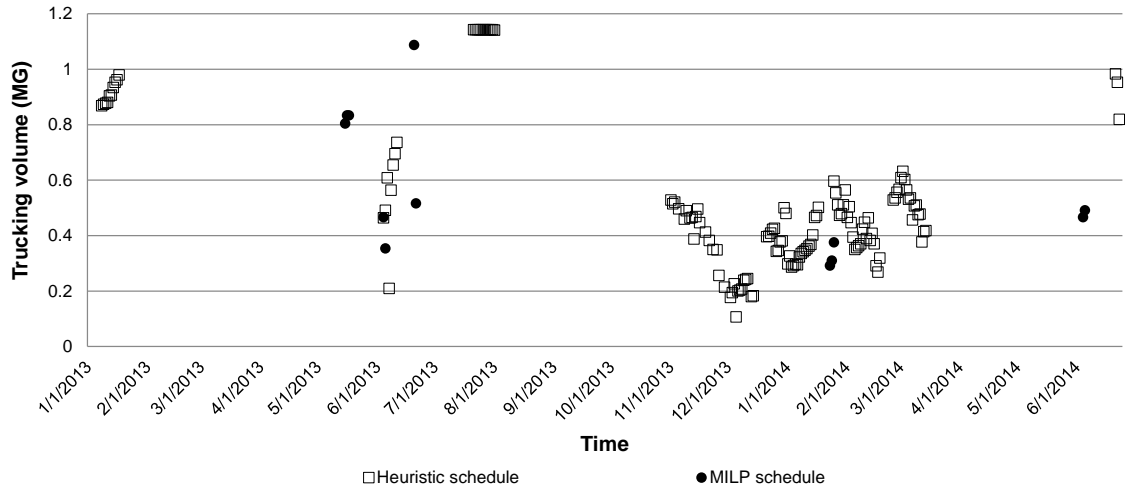


Figure 4.7: Daily truck use comparison.

the optimized schedule fractures H at 4 stages per day since it can be stimulated at a later date when there is more water in the impoundment, so fewer truck trips are required for this specific wellpad.

It is interesting to note that if we solve the MILP model governed by Eqs. (4.3) – (4.10) as a deterministic model using the mean values for the historical flowrate data, this yields a smaller MILP problem with 9,776 binary variables, 57,241 continuous variables, and 10,829 constraints. The problem was solved to optimality in only 18.5 CPUs. However, when we fix the stage-one decisions of deterministic solution, and solve the stochastic programming model over the 30 scenarios, we obtain an expected cost of \$15,796,516, which in fact is worse than the heuristic solution and significantly higher than the expected cost of \$13,360,915. Therefore, the value of the stochastic solution⁸⁶ in this example is \$2,435,601.

4.3 Wastewater handling

4.3.1 Background

In the next section of the paper we extend the MILP model for Problem I so as to account for treatment and reuse of the water. Once the frac fluid is injected into the wellbore, approximately 60-90% of the water used in fracturing does not return to the surface since it is trapped within the formation⁴. In the first few weeks there is flowback water, which is characterized by high volumetric flowrate and relatively low TDS concentration as shown in Figure 4.8. Flowback water includes contaminants such as TDS, total suspended solids (TSS), organics, and metals⁴⁷. The longer the frac fluid remains below ground, the more pollutants the fluid absorbs. For example, Marcellus is a highly desiccated formation due to high capillary binding. As a result, only 10 – 15% of the injected fluid will return as flowback water within the first two weeks. Water that returns to the surface after the initial stage is produced water, which consists of a combination of injected frac fluid as well as the water that exists in the formation. Produced water is removed from the gas at the wellpad before the gas is delivered into the gas pipeline. In general, produced water has high salinity (>120,000 ppm) and low flowrate. Whereas the Marcellus and Utica formations produce less than 0.1 L per m³ of produced water, the Barnett shale play produces 0.3 - 0.8 L per m³. In addition, there is also high variability among the wellpads in terms of the composition of the flowback water. The contaminant levels that are generally of interest are TDS, TSS, calcium, and sulfate.

Following hydraulic fracturing, treated wastewater can be mixed with freshwater for the next operation. The contaminants are removed through a combination of mechanical, chemical, and thermal treatment processes. Typically filtration or electric coagulation is performed to remove TSS, bacteria, and heavy metal present in the flowback water. These recycling options are cheap at around less than \$25/m³. In comparison, it is more costly to reduce the TDS level, which can be accomplished through reverse osmosis, distillation, evaporation, and crystallization, all of which incur high cost that lies in the \$80-120/m³ range. One way to increase the energy efficiency of TDS removal is through a Mechanical

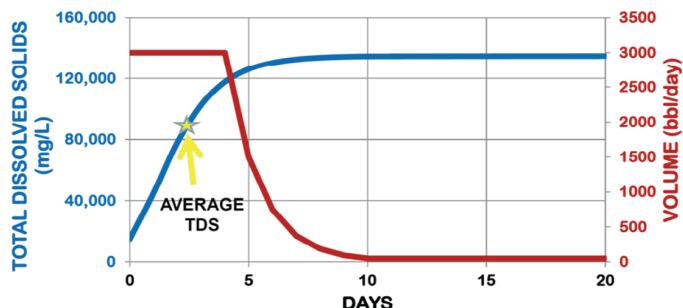


Figure 4.8: Example flowback volume vs. TDS profile³.

Vapor Recompression (MVR) unit⁸⁸. High purity of water is, however, not required for hydraulic fracturing. As a result, salt removal is uncommon among shale gas operations. In order to perform the treatments, there are mobile units and recycling facilities. A mobile treatment unit can be located on a wellpad, whereas a recycling facility is typically further away but has a higher capacity. The mobile treatment unit is highly desirable and takes only 2-3 days to set up. However, the time that is required to obtain the permit for the unit could be very long.

Another major step in water use for shale play involves storage of both freshwater and wastewater. Freshwater is typically stored in open impoundments, while wastewater is heavily regulated and typically stored in frac tanks³. Each barrel of flowback and produced water is tracked. Even after extensive treatment, the flowback water is prohibited from being discharged without extensive permitting. Figure 4.9 shows a wellpad with both an impoundment and frac tanks. When a well is ready to be stimulated, streams from both storage containers and impoundment are mixed together and pumped down the wellbore. Freshwater impoundment costs approximately \$3.86/m³ for the lifetime of the impoundment. In comparison, frac tanks cost \$0.59-1.00/m³/day.

Finally, if needed, disposal of wastewater can be performed using Type II disposal wells. The US Environmental Protection Agency (EPA) implements the Underground Injection Control (UIC) and sets the standards for Class II wells. Most of the underground injection wells in the Marcellus are located in eastern Ohio, and there are only eight permitted disposal wells in Pennsylvania in 2008⁸⁹. The reasons for the difference are: a) Pennsyl-



Figure 4.9: Wellpad impoundment and frac tank aerial view.

vania does not have state level control for permitting Class II wells; and b) the geology in Pennsylvania is not conducive to constructing injection wells. Since Pennsylvania's disposal wells have limited capacity, most Marcellus wastewater is disposed via trucking to West Virginia or Ohio. This is a very expensive option, especially for operations in north-eastern PA that require both wastewater disposal (\$100/m³) and transportation to Ohio. A high wastewater recycle rate is achieved in the Marcellus, partially due to the cost-prohibitive nature of disposal. However, when the natural gas price drops, most gas operators have no choice but to stop stimulating wells, and transport the flowback water to disposal wells.

4.3.2 Problem statement II

In problem statement I only freshwater consumption was considered. However, strategies for reuse, recycle, storage, and disposal options can offer opportunities for reducing overall water management cost. In order to address both water quality and quantity issues, we develop a more comprehensive model by considering the handling of flowback wastewater, as well as the revenue from gas production, which was not considered in problem I.

In addition to the information given for Problem I, we assume that wellpad decline curves (Figure 4.10) are given by Arps decline curve⁹⁰, which indicate the production profile of the wellpad over time.

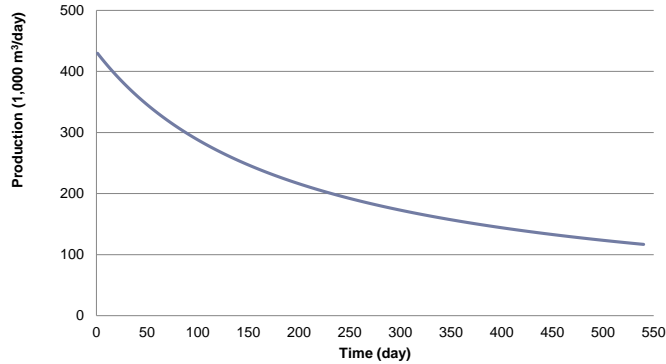


Figure 4.10: Well production decline curve.

The decline curve is described by the following equation,

$$P(t) = \frac{P_0}{(1 + bDt)^{1/b}} \quad (4.11)$$

where P_0 is the initial production level, b and D are adjustable parameters.

There are also a number of frac tanks on the wellpad. The location and capacity of treatment facilities is also given, as well as their capability of removing the contaminants. As in problem I, we assume that the availability of interruptible sources of water is uncertain, and modeled with R scenarios from historical data. Finally, we assume that the price of natural gas is given as a function of time (see Figure 4.11). The goal is then to determine the fracturing schedule as well as the logistics for water acquisition, flowback reuse and treatment. The objective is to maximize the profit given by the income of gas production, minus the expected cost of transportation, treatment, storage, and disposal. We have seen in Problem I that the optimized schedule spans a similar time horizon as the heuristic schedule. However, for Problem II the sooner the wellpads are completed, the sooner they can start producing gas, thereby potentially increasing the income, and hence the profit.

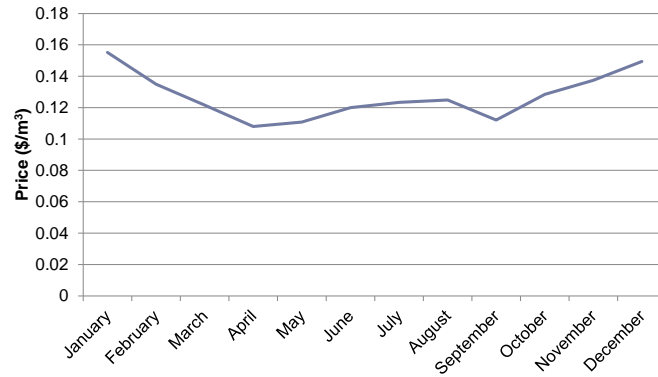


Figure 4.11: Natural gas price profile averaged over the years 2009, 2010, and 2012.

In order to model this problem, we rely on the superstructure representation shown in Figure 4.12 to account for the alternatives of interest. In addition to the freshwater acquisition structure from Problem I, we have additional treatment units for removing TSS in the flowback water, a set of frac tanks at each wellpad to store incoming wastewater, and finally, the unused flowback water a given wellpad can dispose. In terms of the STN, the treatment facilities represent additional tasks, while the treated wastewater corresponds to additional states. The major assumptions for Problem II are as follows:

1. Freshwater trucking cost is only volume-dependent.
2. Wastewater trucking cost is volume and distance-dependent to allow for recycling among geographically proximate wellpads.
3. The wells on each wellpad are aggregated.
4. Arps decline curve is used to estimate gas production profile.
5. A fixed percentage of total water used in fracturing must be freshwater.
6. Only the first two weeks of flowback water can be treated and recycled.
7. There are existing temporary wastewater piping connections between a selected set of wellpads and treatment facilities.

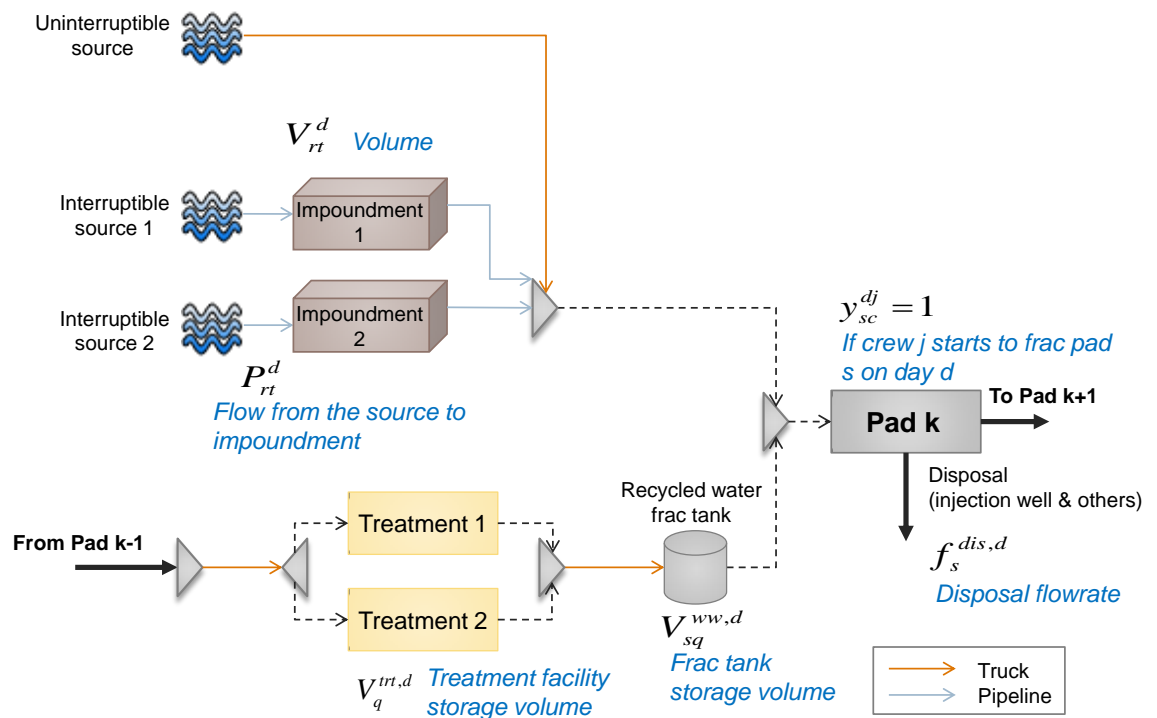


Figure 4.12: Problem 2 superstructure.

4.3.3 Optimization model II

In addition to constraints (4.3) – (4.9), we consider for the two-stage programming model the following additional constraints (4.12) – (4.18) to account for flowback water.

Material balances. Constraint (4.12) is similar to constraint (4.3), and it denotes the daily recycled water needed, which is treated as a stage-one variable. dy_{sc}^{ww} and ds_{sc}^{ww} are parameters that indicate the daily requirement of water to fracture each wellpad.

$$da_s^{ww,d} = \sum_c \sum_j \left(\sum_{d'=d-fD_{sc}+2}^d dy_{sc}^{ww} y_{sc}^{d'j} + \sum_{d'=d-fD_{sc}+1} ds_{sc}^{ww} y_{sc}^{d'j} \right) \quad (4.12)$$

The mass balance for the frac tanks on a given wellpad is represented by (4.13). The volume on a given day, $V_s^{ww,d}$, which is also a stage-one variable, is given by: i) volume from the previous time period, ii) plus flow from treatment facilities to the wellpad $f_{sq}^{wt,d}$, iii) minus consumption for stimulating the wellpad $da_s^{ww,d}$, and iv) plus the fresh make-up water $D_s^{fw,d}$.

$$V_s^{ww,d} = V_s^{ww,d-1} + \sum_q f_{sq}^{wt,d} - da_s^{ww,d} + D_s^{fw,d} \quad \forall s, \forall d \quad (4.13)$$

Constraints (4.14) and (4.15) determine the flowback water produced from each well after completing all the stages for a given wellpad. Constraint (4.14) determines the flowback profile up to two weeks after completion from the parameter $F_s^{fbw,d}$, while constraint (4.15) determines the flowback water that can either be sent to a treatment facility $f_{sq}^{tw,d}$ or disposed $f_s^{dis,d}$. Note that all these variables are stage-one variables.

$$da_s^{fbw,d} = \sum_j \sum_{s \in TP_{s,t}} \sum_{d'=d-d''-fD_{sc}}^{|d'|} \sum_{d''} F_s^{fbw,d'} y_{sc}^{d''j} \quad \forall s, \forall d \quad (4.14)$$

$$da_s^{fbw,d} = \sum_q f_{sq}^{tw,d} + f_s^{dis,d} \quad \forall s, \forall d \quad (4.15)$$

The treatment facility wastewater storage level $V_q^{trt,d}$, also a stage-one variable, is determined by equation (4.16). The daily level connects the following terms: i) storage level of the previous day, ii) plus water transported from the wellpads to the treatment facility $f_{sq}^{tw,d}$, and iii) minus water transported to wellpads from the treatment facility $f_{sq}^{wt,d}$.

$$V_q^{trt,d} = V_q^{trt,d-1} + \sum_s f_{sq}^{tw,d} - \sum_{s'} f_{s'q}^{wt,d} \quad \forall q, \forall d \quad (4.16)$$

Constraint (4.17) specifies the storage capacity CAP_q at the treatment facilities.

$$\sum_s f_{sq}^{wt,d} \leq CAP_q \quad \forall q, \forall d \quad (4.17)$$

Objective. Finally, equation (4.18) represents the objective function of problem II, the expected net profit. It has the following terms: i) expected freshwater transportation cost, ii) flowback water treatment and disposal cost, iii) trucking cost of freshwater to compensate for recycled water deficit, iv) trucking and pumping cost to treatment facility, v) storage of flowback water, and vi) revenue from gas production.

$$\begin{aligned} \text{Expected profit} = & - \sum_s OC_s^{pump,fw} \sum_d \sum_r \sum_{t \in TP_{st}} \frac{P_{rt}^d}{R} + \sum_s OC_s^{truck,fw} \sum_d \sum_r \sum_{t \in TP_{st}} \frac{D_{rt}^d}{R} \\ & - \sum_s \sum_d \sum_q OC_q^{trt} f_{sq}^{wt,d} + \sum_s \sum_d OC_s^{dis} f_s^{dis,d} \\ & - \sum_s \sum_d OC_s^{truck,fw} da_s^{ww,d} \\ & - \sum_s \sum_d \sum_q OC_s^{truck,ww} D_s (1 - yt_q^s) (f_{sq}^{wt,d} + f_{sq}^{tw,d}) \\ & - \sum_s \sum_d \sum_q OC_s^{pump,ww} D_s yt_q^s (f_{sq}^{wt,d} + f_{sq}^{tw,d}) \\ & - \sum_s \sum_d \sum_q OC_s^{st,ww} (V_q^{trt,d} + V_{sq}^{ww,d}) \\ & + \sum_s \sum_d \sum_c \sum_j P_s^{d+f} D_{sc} y_{sc}^{dj} \end{aligned} \quad (4.18)$$

4.3.4 Example 2

We expand on example 1 which has 14 wellpads, 540 days, 2 impoundments. We allow for the addition of a second crew, with which the crews can be assigned to no more than 2 wellpads. In addition, there are two wastewater treatment facilities, one of which uses electric coagulation and the other one uses filtration. The difference between the two treatment facilities lies in the location, the treatment and storage capacity, as well as the cost of treatment. Data of the problem are given in Table 4.4. For each of the wellpads, we assume its flowback curve and decline curve are given to model the wastewater and natural gas production levels as indicated in Figure 4.13. Note that wellpads L and M are the highest producing wellpads, followed by wellpads C and D. In this example, we assume a cost profile of natural gas that is based on the average of the years 2009, 2011, and 2012 as shown in Figure 4.11. Finally, we also assume historical data over 30 years to define the scenarios for the uncertain interruptible water sources.

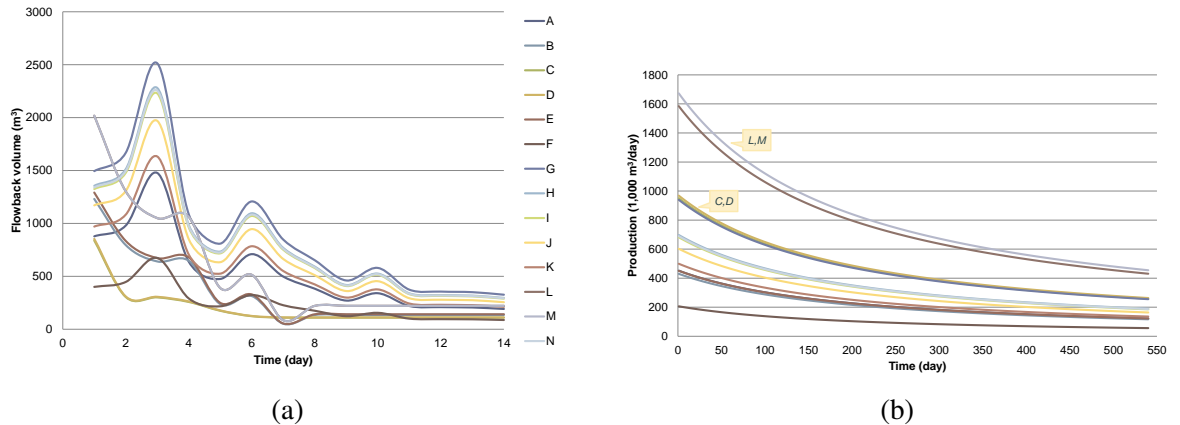


Figure 4.13: Example 2 (a) flowback profile and (b) production profile.

The two-stage stochastic MILP model for this example consists of 540 time periods and has 19,552 binary variables, 220,321 continuous variables, and 90,750 constraints. The MILP was solved in 3,006 CPUs with an optimality gap of 3.9% using CPLEX 12.5.

The result of using the MILP formulation for problem II is shown in Table 4.5, in which the expected profit for the MILP schedule is about 19% higher than the one of the heuristic

Table 4.4: Example 2 parameters and cost coefficients.

Parameter	Symbol	Value
Capacity of treatment facility (m ³)	CAP_q	q1 = 480 q2 = 1,200
Treatment cost (\$/m ³)	OC_q^{trt}	q1 = 25.16 q2 = 12.58
Disposal cost (\$/m ³)	OC^{dis}	134.18
Storage cost (\$/m ³ /day)	$OC^{st,ww}$	0.59
Wastewater pumping cost (\$/km/m ³)	$OC_s^{pump,ww}$	0.28
Wastewater trucking cost (\$/km/m ³)	$OC_s^{truck,ww}$	0.15

schedule (\$214.15 million vs. \$ 180.27 million). There are reductions in both expected freshwater trucking cost and disposal cost, which are important cost factors in the completion process. As a result, the total cost is reduced from \$25.02 million to \$23.41 million. Furthermore, the revenue from gas production is increased from \$205.29 million to \$237.56 million, a 15.7% increase.

Table 4.5: Example 2 solution comparison.

		Heuristic schedule	MILP schedule
Transportation	Freshwater pumping	9.91	10.79
	Freshwater trucking	9.19	7.22
	Wastewater	0.27	0.37
Treatment		0.64	0.7
Disposal		4.93	4.23
Storage		0.08	0.1
Total cost (\$1,000,000)		25.02	23.41
Revenue (\$1,000,000)	Gas production	205.29	237.56
Profit (\$1,000,000)		180.27	214.15

Due to the efficient reuse of flowback water, a saving of 15,860 m³ of freshwater can be achieved out of the total volume required for all 14 wellpads (1.29 million m³). The saving comes from the reduction of freshwater used to make up for the deficit in recycled water. Since the use of recycled water is assumed to be capped at 15% of the total volume required to frac the well, the freshwater saving achievable is relatively small. Nonetheless, the saving in freshwater also implies that less disposal of flowback water is required.

The schedule comparison for fracturing the wellpads is shown in Figure 4.14. There are

three observations worth noting from the resulting schedule. First, unlike the heuristic schedule, there is no break between the first group of wellpads, namely, C,D,G,E,N,A,B, and F. This tightness in schedule improves the recycling efficiency of the flowback water. The second note is that wellpads L and M are stimulated in parallel in the winter when the gas price is high, leading to higher revenue. Finally, most of the wellpads are completed sooner in the optimized schedule, and this front-loading scheme allows for a higher overall production level to be achieved within the time horizon under consideration.

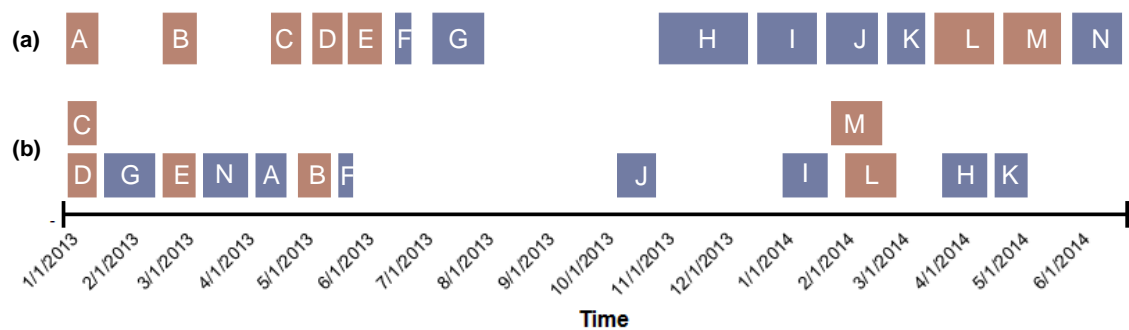


Figure 4.14: Example 2 fracturing schedule from (a) heuristic method (b) MILP model.

4.4 Conclusion

In this chapter, two-stage programming MILP scheduling formulations have been proposed for shale plays water management. The goal in Problem I is to balance the trade-off between water acquisition from uninterrupted sources that are available throughout the year but require more expensive truck transportation, versus acquisition from interruptible sources that can be transported with pipelines at lower costs but are not available throughout the year. An effective STN-based model has been developed for this problem. This model has been extended to handle a combination of disposal options with alternatives for recycling and reuse of flowback water, while accounting for the income from the sales of natural gas. Using two test cases from operations in the Marcellus shale development, we have shown that these models yield cost reduction, revenue enhancement, reduced

freshwater consumption, as well as reduced CO₂ emissions from transportation. Finally, it should be noted that the models proposed in this work can be coupled with investment models for shale gas supply chain such as the MINLP model proposed by Cafaro and Grossmann⁹¹.

Nomenclature

Sets

s, s'	Wellpads
t	An interruptible source and its corresponding impoundment
r	Historical river flowrate data year
d, d', d''	Time interval
c	Stages per day fractured scenarios
j	Frac crew
q	Wastewater treatment facility
TP_{st}	Match between wellpad s and source t

Superscripts

fw	Freshwater
ww	Waste water
fbw	Flowback water
$truck$	Trucking
$pump$	Pumping
trt	Treatment
dis	Disposal
st	Storage
wt	From treatment facility to wellpad
tw	From wellpad to treatment facility

Parameters

$OC_s^{pump, fw}$	Freshwater pumping cost, $\$/m^3$
$OC_s^{truck, fw}$	Freshwater trucking cost, $\$/m^3$
fD_{sc}	Days takes to frac the wellpad, day
dy_{sc}^{fw}	Volume required to frac all but the last day, m^3
ds_{sc}^{fw}	Volume required to frac the last day, m^3
$CT_s^{s'}$	Crew transition time between wellpads, day
sgT_s	Total number of stages at each wellpad
eT	A date to finish a certain number of stages
T	Target number of stages to be completed
hD	Length of frac holiday, day
dy_{sc}^{ww}	Daily wastewater required for all but the last day, m^3
ds_{sc}^{ww}	Daily wastewater required for the last day, m^3
$F_s^{fbw, d}$	Flowback water production, m^3
CAP_q	Capacity of treatment facility q , m^3
OC_q^{trt}	Treatment facility cost, $\$/m^3$
OC^{dis}	Disposal cost, $\$/m^3$
$OC^{st, ww}$	Storage cost, $\$/m^3$
$OC_s^{truck, ww}$	Wastewater trucking cost, $\$/m^3/km$
$OC_s^{pump, ww}$	Wastewater pumping cost, $\$/m^3/km$
D_{sq}	Distance between wellpad s to treatment facility q
P_s^d	Production $\$$
yt_q^s	Wastewater piping connection between wellpads and treatment facilities
P_0	Initial production, m^3
b	Decline exponent, $0 \leq b \leq 1$
D	Initial decline rate parameter
Binary variables	
y_{sc}^{dj}	Defines the beginning of stimulating each wellpad
z^d	Defines the beginning of a a frac holiday
Continuous variables	

CHAPTER 4. OPERATIONAL MODEL FOR SHALE GAS WATER MANAGEMENT

D_{rt}^d	Deficit in impoundment, m ³
$da_s^{fw,d}$	Freshwater deficit at a wellpad, m ³
$to_t^{fw,d}$	Total freshwater required to frac from an impoundment, m ³
V_{rt}^d	Volume of the impoundment, m ³
$V_q^{trt,d}$	Volume of the wastewater in treatment facility, m ³
$V_{sq}^{ww,d}$	Volume of the wastewater in frac tank, m ³
P_{rt}^d	Pumping rate, m ³
$da_s^{ww,d}$	Daily wastewater required, m ³
$da_s^{fbw,d}$	Daily flowback water produced, m ³
$f_{sq}^{tw,d}$	Flowrate from wellpad s to a treatment facility q , m ³
$f_{sq}^{wt,d}$	Flowrate from a treatment facility q to a wellpad s , m ³
$f_s^{dis,d}$	Disposal flowrate, m ³

Chapter 5

Investment optimization model for freshwater acquisition and wastewater handling in shale gas production

5.1 Introduction

The need for infrastructure development arises due to the rapid growth rate in shale gas development. Whereas chapter 4 deals mainly with short-term operations and temporary solutions, the model in this chapter incorporates more permanent trends towards better practice in the long term. Buried water pipelines, for example, can be setup while the gas pipelines are buried to incur less environmental footprint in comparison to overland pipelines and trucks. In addition, constructing centralizing wastewater storage and desalination plant can allow operators to benefit from economies of scale, thereby providing strong incentives for produced water reuse both within and outside the shale gas industry.

The proposed optimization model builds on the MILP model in the previous chapter⁹² for the optimal water management given water sources and treatment facilities for a set of wellpads. It should also be noted that Gao and You⁹³ have addressed a problem similar

to this chapter except that in their case they assumed a fixed schedule for the fracturing, which has a major impact in the revenue.

Chapter 5 is organized as follows. First, we discuss several practical options for desalination processes. We next introduce the general problem statement, its assumptions, and the mathematical formulation. Finally, we provide an example in the Utica shale play to illustrate the application of the model and present several scenarios that evaluate the sensitivity of various aspect of the model.

5.2 Treatment facility

5.2.1 Overview

Flowback water is generated in the first few weeks following well stimulation, although the quantity and quality vary from site to site and from play to play, the general trend of increased salt concentration and decreased flow is predominant. Long-term produced water, which could be up to 70% of the total wastewater generated during the lifetime of a well, has a salinity level that could reach as high as 360,000 ppm⁹⁴. It is estimated that while water acquisition cost will increase by 20% from 2013 to 2022, wastewater treatment cost will increase by 60%, a significant part of which will come from treating the streams to discharge standard. To meet the current and anticipated challenges from these wastewater streams, there are several schemes that can be adopted for wastewater reuse or disposal.

The flowback water profile provides an opportunity for reusing the initial flowback and blending it with freshwater to be used at the next well. Depending on the presence of other constituents in the stream, the next period of flowback can go through primary treatment options including de-oiling and straining for the removal of suspended solids, oil and grease, bacteria, and divalent ions to prepare the stream for reuse⁹⁵. As contaminant concentration increases, intermediate strategies such as disinfection (to remove microbes), organics removal, and softening (to remove divalent metal cations which cause scaling) are

CHAPTER 5. INVESTMENT OPTIMIZATION MODEL FOR FRESHWATER ACQUISITION AND WASTEWATER HANDLING IN SHALE GAS PRODUCTION

Table 5.1: Specifications of desalination technologies.^{1,2}

Technology	Max TDS Concentration (ppm) @ Max Recovery (%)
Reverse osmosis	35,000 @ 50
Forward osmosis	70,000 @ 60
Membrane distillation	300,000 @ 60-95
Mechanical vapor recompression	200,000 @ 50

adopted to treat the stream to reuse standard. This option can be done either onsite through a mobile treatment unit or at a centralized wastewater treatment facility (CWT). The high salinity streams require a level of high integrity in the equipment (added cost) to avoid damaging the environment through spills and leaks. In addition, a major concern is managing the large quantity of produced water once the gas field is saturated with producing wells and the wastewater cannot be internally reused by the operator. Thus, demineralization through more advanced options for additional reuse or discharge to surface water (<500 ppm TDS in the state of Pennsylvania) is considered, although conventional thermal processes are unsuitable due to the prohibitive capital cost, large installation footprint, and significant energy requirement⁹⁴.

5.2.2 Desalination methods

Desalination technologies can be categorized as thermal and membrane processes. The primary challenge is the variability in TDS concentration over the lifetime of the well, which constrains the selection of appropriate treatment technologies. Since produced water management is mainly an economic decision, installation cost, energy cost, and secondary waste management cost are of primary concern. We present several desalination technologies that are suitable for use under the incentive of treating produced water. The feed water TDS level criterion for each technology is specified in Table 5.1. As can be seen, reverse osmosis can typically operate with low salinity level, forward osmosis can be adopted for medium TDS range, and finally, distillation (with or without crystallizer for the concentrated stream) is required to handle waste streams with up to 300,000 ppm of TDS⁹⁵.

Reverse osmosis. Reverse osmosis (RO) is a mature technology and has been widely used in seawater desalination. The membrane permeability in RO allows it to effectively reject monovalent ions and low molecular weight organic compounds⁹⁴. In addition, the process is highly modular and scalable. However, it is used to a much lesser extent in shale gas wastewater treatment since RO units are only able to process low-salinity influent water not exceeding 35,000 ppm of TDS with about 50% recovery level. Further recovery becomes limiting due to the high hydraulic pressure required to overcome the osmotic pressure of high-salinity produced water stream can exceed the allowable pressure of the equipment tolerance⁹⁶.

Forward osmosis. An intermediate range option for desalination is forward osmosis (FO), which is a technology that can avoid some of the drawbacks of pressure-driven membrane processes. A semi-permeable membrane is used to separate the feed from a concentrated draw solution. The osmotic pressure difference across the membrane allows water to diffuse from the feed to the more concentrated draw solution such as thermolytic salts, therefore rejecting TDS as well as suspended solids in the process. The main difference between FO and RO is the driving force for separation. Whereas RO applies hydraulic pressure to overcome osmotic pressure, FO relies on the osmotic pressure differential between the feed and the draw solution that has a higher osmotic pressure to drive the flux. As a result, an additional step is necessary to regenerate the draw solution. FO can be used as a standalone process, or as a pretreatment for RO or distillation. The advantage of FO is that it can operate at relatively low pressure and temperature, which reduces the energy consumption. Unlike RO, FO is not limited by the high-pressure tolerance and is suitable for treating wastewater with less than 70,000 ppm TDS⁹⁷.

Membrane distillation. Membrane distillation (MD) is a thermally-driven process that uses hydrophobic membranes to separate a warm aqueous feed with up to 300,000 ppm of TDS from a cool permeate. The temperature difference across the membrane serves as the driving force for the water transfer. As a result, the flux in MD is not very sensitive to the feed salinity. Another advantage of MD is that low-grade heat such as waste heat in power plant can be used as heat source. Compared to pressure-driven membrane processes, MD uses membranes with larger pores without an applied hydraulic pressure, leading to a lower

propensity for fouling¹. However, pre-treatment is still important since contaminants such as organics and dissolved gas could still reduce the efficacy of the membranes by exerting partial pressures. In order to reduce secondary waste stream, an integration of MD with a crystallization unit could convert the raw brine to high quality water and salt crystals as products at a higher capital cost⁹⁶.

Mechanical vapor recompression. The most widely demonstrated approach, in terms of reliability in demineralization of shale gas wastewater, is the mechanical vapor recompression process (MVR), which uses electrical energy to supply thermal energy. This process has been commercially applied to shale gas water management, mainly in the Barnett shale by Aqua-Pure Ventures⁸⁸. The system includes heating the brine to evaporate the water, which is placed under partial vacuum by a compressor, allowing the water vapor to flow through a heat-exchanger, which recovers heat for the feed stream³. By using a compressor for evaporation instead of traditional heat source, energy savings can be achieved in this energy-intensive process. The unit is less susceptible to fouling and requires less pre-treatment than membrane processes. It can also handle wastewater streams up to 200,000 ppm limited by salt solubility⁸⁸. The recovered distillate is of high quality and can meet the surface water discharge standard in Pennsylvania, or reused as process water in other industrial applications. The concentrated brine can be crystallized and converted to salt cakes or disposed through Class II wells. While the operating and capital costs are lower compared to conventional thermal processes, the energy requirement is relatively high compared to membrane processes¹. However, corrosion and scaling can occur and incur high operating and maintenance costs⁹⁴. Since the Marcellus play has relatively high TDS concentration in comparison with other shale plays, MVR is a feasible desalination option for the region.

5.3 Problem statement

The proposed model extends chapter 4⁹², which dealt only with operations, to include capital investment decisions. Specifically, the objective is to minimize the overall cost

CHAPTER 5. INVESTMENT OPTIMIZATION MODEL FOR FRESHWATER ACQUISITION AND WASTEWATER HANDLING IN SHALE GAS PRODUCTION

including capital cost of impoundment, piping, and treatment facility, as well as operating cost including freshwater, pumping, and treatment. We assume that we are given the potential freshwater source locations and withdrawal data, potential impoundment locations, wellpad locations and total number of stages, and treatment units capability and locations. The goal is to determine the location and capacity of impoundment, the type of piping, treatment facility desalination technology, as well as the frac schedule, and the water sources to obtain freshwater.

The scheduling part of the problem is formulated through a discrete-time MILP model using as a basis the State-Task Network (STN) representation for batch scheduling⁵⁷. The STN representation consists of three major elements: states, tasks, and equipment. Similar to STN-based batch processing models, the processing tasks in the context of this work correspond to the fracturing of the wells on each wellpad. The states correspond to the water sources and impoundments that feed into the wellpads. The investment decisions are superimposed on the scheduling model. The problem is optimized over a long planning horizon, which increases the computational difficulty for solving the MILP model.

The wellpads are divided into multiple areas. The potential water piping connections are highly dependent on the geology of the land. Since the wellpads in each area are close in proximity, pipelines can be placed in between wellpads. Through the extensive use of pipelines, the advantage is that trucking freshwater can be greatly reduced or even avoided altogether, which improves the procedure both economically and environmentally.

Frac fluid is blended using freshwater and wastewater. Since the various contaminants in the wastewater stream could interfere with frac fluid performance, operators fix the wastewater to freshwater ratio in the blending process to maintain the efficacy of the fluid. Since the purpose is to reuse the stream, this approach does not require wastewater streams to be treated to freshwater discharge standard, thereby avoiding extensive and costly treatment procedures. In this problem, we assume that the frac fluid criterion is specified by its TDS concentration level, which requires recycle and reuse of wastewater streams to meet the concentration target.

Freshwater can be obtained from rivers as well as ponds. The availability of water at the

CHAPTER 5. INVESTMENT OPTIMIZATION MODEL FOR FRESHWATER ACQUISITION AND WASTEWATER HANDLING IN SHALE GAS PRODUCTION

takepoint of the river affects the volume that the operator can withdraw from the river. In the problem formulation, we assume that all the freshwater sources are interruptible (i.e. small rivers or creeks close to the wellpads), which means that water can only be withdrawn from the sources if the flowrate in the source is above a threshold. Alternatively, the ponds can serve either as a storage unit or a source. Freshwater sources supply water to the wellpads through either an overland or buried pipelines. Overland pipelines can be rented and leave less environmental footprint. Buried pipelines, however, are mostly owned by the operator and are usually placed at the same time as burying the gas pipelines. Practical issues involve tree clearing, pipe freezing. Impoundments can provide additional storage capacity.

After completion, streams of flowback can go through basic treatment onsite and then recycled at the next wellpad. It can also be trucked to CWT, where the streams are treated to discharge standard to be recycled at the next completion pad or discharged. Since salinity level restricts the type of technology that can be used to treat the feed water, we consider several TDS removal options in the CWT. Depending on the desalination process, a concentrated wastewater stream is generated and trucked to disposal wells. The final option is that the flowback and produced stream can be trucked directly to disposal wells. The choice among these options is highly dependent on the flowback characteristics and handling costs. The locations and potential interconnections of the water sources, wellpads, and impoundments for the corresponding water supply chain are shown in Figure 5.1.

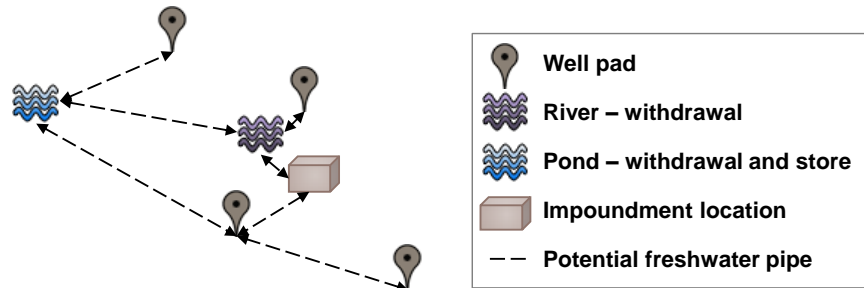


Figure 5.1: Main elements in water supply chain for shale gas production.

The assumptions made in the formulation of the model are as follows:

1. Each well can only be fractured at least two weeks after the well is drilled, and the drilling schedule is fixed.
2. The wells in each wellpad are aggregated so that the wells are all stimulated before the frac crew is transferred to another wellpad. Each wellpad has a fixed number of stages that are available for completion during the time period of interest.
3. Freshwater sources connected to pipelines are interruptible sources and their availability is given by the average historical flowrate data.
4. Each pipeline segment has enough capacity to transfer freshwater used at the wellpads in each time period.
5. The sales value of gas production is known a priori.
6. Flowback volume and composition are known.
7. Frac tanks can only be placed on the completion pad.
8. Onsite treatment process provides adequate removal of most contaminants other than TDS for recycle.
9. CWT has pretreatment capability prior to desalination.
10. The treatment technologies considered can desalinate the water stream to discharge standard.
11. The cost of the desalination plant is annualized over the time horizon and is shared among a number of operators.

5.4 Problem formulation

The problem can be formulated as a MINLP model with the following constraint types: allocation constraints, material balances, logic constraints, and an objective function. The

main decision variables are several 0-1 variables that are associated with various capital investment options. Additionally, y_{skt} is a binary variable that indicates the starting date t for wellpad s stimulation at rate k .

5.4.1 Constraints

Allocation constraints. Constraint (5.1) specifies that each wellpad s has to be fractured exactly once at a given date t , and for a rate to frac per week k .

$$\sum_k \sum_t y_{skt} = 1 \quad \forall s \quad (5.1)$$

Constraint (5.2) represents a backward aggregation constraint from the STN model⁸⁷ that ensures there is no overlap between different wellpad operations,

$$\sum_s \sum_k \sum_{t'=t-SFL_{sk}-STC+1}^t y_{skt'} \leq 1 \quad \forall t \quad (5.2)$$

where SFL_{sk} represents the duration of the hydraulic fracturing for the wellpad s stimulated at the rate of k stages per time period, STC represents the transition time required to move the frac crew from wellpad s to the next wellpad.

Water use at wellpads. Frac fluid at each wellpad can be supplied by a combination of freshwater and wastewater. The total weekly water requirement to frac a wellpad s is represented by constraint (5.3), where f_{st} is a continuous variable that defines the time profile of water use at each wellpad. SDW_s is the constant indicating water requirement for wellpad s during each time period. Water requirement for the remaining stages that are stimulated during the final time period is represented by the parameter SLW_s .

$$f_{st} = \sum_k \left(\sum_{t'=t-SFL_{sk}+2}^t SDW_s y_{skt'} + \sum_{t'=t-SFL_{sk}+1} SLW_s y_{skt'} \right) \quad \forall s, \forall t \quad (5.3)$$

Both freshwater and wastewater can be used in frac fluid and is represented by constraint

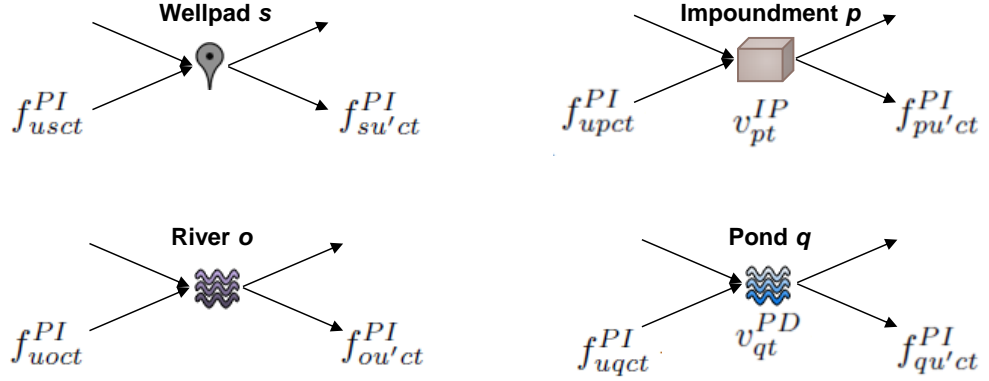


Figure 5.2: Flow directions for wellpads, impoundments, rivers, and ponds.

(5.4), where f_{st}^{FW} indicates the freshwater use and f_{st}^{WW} is the wastewater used at the wellpad.

$$f_{st} = f_{st}^{FW} + f_{st}^{WW} \quad \forall s, \forall t \quad (5.4)$$

The freshwater mass balance at each wellpad is described by the mass balance in (5.5). The continuous variable $f_{uu'ct}^{PI}$ represents the flow using pipeline of type c from location u to u' . The set u represent locations of all wellpads, river sources, pond sources, and impoundments, which are given by the indices s , o , q , and p , respectively. The nomenclature for flow directions at each location type is indicated in Figure 5.2.

$$\sum_{u \in DP_{us}} \sum_c f_{usct}^{PI} = f_{st}^{FW} + \sum_{u' \in DP_{su'}} \sum_c f_{su'ct}^{PI} \quad \forall s, \forall t \quad (5.5)$$

Freshwater source constraints. Constraint (5.6) describes the mass balance for river take-points, where f_{ot}^{RI} is a continuous variable that represents the withdrawal rate from river source o . The utilization of source o is then restricted by the binary variable y_o^{FW} to a

flowrate upper bound of $F_{ot}^{max,RI}$ in constraint (5.7).

$$\sum_{u \in DP_{uo}} \sum_c f_{uoct}^{PI} + f_{ot}^{RI} = \sum_{u' \in DP_{ou'}} \sum_c f_{ou'ct}^{PI} \quad \forall o, \forall t \quad (5.6)$$

$$f_{ot}^{RI} \leq y_o^{FW} F_{ot}^{max,RI} \quad \forall o, \forall t \quad (5.7)$$

Similarly, freshwater can also be obtained from ponds. In addition to withdrawal of freshwater, ponds can serve as storage vessels. The volume of pond q on week t is given by the continuous variable v_{qt}^{PD} , and withdrawal of freshwater from the pond at time t is given by f_{qt}^{PD} . The weekly mass balance is described by constraint (5.8).

$$\sum_{u \in DP_{uq}} \sum_c f_{uqct}^{PI} + v_{qt-1}^{PD} + f_{qt}^{PD} = v_{qt}^{PD} + \sum_{u' \in DP_{qu'}} \sum_c f_{qu'ct}^{PI} \quad \forall q, \forall t \quad (5.8)$$

Constraint (5.9) establishes the use of pond q and withdrawal from the source is limited by water availability in the pond through constraint (5.10). Through the binary variable y_q^{PD} , the volume and withdrawal are zero if the pond is not used, otherwise, these variables are bounded by the maximum capacity CP^{PD} and maximum withdrawal F_{qt}^{PD} from the pond, respectively.

$$v_{qt}^{PD} \leq y_q^{PD} CP^{PD} \quad \forall q, \forall t \quad (5.9)$$

$$f_{qt}^{PD} \leq y_q^{PD} F_{qt}^{PD} \quad \forall q, \forall t \quad (5.10)$$

Additional freshwater storage can be fulfilled by impoundments, which can be either constructed by the operator or rented. v_{pt}^{IP} is the continuous variable indicating the volume of water in impoundment p . The mass balances are given by the following constraint (5.11).

$$\sum_{u \in DP_{up}} \sum_c f_{upct}^{PI} + v_{pt-1}^{IP} = v_{pt}^{IP} + \sum_{u' \in DP_{pu'}} \sum_c f_{pu'ct}^{PI} \quad \forall p, \forall t \quad (5.11)$$

Impoundment capacity l_p^{IP} and water volume v_{pt}^{IP} are bounded by the maximum $CP_p^{max,IP}$ and minimum $CP_p^{min,IP}$ capacity in constraints (5.12) and (5.13). y_p^{IP} and y_{pt}^{IP} indicate the use of impoundment p .

$$CP_p^{min,IP} y_p^{IP} \leq l_p^{IP} \leq CP_p^{max,IP} y_p^{IP} \quad \forall p \quad (5.12)$$

$$v_{pt}^{IP} \leq CP_p^{max,IP} y_{pt}^{IP} \quad \forall p, \forall t \quad (5.13)$$

The volume of water in the impoundment is restricted by the capacity of the impoundment as in constraint (5.14), and constraint (5.15) relates the two binary variables y_p^{IP} and y_{pt}^{IP} to indicate the use of each impoundment.

$$v_{pt}^{IP} \leq l_p^{IP} \quad \forall p, \forall t \quad (5.14)$$

$$y_p^{IP} \geq y_{pt}^{IP} \quad \forall p, \forall t \quad (5.15)$$

Wastewater handling constraints. The superstructure for flowback handling is shown in Figure 5.3.

In constraint (5.16) and (5.17), f_{st}^{FB} and c_{st}^{FB} are continuous variables that indicate flowback flowrate and concentration of each wellpad during time t , which define the profiles over the horizon depending on the frac schedule. SF_{st}^{FB} and SC_{st}^{FB} are parameters that indicate flowback flowrate and TDS concentration.

$$f_{st}^{FB} = \sum_k \sum_{t''} \sum_{t' \in t-t''-SFL_{sk}+1} SF_{st''}^{FB} y_{skt'} \quad \forall s, \forall t \quad (5.16)$$

$$c_{st}^{FB} = \sum_k \sum_{t''} \sum_{t' \in t-t''-SFL_{sk}+1} SC_{st''}^{FB} y_{skt'} \quad \forall s, \forall t \quad (5.17)$$

The flowback stream from wellpad, f_{st}^{FB} , can be treated onsite, trucked to CWT for de-

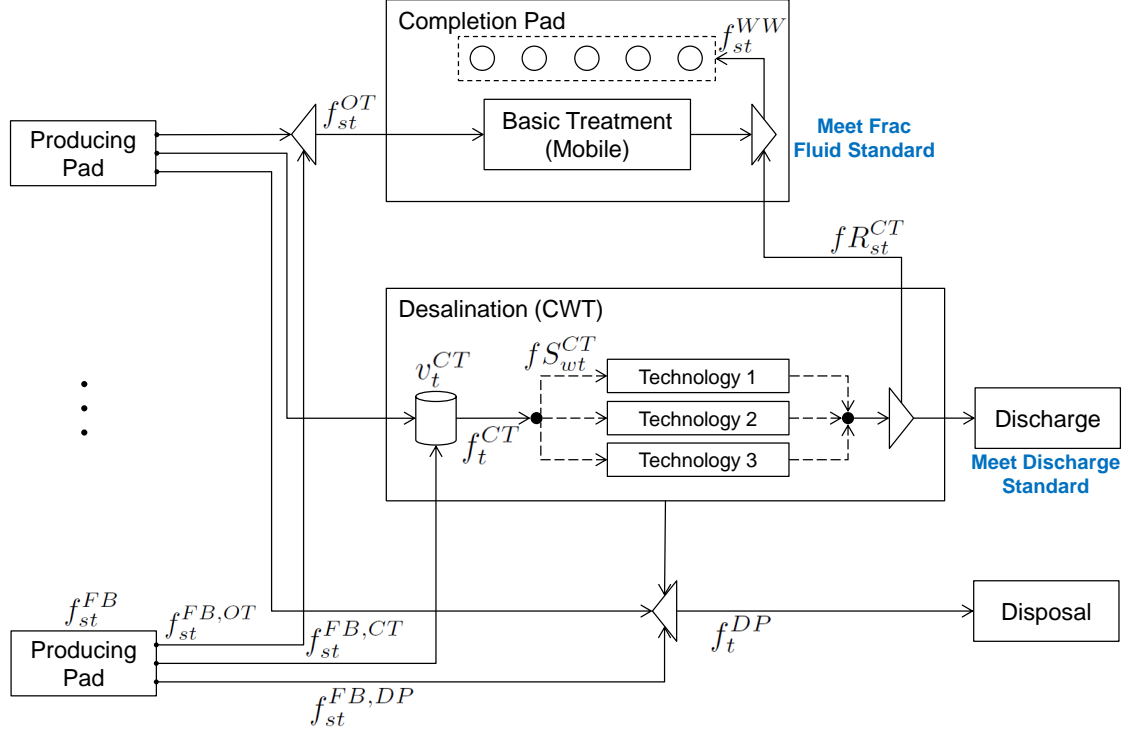


Figure 5.3: Wastewater flows.

salination and discharge, or disposed directly as described in constraint (5.18), and their flowrates are denoted by $f_{st}^{FB,OT}$, $f_{st}^{FB,CT}$, and $f_{st}^{FB,DP}$.

$$f_{st}^{FB} = f_{st}^{FB,OT} + f_{st}^{FB,CT} + f_{st}^{FB,DP} \quad \forall s, \forall t \quad (5.18)$$

f_{st}^{OT} is a continuous variable representing the combined flowback streams from producing wells that is being treated onsite and recycled to wellpad s . f_t^{CT} is the flow trucked to CWT for desalination. The desalination unit is assumed to have gone through pretreatment and the additional cost is incorporated. f_t^{DP} is the flowrate that is trucked to disposal wells.

For the first option, basic onsite treatment, the total mass and TDS balance are represented by constraint (5.19) and (5.20). c_t^{OT} is the TDS concentration of the flowback water trans-

ported to basic treatment.

$$\sum_s f_{st}^{OT} = \sum_{s'} f_{s't}^{FB,OT} \quad \forall t \quad (5.19)$$

$$\sum_s f_{st}^{OT} c_t^{OT} = \sum_{s'} f_{s't}^{FB,OT} c_{s't}^{FB} \quad \forall t \quad (5.20)$$

The second option is desalination at CWT. A wastewater tank (assuming constant mixing) with volume v_t^{CT} is used to temporarily store the flowback streams. The mass balance for the tank is expressed in constraint (5.21). The TDS concentration of the combined flowback stream is denoted by c_t^{CT} and the balance of TDS is represented by constraint (5.22).

$$\sum_s f_{st}^{FB,CT} + v_{t-1}^{CT} = f_t^{CT} + v_t^{CT} \quad \forall t \quad (5.21)$$

$$\sum_s f_{st}^{FB,CT} c_{st}^{FB} + v_{t-1}^{CT} c_{t-1}^{CT} = (f_t^{CT} + v_t^{CT}) c_t^{CT} \quad \forall t \quad (5.22)$$

Several treatment options can be used for TDS reduction in CWT such as reverse osmosis and thermal distillation. The choice of each technology is represented by the binary variable y_w^{CT} , the throughput of each technology is indicated by the continuous variable fS_{wt}^{CT} . Constraint (5.23) allows the problem to choose at most one technology for TDS removal, and constraint (5.24) is the mass balance for flow through the desalination unit.

$$\sum_w y_w^{CT} \leq 1 \quad (5.23)$$

$$\sum_w fS_{wt}^{CT} = f_t^{CT} \quad \forall t \quad (5.24)$$

The flowrate through each technology in CWT is bounded as in constraint (5.25). In addition, each technology is limited to treating feedwater with TDS concentrations given by

CHAPTER 5. INVESTMENT OPTIMIZATION MODEL FOR FRESHWATER ACQUISITION AND WASTEWATER HANDLING IN SHALE GAS PRODUCTION

parameter CU_w^{CT} , as is expressed in constraint (5.26).

$$fS_{wt}^{CT} \leq F_{wt}^{max,CT} y_w^{CT} \quad \forall w, \forall t \quad (5.25)$$

$$c_t^{CT} \leq \sum_w CU_w^{CT} y_w^{CT} \quad \forall t \quad (5.26)$$

A fraction of the desalinated water stream becomes a concentrated waste stream and needs to be disposed, thus the recycle stream from desalination depends on the parameter η_w , the recycle ratio.

$$\sum_w \eta_w fS_{wt}^{CT} \geq \sum_s fR_{st}^{CT} \quad \forall t \quad (5.27)$$

Disposal at an injection well is the final option being considered.

$$f_t^{DP} = \sum_s f_{st}^{FB,DP} \quad \forall t \quad (5.28)$$

fR_{st}^{CT} represents the stream that is recycled to the wellpad s after desalination. Wastewater used at each site is through recycling of the treated water as follows,

$$fR_{st}^{CT} + f_{st}^{OT} = f_{st}^{WW} \quad \forall s, \forall t \quad (5.29)$$

The TDS balance at wellpad s is represented by constraint (5.30). The stream that is treated onsite does not change in TDS concentration since we assume that the onsite treatment does not have desalination capability. The stream of frac fluid from blending recycled wastewater and freshwater on wellpad s has to meet the frac fluid TDS standard CF .

$$CDfR_{st}^{CT} + c_t^{OT} f_{st}^{OT} \leq CFf_{st} \quad \forall s, \forall t \quad (5.30)$$

On the completion pad, the capacity of frac tank at wellpad s is bounded by the maximum

wastewater flowrate used at the wellpad as in constraint (5.31).

$$l_{st}^{ST} \geq f_{st}^{WW} \quad \forall s, \forall t \quad (5.31)$$

f_w^{CT} is a continuous variable indicating the throughput of the desalination plant.

$$f_w^{CT} \geq f_{wt}^{SCT} \quad \forall w, \forall t \quad (5.32)$$

Pipeline constraints. $y_{uu'}^{PI}$ are binary variables that indicate the existence of a pipeline of type c between u and u' . Constraint (5.33) ensures that both flow directions are allowed in any pipe in the structure.

$$y_{uu'}^{PI} = y_{u'uc}^{PI} \quad \forall uu' \in DP_{uu'}, \forall c \quad (5.33)$$

Constraint (5.34) indicates that only one type of pipeline, buried or overland, can be chosen for each segment.

$$\sum_c y_{uu'}^{PI} \leq 1 \quad \forall uu' \in DP_{uu'} \quad (5.34)$$

In addition, pipeline flow capacities are bounded above by UF and below by LF .

$$LF y_{uu'}^{PI} \leq f_{uu'ct}^{PI} \leq UF y_{uu'}^{PI} \quad \forall uu' \in DP_{uu'}, \forall t \quad (5.35)$$

5.4.2 Objective

The objective of the problem involves the sum of the following costs: 1) freshwater cost; 2) impoundment cost; 3) freshwater pipeline cost; 4) frac tank cost; 5) treatment cost; 6) disposal cost; 7) onsite treatment cost; and 8) CWT treatment cost.

Freshwater cost $COST^{FW}$ include set-up cost and withdrawal cost from rivers and ponds. In constraint (5.36), IC_u^{FW} is the set-up cost of source, and OC_u^{FW} is the withdrawal cost

coefficient.

$$\begin{aligned}
 Cost^{FW} = & \sum_o IC_o^{FW} y_o^{RI} + \sum_o \sum_t OC_o^{FW} f_{ot}^{RI} \\
 & + \sum_q IC_q^{FW} y_q^{PD} + OC_q^{FW} \sum_q \sum_t f_{qt}^{PD}
 \end{aligned} \tag{5.36}$$

Impoundments can be either constructed by the operator or rented, and the cost term $Cost^{IP}$ includes both the construction and rental cost. ICB_p^{IP} in constraint (5.37) is the base cost factor of the impoundment, whereas ICI_p^{IP} is the incremental cost based on volume of the impoundment, and OC_p^{IP} is the operating cost of the impoundment.

$$Cost^{IP} = \sum_p (ICB_p^{IP} y_p^{IP} + ICI_p^{IP} l_p^{IP} + OC_p^{IP} \sum_t y_{pt}^{IP}) \tag{5.37}$$

Pipeline cost $Cost^{PI}$ is made up of installation cost and pumping cost as follows,

$$Cost^{PI} = \sum_c \sum_u \sum_{u' \in DP_{uu'}} (IC_c^{PI} UDI_{uu'} y_{uu'}^{PI} + \sum_t (OC_c^{PI} UDI_{uu'} y_{uu'}^{PI} + OCPU f_{uu'}^{PI})) \tag{5.38}$$

where IC_c^{PI} is the pipeline installation cost, OC_c^{PI} is the rental cost of the pipeline, and $OCPU$ is the pumping cost.

Since frac tanks are typically rented, the only coefficient associated with frac tank cost $Cost^{WW,ST}$ is the rental cost $OC^{WW,ST}$.

$$Cost^{WW,ST} = \sum_s \sum_t OC^{WW,ST} l_{st}^{ST} \tag{5.39}$$

Disposal cost $Cost^{DS}$ includes trucking cost from wellpad to disposal well and disposal cost. $OC^{WW,TR}$ is the coefficient of trucking cost, UDS is the distance to disposal site, and $OCDS^{WW}$ is the disposal cost.

$$Cost^{DS} = (OC^{WW,TR} UDS + OCDS^{WW}) \sum_t f_t^{DP} \tag{5.40}$$

Onsite treatment cost $Cost^{OT}$ including onsite treatment cost, $OC^{WW,OT}$ is the cost coef-

ficient for treatment.

$$Cost^{OT} = OC^{WW,OT} \sum_s \sum_t f_{st}^{OT} \quad (5.41)$$

The last term is CWT treatment cost $Cost^{CT}$, which has several components, desalination capital and operating cost, wastewater hauling cost, concentrated stream disposal cost, and desalinated water discharge cost. AR is the annuity factor, $IC_w^{WW,CT}$ and $OC_w^{WW,CT}$ are the capital and operating cost of desalination using treatment process w , $OCDC^{WW}$ is discharge cost for desalinated water, and UDC is the distance to CWT.

$$\begin{aligned} Cost^{CT} = & \sum_w \frac{1}{AR} IC_w^{WW,CT} fT_w^{CT} + \sum_w \sum_t OC_w^{WW,CT} fS_{wt}^{CT} + \sum_t UDC f_t^{CT} \\ & + OCDC^{WW} \sum_t \left(\sum_w \eta_w fS_{wt}^{CT} + \sum_s fR_{st}^{CT} \right) \\ & + OCDS^{WW} \sum_w \sum_t (1 - \eta_w) fS_{wt}^{CT} + OC^{WW,TR} UDS \sum_w \sum_t (1 - \eta_w) fS_{wt}^{CT} \end{aligned} \quad (5.42)$$

The profit from gas revenue can be represented by (5.43), where P_{st} is the parameter representing revenue from production for each wellpad during time period t .

$$Revenue = \sum_s \sum_t \sum_k P_{s,t+SF} L_{sk} y_{skt} \quad (5.43)$$

Combining terms (5.36) - (5.43), we have the objective function (5.44), which defines the total profit,

$$\begin{aligned} \max. \text{ Profit} = & Revenue - (Cost^{FW} + Cost^{IP} \\ & + Cost^{PI} + Cost^{WW,ST} + Cost^{DS} + Cost^{OT} + Cost^{CT}) \end{aligned} \quad (5.44)$$

5.4.3 MILP approximation

The formulation with constraints (5.1)-(5.35) corresponds to an MINLP due to the bilinear terms of flowrate multiplied by concentration in constraints (5.20),(5.22) and (5.30).

In order to eliminate nonlinearities, we discretize concentration variables that are part of the bilinear terms. While it is an approximation, it still allows for enough resolution to distinguish the ability to recycle the stream and the selection of discrete desalination technology choice. Thus, we discretize the concentration terms c_{st}^{FB} and disaggregate the flow f_{st}^{FB} as follows,

$$\left. \begin{aligned} c_{st}^{FB} &= \sum_r CI_r z_{str}^{FB} \quad \forall s, \forall t \\ \sum_r z_{str}^{FB} &= 1 \quad \forall s, \forall t \\ f_{st}^{FB} &= \sum_r \hat{f}_{str}^{FB} \quad \forall s, \forall t \\ \hat{f}_{str}^{FB} &\leq F^{max} z_{str}^{FB} \quad \forall s, \forall t, \forall r \end{aligned} \right\} \quad (5.45)$$

where z_{str}^{FB} are the binary variables selecting the concentration value CI_r and \hat{f}_{str}^{FB} are the disaggregated variables for f_{st}^{FB} . Similarly, the other bilinear terms are approximated in the same fashion. Note we included zero for ensuring that the inequality in (5.26) is satisfied when the technology w is not chosen.

The objective in (5.44), along with the linearized constraints (5.45) and (5.1)-(5.35), form the MILP model for the water source location and treatment management problem.

5.5 Case study in Utica shale

5.5.1 Optimization model

We consider a case study in the Utica shale play with 14 wellpads as shown in Figure 5.4 with production curve shown in Figure 5.5. Each wellpad becomes available at different time as indicated in the figure. They are geographically distributed in two clusters in a given county. There are 5 interruptible river sources, 4 ponds, and 2 impoundments serving the wellpads in the two areas. The time horizon is 3 years and it is discretized into 156 weekly time steps. Three completion rates, 20, 30, and 40 stages per week, are possible.

CHAPTER 5. INVESTMENT OPTIMIZATION MODEL FOR FRESHWATER ACQUISITION AND WASTEWATER HANDLING IN SHALE GAS PRODUCTION

Table 5.2: Case study wellpad data.

Wellpad	s1	s2	s3	s4	s5	s6	s7	s8	s9	s10	s11	s12	s13	s14
# of stages	120	120	210	140	140	210	434	492	280	175	280	175	70	350
Earliest frac time (week)	1	6	19	19	71	71	20	11	19	19	19	71	71	71

The slowest stimulation rate is usually selected during periods of low water availability. The flowback flowrate and TDS level profile are given in Figure 5.6. Choice of two types of pipelines, overland and buried, are incorporated in the model. The buried pipelines are more capital intensive, whereas the overland pipelines cannot be used in the winter due to the possibility of freezing pipelines. Furthermore, three desalination technologies are considered for TDS removal, including membrane distillation, mechanical vapor recompression, and mechanical vapor recompression with crystallizer.

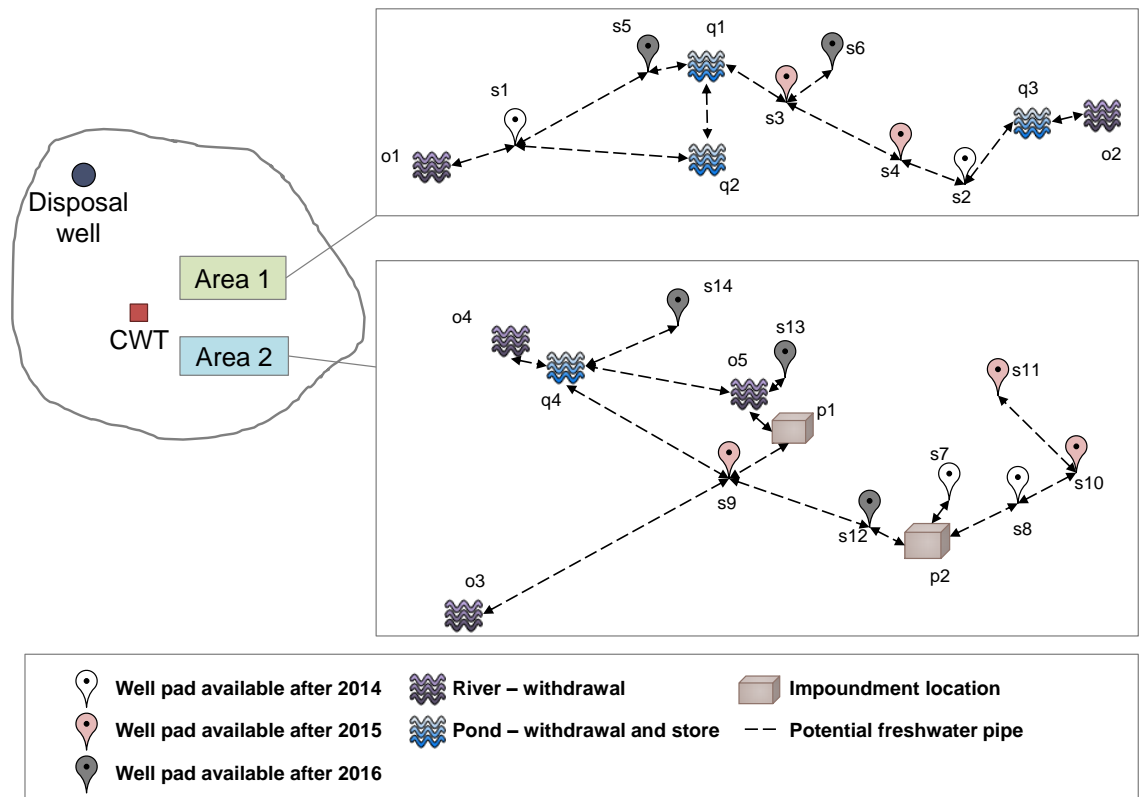


Figure 5.4: Layout of Utica case study.

CHAPTER 5. INVESTMENT OPTIMIZATION MODEL FOR FRESHWATER ACQUISITION AND WASTEWATER HANDLING IN SHALE GAS PRODUCTION

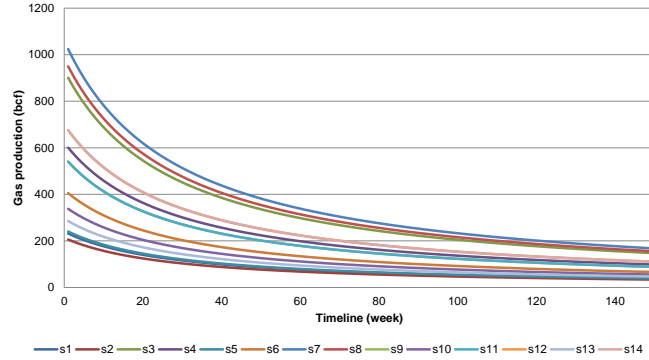
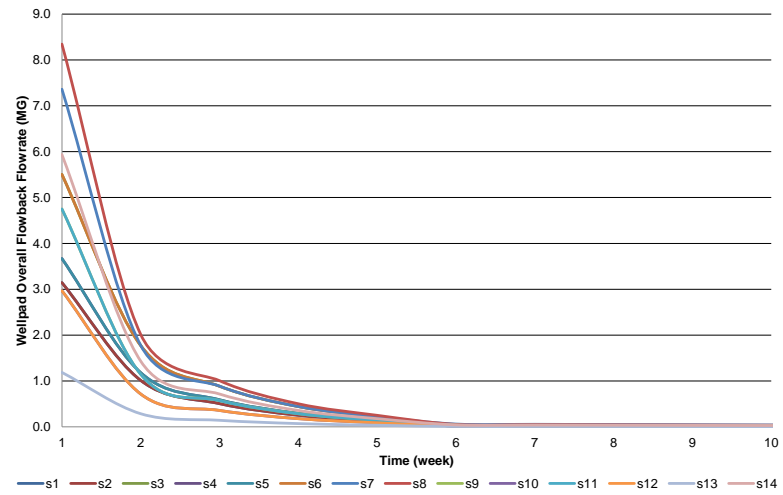


Figure 5.5: Total gas production curve of each wellpad.

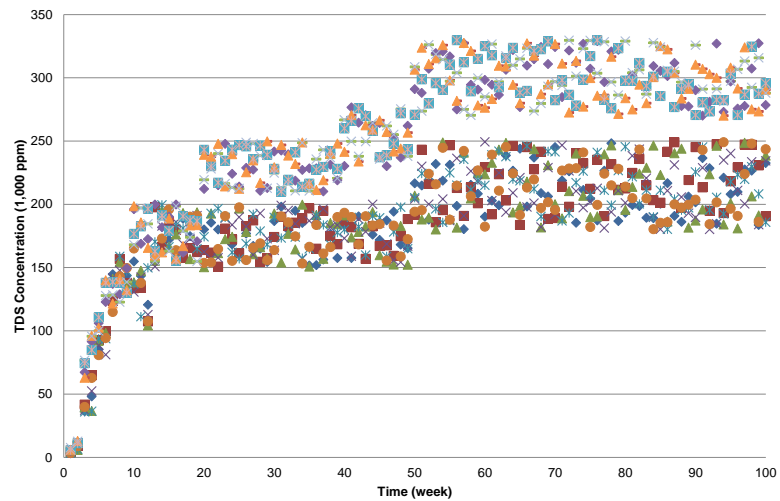
Table 5.3: Case study cost coefficient data. ^{3,2}

Cost coefficient	Unit	Value
ICB_p^{IP}	\$	360,000
ICI_p^{IP}	\$/MG	28,000
$IC_w^{WW,CT}$	\$ million	9 – 15
IC_u^{FW}	\$	50,000 – 100,000
IC_c^{PI}	\$/mi	325,000
OC_p^{IP}	\$/week	10,500
OC_u^{FW}	\$/1,000 gallon	0 – 7.5
$OC^{WW,TR}$	\$/bbl/mi	0.053
$OC^{WW,ST}$	\$/bbl/week	0.56
$OC^{WW,OT}$	\$/bbl	3
$OC_w^{WW,CT}$	\$/bbl	5–10
$OCDC^{WW}$	\$/bbl	0.5
$OCDS^{WW}$	\$/bbl	12
OC_c^{PI}	\$/mi/week	5,500
$OCPU$	\$/week	35,000

CHAPTER 5. INVESTMENT OPTIMIZATION MODEL FOR FRESHWATER ACQUISITION AND WASTEWATER HANDLING IN SHALE GAS PRODUCTION



(a)



(b)

Figure 5.6: Flowback (a) flowrate profile and (b) TDS concentration.

The MILP model consists of 111,399 constraints, 104,188 continuous variables, and 19,954 binary variables. The model is solved using GAMS 24.2/CPLEX 12.6 on an Intel 2.93 GHz Core i7 CPU machine with 4 GB of memory to a 0.1% optimality gap in approximately 7 hours.

The optimized frac schedule leads to a profit of \$1,034,110,429, with \$1,115,618,566 in natural gas revenue. Water-related cost totals \$81,508,137, which is around 7% of the total revenue. All river sources, all four ponds, and one impoundment are included in the configuration. All pipelines are buried since we specified in the problem that overland pipelines cannot be used between the months of December to February. In addition, mechanical vapor recompression is selected as the preferred method for TDS removal in CWT. In the optimal solution, there is no recycle of treated water from the desalination plant to the completion pad. Instead, the desalinated stream is discharged to the environment.

We present several scenarios below that provide variations to the optimal solution in order to gain some insights into the nature of this problem.

5.5.2 Scenario description

Scenario 1: Heuristic schedule.

First, the allocation constraints (5.1) and (5.2) are computationally demanding to solve. Scenario 1 optimizes the problem by fixing a heuristic schedule.

Scenario 2: No desalination unit.

Currently, most shale gas operators do not desalinate wastewater streams due to high cost of mobile unit and the lack of centralized treatment facility. However, there is a number of environmental concerns associated with deep-well injections. Thus in Scenario 2 we assume that a centralized desalination plant can be constructed to serve around 50 wellpads in the proximity (ten miles radius). This problem investigates the economic viability of constructing a desalination plant and the distribution of flowback water if desalination is not an option.

Scenario 3: Allow trucking.

The model in this work considers only freshwater transported through pipelines since truck hauling has negative impact including road damages, traffic accidents, and environmental concerns. As a result, operators are encouraged to draw freshwater from nearby sources. We can modify the model to allow for trucking from an uninterruptible source (i.e. large water body with guaranteed water availability year-round) and examine its effect on the optimal solution.

We introduce the continuous variable f_{st}^{TR} to represent the volume of freshwater trucked to each wellpad s during time period t , and modify the constraint (5.4) to obtain constraint (5.46).

$$f_{st} = f_{st}^{FW} + f_{st}^{WW} + f_{st}^{TR} \quad \forall s, \forall t \quad (5.46)$$

The following term is also added to the objective function indicating the trucking cost and the setup cost for the uninterruptible freshwater source from where the truck hauls water,

$$(OC^{TR} + OC^{FW}) \sum_{st} f_{st}^{TR} + IC^{FW} y^{TR} \quad (5.47)$$

where OC^{TR} is the trucking cost, y^{TR} is a binary variable indicating the use of trucking for freshwater acquisition, OC^{FW} is the withdrawal cost, and IC^{FW} is the perennial source set-up cost. In addition, we assume an additional 10% “bonding” cost for truck use which the operators have to account for to cover road damage.

Scenario 4: Higher flowback volume

In the Marcellus and Utica shale plays, flowback rate is relatively low compared other shale plays, where flowback rate may be as high as 25%. We double the flowback rate in the model (see Figure 5.6a) to analyze the distribution of wastewater as a result of higher flowback rate.

5.5.3 Results and discussion

The computational statistics and objective value from all four scenarios are presented in Tables 5.4 and 5.5, respectively. Both revenue from natural gas sales and water-related costs are considered in the profit maximization under the time horizon of the problem. Note from Table 5.5 that for these 14 wellpads, water-related cost makes up 7% (in the optimal case) to 11% (in scenario 2 where desalination is not considered) of the revenue from gas production, which is quite significant. As can be seen, the heuristic schedule yields the lowest profit during the 3-year period.

Table 5.4: Computational statistics.

	Optimal	1: Heuristic	2: No desalination	3: Freshwater trucking	4: Double flowback volume
# of binary var	19,954	16,831	16,830	16,831	16,830
# of continuous var	111,399	111,399	111,399	113,583	111,399
# of constraints	104,188	104,188	104,188	106,373	104,188

Besides the scenario with heuristic schedule, all other cases converged to the same optimal frac schedule since the high revenue achieved from this schedule is an order of magnitude higher than the cost, thus it is unlikely that a different schedule with lower revenue will yield a low enough cost to compensate for the change in revenue. Both the optimal schedule and heuristic schedule are shown in Figure 5.7. In the optimal solution, all wellpads are stimulated under the fastest completion rate, whereas in the heuristic schedule, most wellpads are stimulated at a slower pace.

In the model, we assumed that the desalination facility could be shared by other operators that have around 200 wells to be completed during the same time period. It is interesting

Table 5.5: Summary of objective values.

	Optimal	1: Heuristic	2: No desalination	3: Freshwater trucking	4: Double flowback volume	
Revenue	1,115,618,566	985,551,244	1,115,618,566	1,115,618,566	1,115,618,566	
Cost	Freshwater-related	57,942,917	58,502,626	60,538,657	52,988,194	53,813,066
	Capital	10,210,311	9,558,868	10,814,192	7,372,340	10,210,311
	Operating	47,732,606	48,943,758	49,724,466	45,615,853	43,602,755
	Wastewater-related	23,565,220	26,404,160	63,313,136	23,278,137	44,467,328
	Capital	3,912,326	3,600,535	0	3,598,665	5,109,462
	Operating	19,652,894	22,803,625	63,313,136	19,679,472	39,357,867
Total cost	81,508,137	84,906,786	123,851,793	76,266,331	98,280,395	
Profit	1,034,110,429	900,644,458	991,766,773	1,039,352,235	1,017,338,171	

CHAPTER 5. INVESTMENT OPTIMIZATION MODEL FOR FRESHWATER ACQUISITION AND WASTEWATER HANDLING IN SHALE GAS PRODUCTION



Figure 5.7: Comparison between the optimal and heuristic schedule.

to note that the cost of Scenario 2 (no desalination) is 52% higher than that of the optimal case, considering that desalination is not a standard practice in the Utica. Scenario 4 assumes that the flowback rate doubles in comparison to the flowback rate in the optimal case. The total water-related cost increases by 21%, which is expected since wastewater handling cost increases significantly. However, the pumping cost in Scenario 4 is actually lower compared to the optimal case, \$38.9 million to \$41.8 million, since Scenario 4 takes advantage of recycling the high flowback rate.

Freshwater-related costs for the various scenarios are summarized in Figure 5.8. The optimal solution, heuristic solution, and Scenario 2 solution have similar freshwater pumping costs at around \$42.8-44.7 million. In addition, Scenario 3 takes advantage of flexibility in truck use. Out of the 1073.8 MG of water used to frac the 14 wellpads, 349.4 MG is freshwater supplied through truck hauling. By allowing trucking, the uninterruptible water source for trucking is set up with four interruptible river sources, whereas the optimal scenario requires all five river sources to be set-up. This allows for more robust freshwater supply during periods of low water availability in the interruptible sources, leading to the highest profit, (\$ 1,039 million). As a result, whereas the optimal scenario requires the construction of a 10 MG impoundment, Scenario 3 does not invest in this impoundment. Figure 5.9 shows the total water availability from the sources chosen in the optimized solution for each of the two areas as well as the cumulative trucking use in the two areas. As can be seen from the figure, there is a correlation between period of low water availability and increases in truck use. Overall, the cost for allowing freshwater truck hauling is lower than the optimal solution without the trucking option (\$81.5 vs 76.3 million). However, if freezing is not issue in a shale play region, overland pipeline can offer an even less expensive option.

CHAPTER 5. INVESTMENT OPTIMIZATION MODEL FOR FRESHWATER ACQUISITION AND WASTEWATER HANDLING IN SHALE GAS PRODUCTION

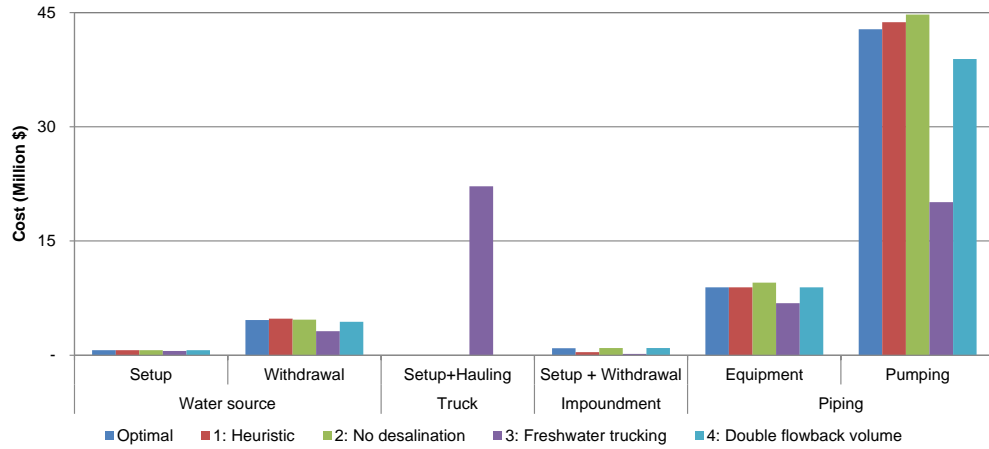


Figure 5.8: Freshwater cost comparison for all scenarios.

Wastewater cost distribution for the four scenarios is presented in Figure 5.10. For the optimal solution, the total cost for desalination (annualized capital cost, operating cost, sludge disposal, discharge cost, and trucking cost from desalination plant to disposal well) is \$20.8 million for 66.1 MG of flowback water, whereas onsite treatment costs \$2.5 million for a total throughput of 35.2 MG. All the scenarios (other than scenario 2) select mechanical vapor recompression as the choice for desalination. Note that other than Scenario 2 where desalination is not an option, none of the other scenarios use direct disposal through Class II injection well. This is mainly due to the relative distance between the centralized desalination plant and the disposal well with respect to the wellpads (13 mi vs 30 mi) for this specific example.

In the problem formulation, we determine the volume of flowback water to recycle for frac fluid by using an upper bound for the concentration (50,000 ppm of TDS), whereas operators use a percentage value (15% of flowback water) to limit recycle. The percentage limit is a convenient measure to evaluate. However, the physical limitation of TDS presence in frac fluid is determined by the concentration. The advantage of the current approach can be seen in the result from the optimal scenario as shown in Figure 5.11. The figure on the left indicates the overall frac fluid composition for each wellpad. Wellpad

CHAPTER 5. INVESTMENT OPTIMIZATION MODEL FOR FRESHWATER ACQUISITION AND WASTEWATER HANDLING IN SHALE GAS PRODUCTION

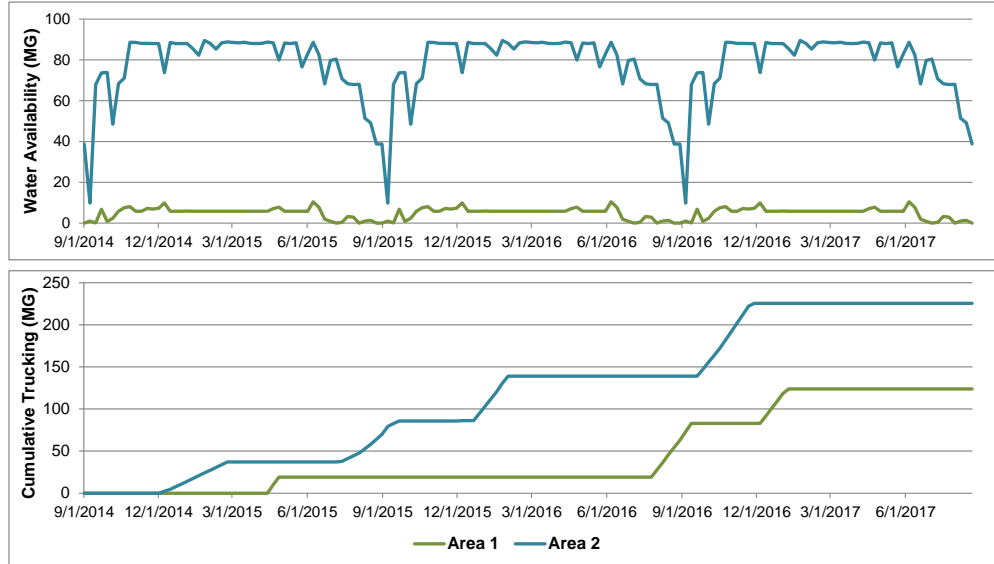


Figure 5.9: Scenario 3 freshwater availability and trucking use.

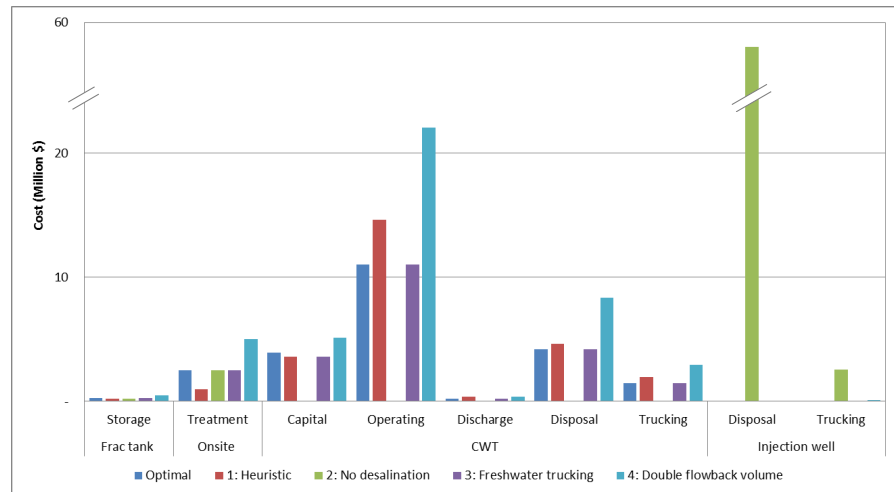


Figure 5.10: Wastewater cost comparison for all scenarios.

1 uses only freshwater since it is the first one to be stimulated. All the wellpads use less than 15% of recycled water. However, if we examine the second figure, which represents the composition over time for wellpad 3, we can see that both in week 1 and week 7, the

recycled water flowrate makes up about 20% of frac fluid. The first week of recycled water mainly comes from the initial flowback of wellpad 8, which has low TDS concentration. The last week of recycled water comes from desalinated wastewater, since the later period of flowback has high TDS concentration.

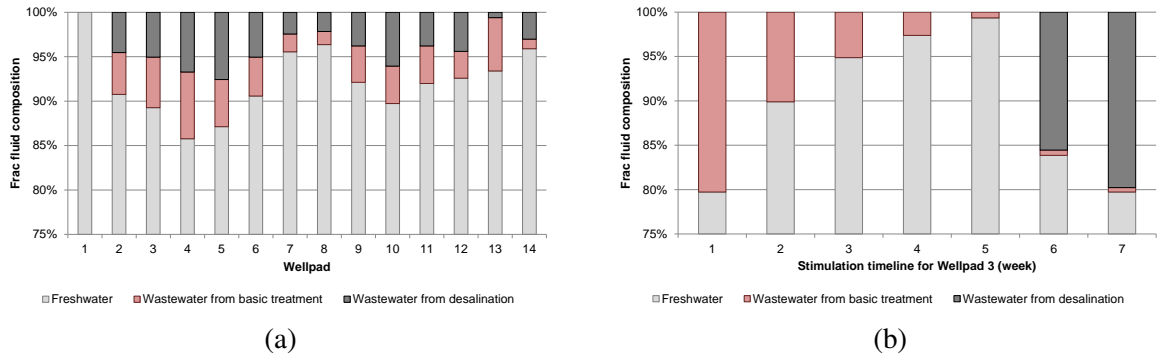


Figure 5.11: Frac fluid composition in the optimal scenario for (a) all wellpads averaged over time and (b) wellpad 3.

Note that the total freshwater-related cost is significantly higher than wastewater handling cost. One reason for this is that only less than three years (time horizon of the example) of produced water is considered in this example. However, operators expect around 10 bbl of produced water per month for each well for the lifetime of the well. This small stream of high salinity produced water requires proper handling and can incur a high cost.

5.6 Conclusion

An MILP formulation has been proposed for capital investment decisions related to freshwater sources, storage, and flowback treatment facility for managing water in shale gas development. We have presented a case study with 14 wellpads, 9 freshwater sources, and 3 desalination technologies from Utica shale analyzing water-related costs under a number of scenarios. From the results, the importance of simultaneously optimizing completion schedule with water acquisition, transportation, storage, and treatment has been demonstrated. Also, it has been shown that desalination can be cost-effective for operators in

the Utica if collaboration could be established. Although transporting freshwater through truck is relatively expensive and environmentally unfriendly, allowing truck hauling, in addition to pipeline transportation, can still provide enough flexibility to guarantee freshwater supply so that less freshwater sources need to be set-up for pipeline transportation and less capital investment is required for impoundment construction. Finally, we have shown that for regions with high flowback rate, the wastewater handling cost does increase as expected. However, with proper recycling schemes, the flowback water can be blended for frac fluid use and reduce freshwater supply cost.

Nomenclature

Sets	
t, t', t''	Time interval
k	Stages per day fractured scenarios
u, u'	All locations
s_u, s'_u	Wellpads
o_u	Freshwater source river
q_u	Freshwater source pond
p_u	Impoundment
c	Pipeline type
r	Concentration discretization intervals
$DP_{u,u'}$	Potential pipeline
Superscripts	
FW	Freshwater
FB	Flowback water
WW	Wastewater
IP	Impoundment
PD	Pond

CHAPTER 5. INVESTMENT OPTIMIZATION MODEL FOR FRESHWATER ACQUISITION AND WASTEWATER HANDLING IN SHALE GAS PRODUCTION

RI	River
PI	Pipeline
TR	Truck
ST	Frac tank storage
OT	Onsite treatment
CT	CWT
DP	Disposal
max	Upper bound
min	Lower bound
Parameters	
F_{qt}^{PD}	Water flowrate available for withdrawal
$F_{ot}^{max,RI}$	maximum withdrawal rate from river, MG
$F_{wt}^{max,CT}$	Maximum CWT capacity, MG
SF_{st}^{FB}	Flowback/produced water flowrate per time period t, MG
SC_{st}^{FB}	Flowback/produced water concentration in time period t, ppm
SFT_{st}	Remaining flowback/produced water in the next 20 years, MG
STC	Crew transition period, week
STF_k	Frac rate, stage/week
SFL_{sk}	Frac weeks of each wellpad
SDW_s	Freshwater use at each wellpad in each period, MG
SLW_s	Freshwater use at each wellpad in the last period, MG
AR	Annualized factor for investment on treatment units
P_{st}	Revenue from gas production at each wellpad, \$
$UDI_{uu'}$	Distance between u and u', mi
UDC	Distance to desalination facility, mi
UDS	Distance to disposal, mi
UF	Maximum pipe capacity, MG
LF	Minimum Pipe capacity, MG
ICB_p^{IP}	Base investment cost for impoundment, \$

CHAPTER 5. INVESTMENT OPTIMIZATION MODEL FOR FRESHWATER ACQUISITION AND WASTEWATER HANDLING IN SHALE GAS PRODUCTION

ICI_p^{IP}	Incremental investment cost for impoundment, \$/MG
$IC_w^{WW,CT}$	Investment cost for desalination technology, \$
IC_u^{FW}	Freshwater source set-up cost, \$
IC_c^{PI}	Capital cost of pipelines, \$/mi
OC_p^{IP}	Operating cost for impoundment, \$/week
OC_u^{FW}	Freshwater cost from source u, \$/MG
$OC^{WW,TR}$	Wastewater trucking cost, \$/bbl/mi
$OC^{WW,ST}$	Wastewater frac tank storage cost, \$/bbl/week
$OC^{WW,OT}$	Wastewater onsite treatment cost, \$/bbl
$OC_w^{WW,CT}$	CWT treatment cost, \$/bbl
$OCDC^{WW}$	Desalinated water discharge cost, \$/bbl
$OCDS^{WW}$	Disposal cost, \$/bbl
OC_c^{PI}	Operating cost of pipelines, \$/mi/week
$OCPU$	Pumping cost, \$/week
CF	Concentration upper bound in frac fluid, ppm
CD	TDS discharge concentration tolerance, ppm
CU_w^{CT}	Concentration upper bound in desalination unit inlet, ppm
η_w	Desalination recovery
CP^{PD}	Upper bound capacity of pond, MG
$CP_p^{IP,max}$	Upper bound capacity of impoundment, MG
$CP_p^{IP,min}$	Lower bound capacity of impoundment, MG
Binary variables	
y_{skt}	Defines the beginning of stimulating each wellpad
$y_{uu'c}^{PI}$	Defines existence of piping connections
y_o^{RI}	River o is set up
y_q^{PD}	Pond o is set up
y_p^{IP}	Impoundment p is set up
y_{pt}^{IP}	Impoundment p is used
y_w^{CT}	Indicates the technology for desalination

CHAPTER 5. INVESTMENT OPTIMIZATION MODEL FOR FRESHWATER ACQUISITION AND WASTEWATER HANDLING IN SHALE GAS PRODUCTION

Continuous variables

f_{qt}^{PD}	Pond withdrawal from precipitation, MG
f_{ot}^{RI}	River allowed withdrawal, MG
$f_{uu'/ct}^{PI}$	Freshwater flow from one location to the next, MG
f_{st}	Total water use at each wellpad per time period, MG
f_{st}^{FW}	Freshwater supplied through pipe and used at each wellpad, MG
f_{st}^{WW}	Wastewater use at each wellpad, MG
f_{st}^{TR}	Freshwater transported to each wellpad through trucking, MG
f_{st}^{FB}	Wastewater flowback at each wellpad, MG
f_{st}^{OT}	Onsite treatment throughput, MG
f_t^{CT}	Total wastewater processed through desalination, MG
f_{wt}^{SCT}	Wastewater processed through desalination unit w , MG
f_{st}^{RCT}	Desalinated wastewater recycled to the completion pad, MG
f_t^{DP}	Wastewater disposed, MG
$f_{st}^{FB,OT}$	Flowback water to be transported to basic treatment, MG
$f_{st}^{FB,CT}$	Flowback water to be desalinated, MG
$f_{st}^{FB,DP}$	Flowback water to be disposed at an injection well, MG
f_w^{TCT}	Desalination plant throughput, MG
c_{st}^{FB}	Wellpad flowback TDS concentration, ppm
c_t^{OT}	TDS concentration of flowback transported to basic treatment, ppm
c_t^{CT}	TDS concentration of the feedwater stream to desalination, ppm
v_{pt}^{IP}	Volume of impoundment, MG
v_{qt}^{PD}	Volume of pond, MG
v_t^{CT}	CWT wastewater storage tank, MG
l_p^{IP}	Capacity of impoundment, MG
l_{st}^{ST}	Capacity of wastewater tanks, MG

Chapter 6

Conclusion

This work has focused on the reduction of water-related costs in both chemical processes and unconventional natural gas development. The first part (chapters 2 and 3) involves the application of process models with water-using units as well as wastewater treatment processes. The second half (chapters 4 and 5) deals with water management strategies in Shale plays, where water use volume and cost become more significant than most conventional applications. Options for reducing freshwater consumption can be achieved through reuse, recycle, and regeneration. The objective is to systematically optimize for both conventional and novel applications in a superstructure-based design. In this final chapter, we first summarize the four major chapters of the thesis, then list the main contributions of this work, followed by a discussion of the recommendations for future work.

6.1 Summary of thesis

6.1.1 Water targeting model for water-using process units

Chapter 2 presents an approach to perform simultaneous optimization of heat and water integration for a process flowsheet. Simultaneous optimization allows for complex trade-

offs among raw materials, investment cost, and energy and water consumption in a process flowsheet, which leads to lower cost solutions with efficient use of energy and water. We have proposed a solution methodology where a simplified targeting formulation that can predict the minimum freshwater consumption is required. NLP formulations are typically used to describe a superstructure-based multi-contaminant WN. The nonlinearity is mainly due to the bilinear term of flow multiplied by concentration in the mixer units. To this end, an LP formulation for freshwater targeting based on a WN superstructure has been developed. The formulation for multi-contaminant WN problems with only water-using process units has been shown to be exact under a certain assumption, and it yields a tight upper bound in cases where the assumption does not hold true. We then apply this targeting formulation to two examples, methanol and bioethanol processes, using simultaneous optimization strategy, and demonstrate the effectiveness of the simultaneous approach in improving both the quality and computational effort of the solution. In the methanol synthesis example, the simultaneous optimization approach enables an improvement in the profit from 62.7MM\$ to 73.4MM\$ per year, a 17% increase. This formulation is also combined with the heat targeting model by Duran and Grossmann²⁷ to determine the minimum utility and water requirement for heat-integrated WNs. An example from Bogataj and Bagajewicz⁶² with four water-using process units operating at different temperatures is used to compare the targeting formulation and the detailed MINLP network synthesis model. The detailed model from literature is an MINLP with 749 continuous variables and 115 binary variables, while the targeting formulation (NLP) contains only 206 continuous variables and no binary variables. The solutions from both methods identify the same heating, cooling, and freshwater consumption.

6.1.2 Wastewater regeneration models for water network optimization

Chapter 3 describes an approach combining various technologies capable of removing all the major types of contaminants through the use of more realistic models. The following improvements are made over the typical superstructure-based water network models.

First, since the most common model for treatment units is relating the inlet and outlet concentrations of each contaminant by a removal ratio, we have developed unit-specific short-cut models in place of the fixed contaminant removal model to describe contaminant mass transfer in wastewater treatment units. We have developed short-cut models for reverse osmosis, activated sludge, etc. Short-cut wastewater treatment cost functions are also incorporated into the model. By considering the use of short-cut models, we are able to exploit the trade-offs between treatment cost and removal efficiency of the units. In addition, uncertainty in mass load of contaminant is considered through multiple scenarios (e.g. best, average, and worst) to account for the range of operating conditions. In the illustrative example, the total network cost for optimizing for the worst scenario is \$565,828.80, whereas the cost is \$543,008.65 for optimizing over all three scenarios. In addition, the superstructure is modified to accommodate realistic potential structures. We have also presented a modified Lagrangean-based decomposition algorithm in order to solve the resulting nonconvex MINLP problem efficiently. The effectiveness of the algorithm is demonstrated in Example 1, which has two water-using PUs and two sets of wastewater treatment technologies. The resulting choice of treatment technology is different (ion exchange vs. reverse osmosis) from the simplified model used in the illustrative example. The decomposition algorithm is able to reduce the computational effort by almost a factor of five.

6.1.3 Operational model for shale gas water management

Compared to the process industries, the quality and quantity of freshwater supply is even more significant for shale gas operators. In addition, flowback water management presents a major challenge to the industry. In collaboration with Carrizo Oil & Gas, we have proposed a two-stage programming MILP scheduling formulation to address the various concerns regarding water usage. The goal in Problem I is to balance the trade-off between water acquisition from uninterruptible sources (e.g. large rivers) that are available throughout the year but require more expensive truck transportation, versus acquisition from interruptible sources (e.g. creeks) that can be transported with pipelines at lower costs but are not

available throughout the year. An effective STN-based model has been developed for this problem, and we have applied this model to Carrizo's operation in the Marcellus play in Example 1 with data provided by the operator. The optimized stimulation schedule leads to an order magnitude reduction in freshwater trucking cost (\$5.9 million to \$569,000) compared to a heuristic schedule proposed by the operator. As a result, only 2.4% of the total freshwater required for frac fluid is supplied by truck hauling, while the rest is transported through pipelines. This model has been extended to handle a combination of disposal options with alternatives for recycling and reuse of flowback water, while accounting for the income from the sales of natural gas (Example 2). The inclusion of the sales revenue leads to a more aggressive stimulation schedule that increases the revenue from 181.43 MM\$ to 237.56 MM\$. Although the trucking cost does not experience a significant reduction as seen in Example 1, the overall cost is still reduced from 25.02 to 23.41 MM\$.

6.1.4 Investment optimization model for freshwater acquisition and wastewater handling in shale gas production

With the rapid increase in shale gas production, wastewater management becomes a major issue. As a result, operators need to start making long-term investment decisions to handle flowback and produced water efficiently. In chapter 5, we focus on making investment decisions, including freshwater source setup cost, piping setup cost, freshwater impoundment setup cost, and annualized desalination plant, in order to determine an overall cost-saving strategy. The goal is to determine the optimal freshwater sources for the given set of wellpads based on their respective location, availability, and cost. Treatment facility capacity and removal options that cater to the flowback and produced water characteristics of the region are optimized in addition to the frac schedule. We have presented a case study and several scenarios from the Utica shale to illustrate the model. First, by simultaneously optimizing frac schedule and costs as opposed to optimizing the cost model with fixed frac schedule, a 14.8% improvement in profit can be achieved. Also, we have found that desalinating flowback water not only allows for a higher recycle ratio of the wastewater, but also cost reduction in freshwater supply. Freshwater trucking is allowed

in a third scenario, the result of which indicates that trucking improves the economic and robustness of the operation since freshwater supply in the region is highly intermittent. Finally, we analyzed the effect that increased flowback water flowrate has on the overall cost. Even though treating the flowback becomes more expensive, there is a reduction in freshwater supply cost due to a higher recycle rate, which leads to an overall cost increase by 21%.

6.2 Research contribution

1. An LP formulation has been developed for targeting minimum freshwater consumption for a set of water-using process units with multiple contaminants.
2. The LP targeting method has been used for simultaneous flowsheet optimization with heat and water integration, thereby avoiding the use of detailed NLP or MINLP models for water network synthesis. Since the formulation is linear, it does not contribute significantly to the computational difficulty of the simultaneous optimization of flowsheet formulation.
3. The water targeting formulation has been simultaneously optimized with heat targeting formulation to determine the minimum utilities required for heat-integrated water networks. The problem has smaller size and requires less computational effort compared to solving the detailed HEN and WN superstructures.
4. Wastewater treatment design models based on short-cut models have been developed for several technologies (reverse osmosis, ion exchange, sedimentation, ultra-filtration, activated sludge, and trickling filter) to improve the accuracy of WN with wastewater treatment units. The model can determine the optimal trade-off between treatment unit removal efficiency and capital and operation cost.
5. A Lagrangean decomposition algorithm has been developed to synthesize the water networks with short-cut models under multiple scenarios.
6. A novel MILP model has been proposed to determine the schedule for fracturing a

set of wellpads as well as the acquisition of water from uninterrupted or interruptible sources with both pipelines and trucks.

7. The proposed MILP model has been applied to real shale gas operation in the Marcellus play, yielding significant cost reductions and revenue enhancement in comparison to heuristic schedule developed by shale gas operators.
8. The MILP model has been expanded to incorporate investment decisions in freshwater acquisition, wastewater treatment, storage, and transportation. The model can cater to regional differences, and it has been applied to shale gas operation in the Utica shale.

6.3 Future research directions

6.3.1 Process water network

Predicting contaminant loads. The water-using process units in the water network are characterized by maximum concentration limits on the inlet streams as well as the mass load of contaminants released from the unit into the water stream. Typical water use such as vessel cleaning or solvent extraction emphasizes the mass load of contaminants to be removed, and the water loss or gain is assumed to be negligible¹⁸. Another type of processes such as cooling water cycle concerns more with water flowrate in the process. The need for retrofitting water networks arises from capacity increase, product quality change, and environmental regulations⁹⁸. Methods assuming constant load of contaminants are more appropriate for retrofit, since the specific performance data can be measured in the plant. However, for grass-root design models are required to predict contaminant loads^{32,20}. In chapter 3, we have used a three-scenario model to account for the uncertainty of the processing conditions during the course of the operations. However, a more fundamental approach for modeling contaminants would be desirable. One extension of this work is to predict contaminants loads based on the characteristics of actual process unit operations. By developing more rigorous process models, one can better estimate the mass load and

contaminant concentration in the water streams.

6.3.2 Shale gas water management

Long-term wastewater handling. Long term produced water needs to be handled efficiently. Currently, once an operator stops stimulating or completes all the wells in a region, the wastewater produced thereafter is typically disposed. Sharing of flowback and produced water among operators is prohibited due to regulatory restrictions. In addition, unlike conventional facilities that typically operate at steady state, shale gas flowback water exhibit a decaying profile with fluctuations in the impurity concentration level. As a next step, one could investigate the cost savings assuming it is possible to transfer liability of wastewater to encourage more collaboration. In addition, more detailed models should be developed since the choice of desalination technologies suitable for treating high-TDS water (e.g. forward osmosis, mechanical vapor compression, and membrane distillation¹) is mainly an economic decision.

Wellpad drilling logistics. Another consideration is that drilling decisions could be optimized with water use logistics⁹⁹. The operators need to decide the number of wells to drill at each wellpad during each time period. The length of each well and the spacing between two wells have significant impact on the well's productivity. An increase in the length of the well leads to a higher gas production. However, drilling at such a distance from the wellbore becomes much more difficult, thus increasing the drilling cost significantly. Alternatively, the operators could set up another wellpad in close proximity to the previous pad, and it is possible to have the two wells at the different wellpads to crossover. Since the volume of water used is determined by the number of stages drilled at each wellpad, and the type of frac fluid used at each pad is mainly dependent on the geological formation, the drilling schedule could have significant impact on the water management strategies adapted at each site.

Uncertainty. Freshwater availability is highly seasonal and the fluctuation can affect the frac schedule. We have included the uncertainty associated with freshwater availability of interruptible sources in the operation model for shale plays. Other fluctuating factors

that could affect the optimization result are gas production profile and flowback water flowrate profile. Typically, at each wellpad, operators would drill a test well to determine the productivity of its nearby wells. As more wells are drilled in close proximity, one can better estimate the composition and production profile of the wells in each wellpad. The next step could take this uncertainty into consideration and formulate a stochastic programming problem to better estimate the expected profit related to the wellpads⁸⁶.

Environmental risk measures. One of the major issues in shale gas operations is the potential adverse impact on the environment, namely wastewater disposal, waste transport emission, and water source pollution. Developing criteria for estimating environmental risks from shale gas development then becomes an important consideration^{100,101}.

The bi-criterion optimization approach both maximizes net present value (NPV) and minimizes environmental impact (ENV) as seen in model (6.1).

$$\begin{aligned}
 \max. \quad & NPV = f_1(x, y) \\
 \min. \quad & ENV = f_2(x, y) \\
 \text{s.t.} \quad & g(x, y) \leq 0 \\
 & x \in X, \quad y \in \{0, 1\}
 \end{aligned} \tag{6.1}$$

The bi-criterion approach can be solved using the ϵ -constrained method, which relies on obtaining a series of Pareto-optimal solutions. The environmental objective (ENV) is set as an inequality constraint where $ENV \leq \epsilon$, and the problem is solved for different values of ϵ .

The environmental model itself can be evaluated through Life Cycle Analysis (LCA). LCA is a method to assess environmental impacts associated with a product or process over all the stages. This is achieved by expanding the boundaries to include the upstream (its primary resources) and downstream (final disposal) activities related to the main process itself. Indicators such as ReCiPe¹⁰² and Eco-indicator 99¹⁰³ can also aid in developing optimal water management strategies. A synergy can be created between the reduction of capital and operation cost and the reduction in environmental disturbances. A major chal-

lenge, however, is that data in these LCA systems is either highly uncertain or unavailable for shale gas (e.g. methane emissions)¹⁰⁴. Therefore, prediction of emissions in shale gas operations is also an important future research direction.

Appendix A

LP Targeting Model for Single Contaminant System

This appendix makes a comparison of the superstructure and formulation of two models for predicting freshwater target in the context of single-contaminant WN. Even though the solutions of two models lead to different optimal WN structures, the freshwater targets obtained are the same for each water-using process unit.

The original LP formulation,

$$\begin{aligned} \min. \quad & \sum_j FW_j^w \\ \text{s.t.} \quad & FW_j^w + \sum_i F_{i,j} - \sum_k F_{j,k} - F_{j,out} = 0 \quad \forall j \in N, i \in P_j, k \in R_j \\ & F_h^w - \frac{L_h}{C_{h,out}^{max}} = 0 \quad \forall h \in H \\ & \sum_i F_{i,j} (C_{i,out}^{max} - C_{j,in}^{max}) - F_j^w C_{j,in}^{max} \leq 0 \quad \forall j \in H, i \in P_j \\ & \sum_i F_{i,j} (C_{i,out}^{max} - C_{j,out}^{max}) - F_j^w C_{j,out}^{max} + L_j = 0 \quad \forall j \in H, i \in P_j \end{aligned} \tag{A.1}$$

was developed by Bagajewicz¹⁹ is designed for the single-contaminant Water-Allocation

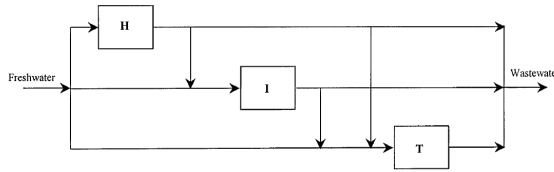


Figure A.1: Schematic representation of a water network.

Planning (WAP) problem. A.1⁵⁹ illustrates the alignment of different types of water-using process units. The sets H represents head process is a water-user that utilizes only fresh water; I is the set of intermediate water user processes that receive streams from other units and feeds water streams to other units; finally, T is the set of terminal processes that receive streams from other processes, and they discharge their outlet water streams to treatment. The set of interconnections among the process units are shown in A.1 and A.2¹⁹.

The freshwater minimization in the work by Savelski and Bagajewicz⁵⁹, which we will refer to as “Model 1”, assumes a mass-transfer model, which applies to water-using process units that have fixed loads of contaminant to be removed. The units are also characterized by their maximum inlet and outlet concentrations for the contaminant. Savelski and Bagajewicz proved that the outlet stream of a process unit reaches its contaminant concentration upper bound for a network solution that consumes minimum freshwater flowrate. Thus, this condition of optimality fixes the outlet concentration for a process unit to its upper bound. The flowrate through a process unit can be varied with the process inlet concentration. On the other hand, the model (NLP-1) used in chapter 2, which we will refer to as “Model 2”, assumes fixed demand of water flowrate through a process unit in addition to fixed load of contaminant. This condition was used in¹⁶, and in essence, it fixes the inlet and outlet concentration difference. It can be shown that even though the two models provide different optimal WN connectivities and flowrates, they provide equivalent freshwater targets.

We can compare the two models by considering the ten-processes problem in¹⁹ (whose data is omitted here). Model 1 predicts a minimum freshwater usage of 165.94 ton/hr. By applying (NLP-1) to this problem and restricting process stream connectivities and flowrates based on the result obtained in Model 1, we also obtain a minimum freshwater

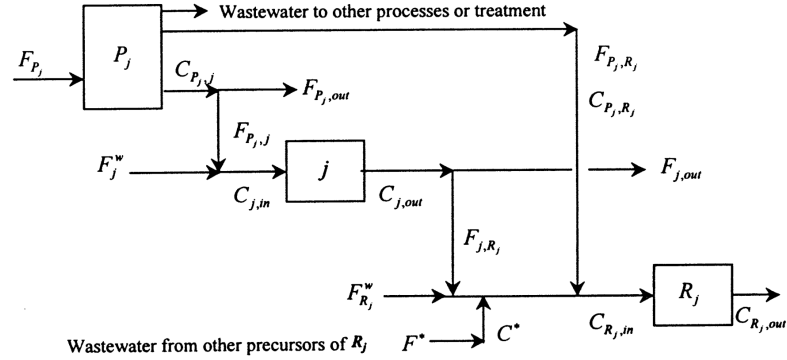


Figure A.2: Precursor and receivers of a process.

consumption of 165.94 ton/hr (this target can also be obtained by (LP-1)).

A closer look at the solutions shows that two cases arise from the two models - the process units could either have different flowrates (thus different inlet concentrations) or the same flowrate (the inlet concentration reaches its upper bound). The former case can be observed in Model 1, where two of the process units use only freshwater to satisfy contaminant removal demands. Therefore, their inlet concentrations are zero, even though the maximum inlet concentration for those units are greater than zero. In Model 2, however, the same two process units allow their inlet streams to reach upper bounds, thus the flowrates through those units are higher than predicted in Model 1. This difference between the two models is reconciled by the local recycle stream allowed in Model 2 as shown in A.3. In the second case where the two models predict the same water flowrate through a process unit, the resulting structure demands for reuse streams from other process units, with or without freshwater consumption to that given process units. This is shown in A.4.

Note that in Model 1, only one direction is allowed for reuse based on the concentration monotonicity proved by Savelski and Bagajewicz⁵⁹. However, Model 2 contains more structural possibilities that could be useful, especially when dealing with multiple contaminants. In that sense, Model 1 can be regarded as a restricted form of Model 2 as shown in A.6. For this case, taking into account Proposition 1, the model (NLP-1) reduces

APPENDIX A. LP TARGETING MODEL FOR SINGLE CONTAMINANT SYSTEM

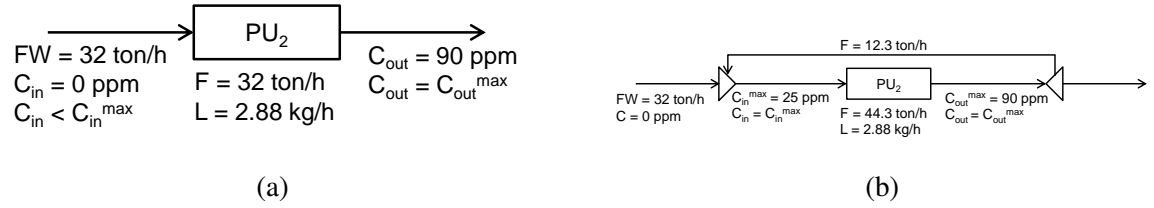


Figure A.3: PU2 stream parameters and variables obtained in (a) Model 1 and (b) Model 2.

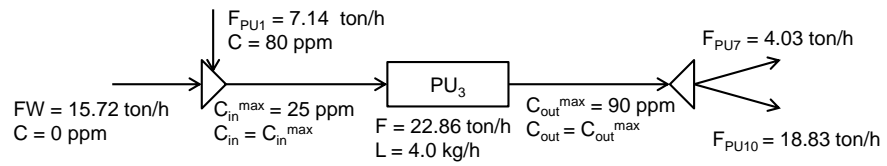


Figure A.4: PU3 stream parameters and variables obtained in Model 1 and Model 2.

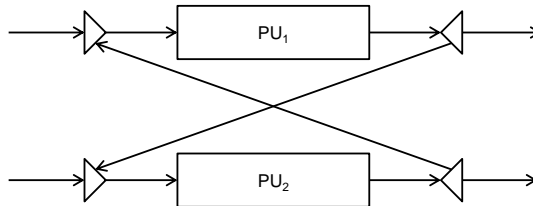


Figure A.5: Excluded structural connectivity in Model 1.

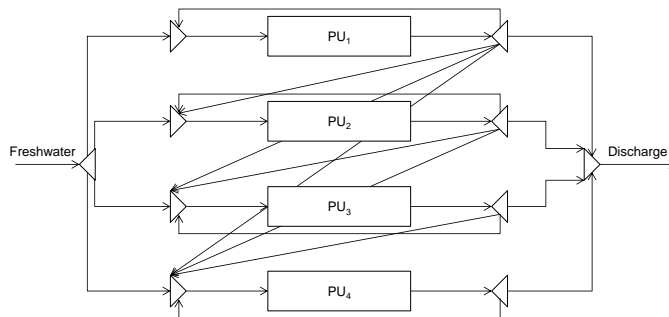


Figure A.6: Representation of Model 1 using Model 2 superstructure.

APPENDIX A. LP TARGETING MODEL FOR SINGLE CONTAMINANT SYSTEM

for the case of a single contaminant to the following LP, where all the concentrations reach their maximum concentrations, and the only variables are the flowrates, F^k and F^i .

$$\begin{aligned}
 \text{min.} \quad & FW \\
 \text{s.t.} \quad & FW = \sum_{k \in SU_{in}} F^k \\
 & F^k = \sum_{i \in m_{in}} F^i \quad \forall m \in MU, k \in m_{out} \\
 & F^k C^{k,max} = \sum_{i \in m_{in}} F^i C^{i,max} \quad \forall m \in MU, k \in m_{out} \quad (\text{LP-s}) \\
 & F^k = \sum_{i \in s_{out}} F^i \quad \forall s \in SU, k \in s_{in} \\
 & P^p C^{k,max} + L^p = P^p C^{i,max} \quad \forall p \in PU, \forall k \in p_{in}, i \in p_{out} \\
 & F^{k,min} \leq F^k \leq F^{k,max} \quad \forall k
 \end{aligned}$$

Model (LP-s), which is for single contaminant, can be shown (we omit the detailed derivation) to provide the same freshwater consumption as the LP in (A.1).

Appendix B

Convex Envelopes

- Bilinear terms⁶⁰: $FC \rightarrow f$

$$\left. \begin{aligned} f &\geq F^{min}C + C^{min}F - F^{min}C^{min} \\ f &\geq F^{max}C + C^{max}F - F^{max}C^{max} \\ f &\leq F^{min}C + C^{max}F - F^{min}C^{max} \\ f &\leq F^{max}C + C^{min}F - F^{max}C^{min} \end{aligned} \right\} \quad (\text{B.1})$$

- Concave term: $F^\alpha \rightarrow \Theta$

$$\Theta \geq (F^{min})^\alpha + \left(\frac{(F^{max})^\alpha - (F^{min})^\alpha}{F^{max} - F^{min}} \right) (F - F^{min}) \quad (\text{B.2})$$

- $\sqrt{V} \rightarrow V_{new}$ (From trickling filter formulation (3.17) and (3.19))

$$V_{new}^2 - V \leq 0 \quad (\text{B.3})$$

Bibliography

- [1] Shaffer D. L, Arias Chavez L. H, Ben-Sasson M, Romero-Vargas Castrilln S, Yip N. Y, Elimelech M. Desalination and Reuse of High-Salinity Shale Gas Produced Water: Drivers, Technologies, and Future Directions *Environmental Science & Technology*. 2013;47:9569–9583.
- [2] An Integrated Framework for Treatment and Management of Produced Water. RPSEA Project 07122-12 Colorado School of Mines 2009.
- [3] Slutz J, Anderson J, Broderick R, Horner P. Key Shale Gas Water Management Strategies: An Economic Assessment Tool *SPE/APPEA International Conference on Health, Safety, and Environment in Oil and Gas Exploration and Production*. 2012.
- [4] Abdalla C, Drohan J, Rahm B, et al. Waters Journey Through the Shale Gas Drilling and Production Processes in the Mid-Atlantic Region *Penn State Extension*. 2011.
- [5] Crittenden J. C, Trussell R. R, Hand D. W, Howe K. J, Tchobanoglous G. *MWHs Water Treatment Principles and Design*. Wiley 2012.
- [6] ERM . CDP Water Disclosure 2010 Global Report tech. rep. Carbon Disclosure Projects 2010.
- [7] Hohmann E. *Optimum networks for heat exchange*. PhD thesis Univ. Southern California 1971.

- [8] Linnhoff B, Flower J. R. Synthesis of heat exchanger networks: I. Systematic generation of energy optimal networks *AIChE Journal*. 1978;24:633-642.
- [9] Yee T, Grossmann I. Simultaneous optimization models for heat integration –II. Heat exchanger network synthesis *Computers & Chemical Engineering*. 1990;14:1165 - 1184.
- [10] Papoulias S. A, Grossmann I. E. A structural optimization approach in process synthesis –II: Heat recovery networks *Computers & Chemical Engineering*. 1983;7:707 - 721.
- [11] Wang Y, Smith R. Wastewater minimisation *Chemical Engineering Science*. 1994;49:981 - 1006.
- [12] Kuo W.-C. J, Smith R. Effluent treatment system design *Chemical Engineering Science*. 1997;52:4273 - 4290.
- [13] Manan Z. A, Tan Y. L, Foo D. C. Y. Targeting the minimum water flow rate using water cascade analysis technique *AIChE Journal*. 2004;50:3169-3183.
- [14] Takama N, Kuriyama T, Shiroko K, Umeda T. Optimal water allocation in a petroleum refinery *Computers & Chemical Engineering*. 1980;4:251 - 258.
- [15] Huang C.-H, Chang C.-T, Ling H.-C, Chang C.-C. A Mathematical Programming Model for Water Usage and Treatment Network Design *Industrial & Engineering Chemistry Research*. 1999;38:2666-2679.
- [16] Karuppiah R, Grossmann I. E. Global optimization for the synthesis of integrated water systems in chemical processes *Computers & Chemical Engineering*. 2006;30:650 - 673.
- [17] Teles J, Castro P. M, Novais A. Q. LP-based solution strategies for the optimal design of industrial water networks with multiple contaminants *Chemical Engineering Science*. 2008;63:376 - 394.
- [18] Foo D. C. Y. State-of-the-Art Review of Pinch Analysis Techniques for Water

- Network Synthesis *Industrial & Engineering Chemistry Research*. 2009;48:5125-5159.
- [19] Bagajewicz M. A review of recent design procedures for water networks in refineries and process plants *Computers & Chemical Engineering*. 2000;24:2093 - 2113.
- [20] Jezowski J. Review of Water Network Design Methods with Literature Annotations *Industrial & Engineering Chemistry Research*. 2010;49:4475-4516.
- [21] Karuppiah R, Peschel A, Grossmann I. E, Martín M, Martinson W, Zullo L. Energy optimization for the design of corn-based ethanol plants *AIChE Journal*. 2008;54:1499-1525.
- [22] Biegler L. T, Grossmann I. E, Westerberg A. W. *Systematic Methods of Chemical Process Design*. Prentice Hall 1997.
- [23] Lang Y.-D, Biegler L, Grossmann I. Simultaneous optimization and heat integration with process simulators *Computers & Chemical Engineering*. 1988;12:311 - 327.
- [24] Furman K. C, Sahinidis N. V. A Critical Review and Annotated Bibliography for Heat Exchanger Network Synthesis in the 20th Century *Industrial & Engineering Chemistry Research*. 2002;41:2335-2370.
- [25] Gundersen T, Naess L. The synthesis of cost optimal heat exchanger networks: An industrial review of the state of the art *Computers & Chemical Engineering*. 1988;12:503-530.
- [26] Grossmann I, Caballero J, Yeomans H. Mathematical programming approaches to the synthesis of chemical process systems *Korean Journal of Chemical Engineering*. 1999;16:407-426.
- [27] Duran M. A, Grossmann I. E. Simultaneous optimization and heat integration of chemical processes *AIChE Journal*. 1986;32:123-138.
- [28] Ahmetović E, Grossmann I. E. Global superstructure optimization for the design of integrated process water networks *AIChE Journal*. 2011;57:434-457.

- [29] Alva-Argez A, Vallianatos A, Kokossis A. A multi-contaminant transshipment model for mass exchange networks and wastewater minimisation problems *Computers & Chemical Engineering*. 1999;23:1439 - 1453.
- [30] Galan B, Grossmann I. E. Optimal Design of Distributed Wastewater Treatment Networks *Industrial & Engineering Chemistry Research*. 1998;37:4036-4048.
- [31] Savelski M, Bagajewicz M. On the necessary conditions of optimality of water utilization systems in process plants with multiple contaminants *Chemical Engineering Science*. 2003;58:5349 - 5362.
- [32] Faria D. C, Bagajewicz M. J. Planning Model for the Design and/or Retrofit of Industrial Water Systems *Industrial & Engineering Chemistry Research*. 2011;50:3788-3797.
- [33] Khor C. S, Shah N, Mahadzir S, Elkamel A. Optimisation of petroleum refinery water network systems retrofit incorporating reuse, regeneration and recycle strategies *The Canadian Journal of Chemical Engineering*. 2012;90:137–143.
- [34] Dzhygyrey I, Jezowski J, Kvitka O, Statyukha G. Distributed wastewater treatment network design with detailed models of processes in *19th European Symposium on Computer Aided Process Engineering* (Jezowski J, Thullie J. , eds.);26 of *Computer Aided Chemical Engineering*:853 - 858Elsevier 2009.
- [35] Karuppiah R, Grossmann I. E. Global optimization of multiscenario mixed integer nonlinear programming models arising in the synthesis of integrated water networks under uncertainty *Computers & Chemical Engineering*. 2008;32:145 - 160.
- [36] Davis M. L. *Water and Wastewater Engineering, Design Principles and Practices*. McGraw-Hill 2010.
- [37] Commission E. Integrated Pollution Prevention and Control Reference Document on Available Techniques in Common Waste Water and Waste Gas Treatment/Management Systems in the Chemical Sector 2011.

- [38] El-Halwagi M. M. Synthesis of reverse-osmosis networks for waste reduction *AIChE Journal*. 1992;38:1185–1198.
- [39] Lu Y, Hu Y, Xu D, Wu L. Optimum design of reverse osmosis seawater desalination system considering membrane cleaning and replacing *Journal of Membrane Science*. 2006;282:7 - 13.
- [40] Saif Y, Elkamel A, Pritzker M. Optimal design of reverse-osmosis networks for wastewater treatment *Chemical Engineering and Processing: Process Intensification*. 2008;47:2163 - 2174.
- [41] Khor C. S, Foo D. C. Y, El-Halwagi M. M, Tan R. R, Shah N. A Superstructure Optimization Approach for Membrane Separation-Based Water Regeneration Network Synthesis with Detailed Nonlinear Mechanistic Reverse Osmosis Model *Industrial & Engineering Chemistry Research*. 2011;50:13444-13456.
- [42] Karuppiah R, Bury S. J, Vazquez A, Poppe G. Optimal design of reverse osmosis-based water treatment systems *AIChE Journal*. 2012;58:2758–2769.
- [43] Stevens P. The 'Shale Gas Revolution': Developments and Changes tech. rep.Chatham House 2012.
- [44] Permits Issued and Wells Drilled Maps tech. rep.Pennsylvania Department of Environmental Protection 2013.
- [45] Mielke E, Anadon L. D, Narayanamurti V. Water Consumption of Energy Resource Extraction, Processing, and Conversion tech. rep.Energy Technology Innovation Policy research group, Belfer Center for Science and International Affairs, Harvard Kennedy School 2010.
- [46] Holditch S. A. Getting the Gas Out of the Ground *Chemical Engineering Progress*. 2012.
- [47] Gay M. O, Fletcher S, Meyer N, Gross S. Water Management in Shale Gas Plays tech. rep.IHS Water White Paper 2012.
- [48] Ghaffour N, Missimer T. M, Amy G. L. Technical review and evaluation of the

- economics of water desalination: Current and future challenges for better water supply sustainability *Desalination*. 2013;309:197 - 207.
- [49] Wolsey L. A, Nemhauser G. L. *Integer and Combinatorial Optimization*. Wiley 1 ed ed. 1999.
- [50] Biegler L. T. *Nonlinear Programming: Concepts, Algorithms, and Applications to Chemical Processes*. SIAM-Society for Industrial and Applied Mathematics 2010.
- [51] Drud A. CONOPT: A GRG code for large sparse dynamic nonlinear optimization problems *Mathematical Programming*. 1985.
- [52] Wächter A, Biegler L. T. On the implementation of an interior-point filter line-search algorithm for large-scale nonlinear programming *Mathematical Programming*. 2006.
- [53] Sahinidis N. BARON: A general purpose global optimization software package *Journal of Global Optimization*. 1996;8:201205.
- [54] Geoffrion A. Generalized Benders Decomposition *Journal of Optimization Theory and Applications*. 1972;10:237-260.
- [55] Duran M. A, Grossmann I. E. An outer-approximation algorithm for a class of mixed-integer nonlinear programs *Mathematical Programming*. 1986;36:307 - 339.
- [56] Westerlund T, Pettersson F. An extended cutting plane method for solving convex MINLP problems *Computers & Chemical Engineering*. 1995;19, Supplement 1:131 - 136. European Symposium on Computer Aided Process Engineering.
- [57] Kondili E, Pantelides C, Sargent R. A general algorithm for short-term scheduling of batch operations –I. MILP formulation *Computers & Chemical Engineering*. 1993;17:211 - 227.
- [58] Balakrishna S, Biegler L. T. Targeting strategies for the synthesis and energy integration of nonisothermal reactor networks *Industrial & Engineering Chemistry Research*. 1992;31:2152-2164.

- [59] Savelski M. J, Bagajewicz M. J. On the optimality conditions of water utilization systems in process plants with single contaminants *Chemical Engineering Science*. 2000;55:5035 - 5048.
- [60] McCormick G. P. Computability of global solutions to factorable nonconvex programs: Part I Convex underestimating problems *Mathematical Programming*. 1976;10:147-175.
- [61] Savelski M, Bagajewicz M. On the necessary conditions of optimality of water utilization systems in process plants with multiple contaminants *Chemical Engineering Science*. 2003;58:5349 - 5362.
- [62] Bogataj M, Bagajewicz M. J. Synthesis of non-isothermal heat integrated water networks in chemical processes *Computers & Chemical Engineering*. 2008;32:3130 - 3142.
- [63] Dong H.-G, Lin C.-Y, Chang C.-T. Simultaneous optimization approach for integrated water-allocation and heat-exchange networks *Chemical Engineering Science*. 2008;63:3664 - 3678.
- [64] Leewongtanawit B, Kim J.-K. Synthesis and optimisation of heat-integrated multiple-contaminant water systems *Chemical Engineering and Processing: Process Intensification*. 2008;47:670 - 694.
- [65] Kim J, Kim J, Kim J, Yoo C, Moon I. A simultaneous optimization approach for the design of wastewater and heat exchange networks based on cost estimation *Journal of Cleaner Production*. 2009;17:162 - 171.
- [66] Savulescu L, Kim J.-K, Smith R. Studies on simultaneous energy and water minimisation –Part I: Systems with no water re-use *Chemical Engineering Science*. 2005;60:3279 - 3290.
- [67] Turkay M, Grossmann I. E. Structural flowsheet optimization with complex investment cost functions *Computers & Chemical Engineering*. 1998;22:673 - 686.
- [68] Ahmetović E, Martín M, Grossmann I. E. Optimization of Energy and Water Con-

- sumption in Corn-Based Ethanol Plants *Industrial & Engineering Chemistry Research*. 2010;49:7972-7982.
- [69] Brooke A, Kendrick D, Meeraus A, Raman R. *GAMS: A Users Guide*. GAMS Development Corporation 2012.
- [70] Faria D. C, Bagajewicz M. J. On the appropriate modeling of process plant water systems *AIChE Journal*. 2010;56:668–689.
- [71] Faria D. C, Bagajewicz M. J. A new approach for global optimization of a class of MINLP problems with applications to water management and pooling problems *AIChE Journal*. 2012;58:2320–2335.
- [72] Vince F, Marechal F, Aoustin E, Brant P. Multi-objective optimization of RO desalination plants *Desalination*. 2008;222:96 - 118.
- [73] George Tchobanoglous F. L. B, Stensel H. D. *Wastewater Engineering: Treatment and Reuse*. McGraw-Hill 2003.
- [74] Qasim S. R. *Wastewater Treatment Plants: Planning, Design, and Operation*. CRC Presssecond ed. 1998.
- [75] Sharma J. R. Development of a Preliminary Cost Estimation Method for Water Treatment Plants Master's thesisThe University of Texas at Arlington 2010.
- [76] Intelligen, Inc*SuperPro Designer Users Guide* 2007.
- [77] Terrazas-Moreno S, Trotter P. A, Grossmann I. E. Temporal and spatial Lagrangean decompositions in multi-site, multi-period production planning problems with sequence-dependent changeovers *Computers & Chemical Engineering*. 2011;35:2913 - 2928.
- [78] Grossmann I. E, Ruiz J. P. Generalized Disjunctive Programming: A Framework for Formulation and Alternative Algorithms for MINLP Optimization in *Mixed Integer Nonlinear Programming* (Lee J, Leyffer S. , eds.);154 of *The IMA Volumes in Mathematics and its Applications*:93-115Springer New York 2012.

- [79] Oliveira F, Gupta V, Hamacher S, Grossmann I. A Lagrangean decomposition approach for oil supply chain investment planning under uncertainty with risk considerations *Computers & Chemical Engineering*. 2013;50:184 - 195.
- [80] GAMS Development Corporation (2009)*EMP, Users Manual* 2009.
- [81] Viswanathan J, Grossmann I. A combined penalty function and outer-approximation method for MINLP optimization *Computers & Chemical Engineering*. 1990;14:769 - 782.
- [82] Lindo Systems Inc *LINDO Driver* 2011.
- [83] Grossmann I. E, Trespalacios F. Systematic modeling of discrete-continuous optimization models through generalized disjunctive programming *AIChE Journal*. 2013;59:3276–3295.
- [84] Ullmer C, Kunde N, Lassahn A, Gruhn G, Schulz K. WADO™: water design optimization methodology and software for the synthesis of process water systems *Journal of Cleaner Production*. 2005;13:485 - 494.
- [85] National Water Information System tech. rep.USGS 2013.
- [86] Birge J. R, Louveaux F. *Introduction to Stochastic Programming*. Springer 2011.
- [87] Shah N, Pantelides C, Sargent R. A general algorithm for short-term scheduling of batch operations – II. Computational issues *Computers & Chemical Engineering*. 1993;17:229 - 244.
- [88] Horner P, Halldorson B, Slutz J. Shale Gas Water Treatment Value Chain - A Review of Technologies, including Case Studies *SPE Annual Technical Conference and Exhibition*. 2011.
- [89] Gaudlip A, Paugh L, Hayes T. Marcellus Shale Water Management Challenges in Pennsylvania *SPE Shale Gas Production Conference*. 2008.
- [90] Arps J. Analysis of Decline Curves *Trans. AIME*. 1945.

- [91] Cafaro D. C, Grossmann I. E. Strategic planning, design, and development of the shale gas supply chain network *AIChE Journal*. 2014.
- [92] Yang L, Grossmann I. E, Manno J. Optimization models for shale gas water management *AIChE Journal*. 2014:n/a–n/a.
- [93] Gao J, You F. Optimization of Water Supply Chain Design and Long-Term Planning for Shale Gas Production: Milfp Model and Algorithms 2014. AIChE Annual Meeting, Atlanta, GA.
- [94] Coday B. D, Xu P, Beaudry E. G, et al. The sweet spot of forward osmosis: Treatment of produced water, drilling wastewater, and other complex and difficult liquid streams *Desalination*. 2014;333:23 - 35.
- [95] Mauter M, Palmer V. Expert Elicitation of Trends in Marcellus Oil and Gas Wastewater Management *Journal of Environmental Engineering*. 2014;140:B4014004.
- [96] Guan G, Wang R, Wicaksana F, Yang X, Fane A. G. Analysis of Membrane Distillation Crystallization System for High Salinity Brine Treatment with Zero Discharge Using Aspen Flowsheet Simulation *Industrial & Engineering Chemistry Research*. 2012;51:13405-13413.
- [97] McGinnis R. L, Hancock N. T, Nowosielski-Slepowron M. S, McGurgan G. D. Pilot demonstration of the NH₃/CO₂ forward osmosis desalination process on high salinity brines *Desalination*. 2013;312:67 - 74. Recent Advances in Forward Osmosis.
- [98] Faria D. C, Bagajewicz M. J. Profit-based grassroots design and retrofit of water networks in process plants *Computers & Chemical Engineering*. 2009;33:436 - 453.
- [99] Drouven M. G, Grossmann I. E. A New Multi-Period MINLP Model for Optimal Long-Term Shale Gas Development Planning AIChE Annual Meeting 2014.
- [100] Laurenzi I. J, Jersey G. R. Life Cycle Greenhouse Gas Emissions and Freshwa-

- ter Consumption of Marcellus Shale Gas *Environmental Science & Technology*. 2013;47:4896-4903.
- [101] Clark C. E, Horner R. M, Harto C. B. Life Cycle Water Consumption for Shale Gas and Conventional Natural Gas *Environmental Science & Technology*. 2013;47:11829-11836. PMID: 24004382.
- [102] Goedkoop M, Heijungs R, Huijbregts M, Schryver A. D, Struijs J, Zelm R. V. ReCiPe 2008, A life cycle impact assessment method which comprises harmonised category indicators at the midpoint and the endpoint level January 2009.
- [103] Goedkoop M, Spriensma R. The Eco-indicator99: a damage oriented method for life cycle impact assessment: methodology report tech. rep.PRe Consultants B.V. 2001.
- [104] Venkatesh A, Jaramillo P, Griffin W. M, Matthews H. Uncertainty analysis of life cycle greenhouse gas emissions from United States natural gas end-uses and its effects on policy *Environmental Science & Technology*. 2011;45:8182-8189.